

**DIRECTING VASCULAR CELLS BY CYCLIC TENSILE STRAIN:
CONTEXTUAL ROLE IN ANGIOGENESIS**

by

Yu Ching Yung

A dissertation submitted in partial fulfillment
of the requirements for the degree of
Doctor of Philosophy
(Chemical Engineering)
in The University of Michigan
2008

Doctoral Committee:

Professor David J. Mooney, Co-Chair, Harvard University
Professor Robert M. Ziff, Co-Chair
Professor Paul H. Krebsbach
Assistant Professor Joerg Lahann

“.....the best is yet to be.”

- Robert Browning



© Yu Ching Yung

All Rights Reserved
2008

This thesis is dedicated to:

My parents and my husband
for their love and unwavering faith in me

ACKNOWLEDGEMENTS

There are many people I would like to thank for playing a role in my development, both as an individual and intellectually. I would like to begin by thanking my thesis advisor, Professor David J. Mooney, for giving me the opportunity to grow as a critical scientist under the guidance of his clarity and insights. It has been an invaluable experience to conduct research in an environment that fosters independent and creative thinking, driven primarily by one's own accord to excel. I feel fortunate to have had this opportunity to learn from him and will carry my appreciation with me as I move on to new endeavors.

I would like to thank my thesis committee, Professors Bob Ziff, Paul Krebsbach, and Joerg Lahann, for their valuable suggestions and input during the course of my thesis. I would also like to thank the past and present members of the Mooney lab, from Michigan and at Harvard. I will treasure the laughter, the tears, the “brotherhoods”, and the friendships. I have greatly appreciated the wonderful administrative staff from Michigan and Harvard: Arlene Stevens (HSEAS), Susan Hamlin (UM-ChemEng), and Elizabeth Rodriguez (UM-DBMS), for always being so helpful and so encouraging.

I extend special thanks to several individuals, whom perhaps unknowingly, have played significant roles during my doctoral studies (in chronological order): Brendan Looyenga,

for showing me the beauty of cell biology; Herman Vandenburg, for giving me direction and being a great mentor; Jeiwook Chae, for teaching me so much more than just molecular biology; Monica Carasco, for generously lending me her device; and the Harvard Machine shop folks: Louie, Richard, and Al for their excellent machine work; and last but not least, Mike Greenberg, for his expertise with AutoDesk. I am fortunate to have had the opportunity to work with and learn from all these unique individuals and look forward to many future interactions.

Most importantly, I would like to thank my parents for teaching us through their actions, the value of perseverance and integrity. It is because of their iron will and courage that I have grown into the individual I am today. Thank you for always encouraging us children to pursue our dreams, with endless love and support. I would also like to thank the rest of my family, in particular my brother, Dr. Chong Yung, who has always inspired me with his kindness and ingenuity; and Dr. Alice Yung, for being my first “teacher” and for impressing upon me, her diligence and caring heart.

Finally, I would like to thank my dearest husband, Markus, who has been an inspirational role model, as a person with integrity and as a scientist. Thank you for always being so supportive and for always looking out, first and foremost, for my best interest then my happiness. I am in awe by your kindness and beauty with which it brings, and I look forward to growing old with you.

TABLE OF CONTENTS

DEDICATION	ii
ACKNOWLEDGEMENTS	iii
LIST OF FIGURES	viii
LIST OF APPENDICES	x
ABSTRACT	xi
CHAPTER 1: INTRODUCTION	
1.1 Problem Statement.....	1
1.2 Hypothesis.....	4
1.3 Specific Aims.....	4
1.4 Significance.....	5
1.5 Outline of Thesis.....	5
1.6 References.....	8
CHAPTER 2: REVIEW OF MECHANOTRANSDUCTION IN VASCULAR CELLS	
2.1 Introduction.....	9
2.2 Role of Endothelial Cells in Vascular Remodeling.....	10
2.3 Tissue Engineering of Smooth Muscle	13

2.4	Mechanotransduction and Extracellular Signaling	22
2.5	Summary	29
2.6	References.....	31
CHAPTER 3:	DESIGN AND CONSTRUCTION OF A COMPUTER CONTROLLED: STRAIN MECHANICS ASSESSING RESEARCH TOOL (S.M.A.R.T.)	
3.1	Introduction.....	52
3.2	Materials and Methods.....	55
3.3	Results.....	66
3.4	Discussion.....	71
3.5	References.....	74
CHAPTER 4:	MECHANISM OF CYCLIC TENSILE STRAIN REGULATION OF ENDOTHELIAL CELL ANGIOGENIC PROCESSES	
4.1	Introduction.....	78
4.2	Materials and Methods.....	79
4.3	Results.....	86
4.4	Discussion.....	90
4.5	References.....	96

CHAPTER 5:	ROLE OF CYCLIC STRAIN IN MODULATING RECRUITMENT OF SMOOTH MUSCLE CELLS TOWARDS MIGRATING ENDOTHELIAL CELLS	
5.1	Introduction.....	101
5.2	Materials and Methods.....	102
5.3	Results.....	109
5.4	Discussion.....	117
5.5	References.....	120
CHAPTER 6:	SUMMARY, CONCLUSIONS, IMPLICATIONS AND FUTURE DIRECTIONS	
6.1	Summary.....	126
6.2	Conclusions.....	127
6.3	Implications and Future Directions	128
6.4	References.....	133
APPENDICES		134

LIST OF FIGURES

CHAPTER 1:

Figure 1.1:	Mortality rates for leading causes of death in the United States..	2
Figure 1.2:	Primary areas of research in tissue engineering.....	6

CHAPTER 2:

Figure 2.1:	Mechanisms of blood vessel formation.....	11
Figure 2.2:	Mechanisms of Extracellular Signaling.....	28

CHAPTER 3:

Figure 3.1:	Design chart of S.M.A.R.T system.....	56
Figure 3.2:	Large scale S.M.A.R.T. device and principle of strain.....	58
Figure 3.3:	Microscope adaptable mini S.M.A.R.T.	61
Figure 3.4:	PDMS clamp unit, mold, and plate.	63
Figure 3.5:	Method to create PDMS wells with strain gradient.....	65
Figure 3.6:	Force Profile per PDMS well.....	68
Figure 3.7:	Applied strain is directly conferred in 2D	69
Figure 3.8:	Strain gradient within PDMS well for 2D cultures.....	70
Figure 3.9:	Applied strain is conferred, integrity maintained in 3D gels.....	72

CHAPTER 4:

Figure 4.1:	Method to <i>in vitro</i> angiogenesis: sprouting assay.....	82
Figure 4.2:	Sprout formations by HUVECs.....	84
Figure 4.3:	Cyclic strain enhanced EC migration and sprout formation.....	87
Figure 4.4:	Cyclic strain regulates temporal secretion of angiogenic factors..	89
Figure 4.5:	Ang-2 and VEGF enhance EC migration and sprout formation...	91
Figure 4.6:	Knockdown of Ang-2 decrease EC responsiveness to strain.....	92

CHAPTER 5:

Figure 5.1:	Method to culture a precise array of ECs and SMCs	105
Figure 5.2:	Array of vascular cell colonies in PDMS well with strain gradient.	106
Figure 5.3:	Response of EC migration to increasing strain magnitudes.....	110
Figure 5.4:	Response of SMC migration to increasing strain magnitudes.....	111
Figure 5.5:	Model of PDGF concentration profile and SM migration to PDGF.	113
Figure 5.6:	Bioactivity of SM PDGF-R enhanced by cyclic strain and rhPDGF.	115
Figure 5.7:	Cyclic strain mediates EC paracrine effects on SMC recruitment..	116

CHAPTER 6:

Figure 6.1:	Suggestion for a new tissue Engineering Approach	132
--------------------	---	------------

LIST OF APPENDICES

Appendix A.	Schematics for S.M.A.R.T.....	134
Appendix B.	Protocol to create Mosaic Images.....	135
Appendix C.	Protocol to Sprouting Assay.....	136
Appendix D.	Protocol to Cloning pSilencer-neo.....	137
Appendix E.	Protocol to Pattern Array of Vascular Cell Colonies.....	138

ABSTRACT

DIRECTING VASCULAR CELLS BY CYCLIC TENSILE STRAIN: CONTEXTUAL ROLE IN ANGIOGENESIS

by

Yu Ching Yung

Co-Chairs: David J. Mooney and Robert M. Ziff

Mechanical stretch, a normal physiologic signal in the vascular system, regulates vascular development and regeneration, but the mechanisms underlying these endothelial (EC) and smooth muscle cell (SMC) responses remain unclear. We hypothesized that cyclic tensile strain can regulate autocrine or paracrine signaling between vascular cells to activate concerted angiogenic responses. In order to systematically examine vascular cell response to cyclic tensile strain, a high precision computer controlled strain device was designed and elastomeric substrates to present defined strain profiles, for 2D and 3D studies, were created.

It has been demonstrated that cyclic strain can alter EC phenotype and Angiopoietin-2 (Ang-2) expression, and the alterations in Ang-2 mediated changes in EC migration, and in vitro capillary formation. Knockdown of endogenous Ang-2 expression via RNAi, however, decreased EC responsiveness to strain mediated EC angiogenic processes. We

concluded that autocrine signaling via activation of Ang-2 may be one of the mechanistic pathways by which ECs transduce mechanical strain signals to process early angiogenic responses. Cyclic strain also regulated EC secretion of platelet derived growth factor (PDGF), a known chemotactant for SMCs. Application of strain gradients on isolated vascular EC and SMC colonies in co-culture regulated EC secretion of chemotactic gradients, and this gradient directed SMC recruitment towards strain-mediated EC migration. It is concluded that cyclic strain can modulate the intercellular communication between ECs and SMCs by mediating chemotactic paracrine factors. Taken together, our studies show that the application of precise local cyclic tensile strain signals enables one to regulate the behavior of cells at the molecular level by regulating autocrine signals (EC to EC) via Ang-2 and paracrine signals (EC to SMC) via PDGF to give vascular cells directional cues to direct angiogenic phenotypes at physiologic length scales.

CHAPTER 1

INTRODUCTION

1.1 Problem Statement

Tremendous achievements in science over the past centuries have laid platform for medical discoveries that largely impact today's society. These advancements provide enumerable cures and treatments that improve our lives in many aspects. Benefits from enhanced awareness due to scientific research and resultant treatments is clear in diseases associated with the cardiovascular where mortality rates have diminished by 4 million individuals over the past 50 years¹. However, over 25 million people still continue to suffer annually due to heart disease related issues, the leading cause of death in the United States (Figure 1.1).

Tissue engineering has emerged over the past three decades to address the growing need for biological substitutes to restore or replace damaged tissues and organs² (Figure 1.2). Current approaches to organ repair rely primarily on transplantation of whole or partial organs and tissues. The imbalance of need versus availability of organs poses as a significant and inherent limitation to this method³. Tissue engineering promises an alternative via rebuilding tissues or organs from targeted cell populations, often with the

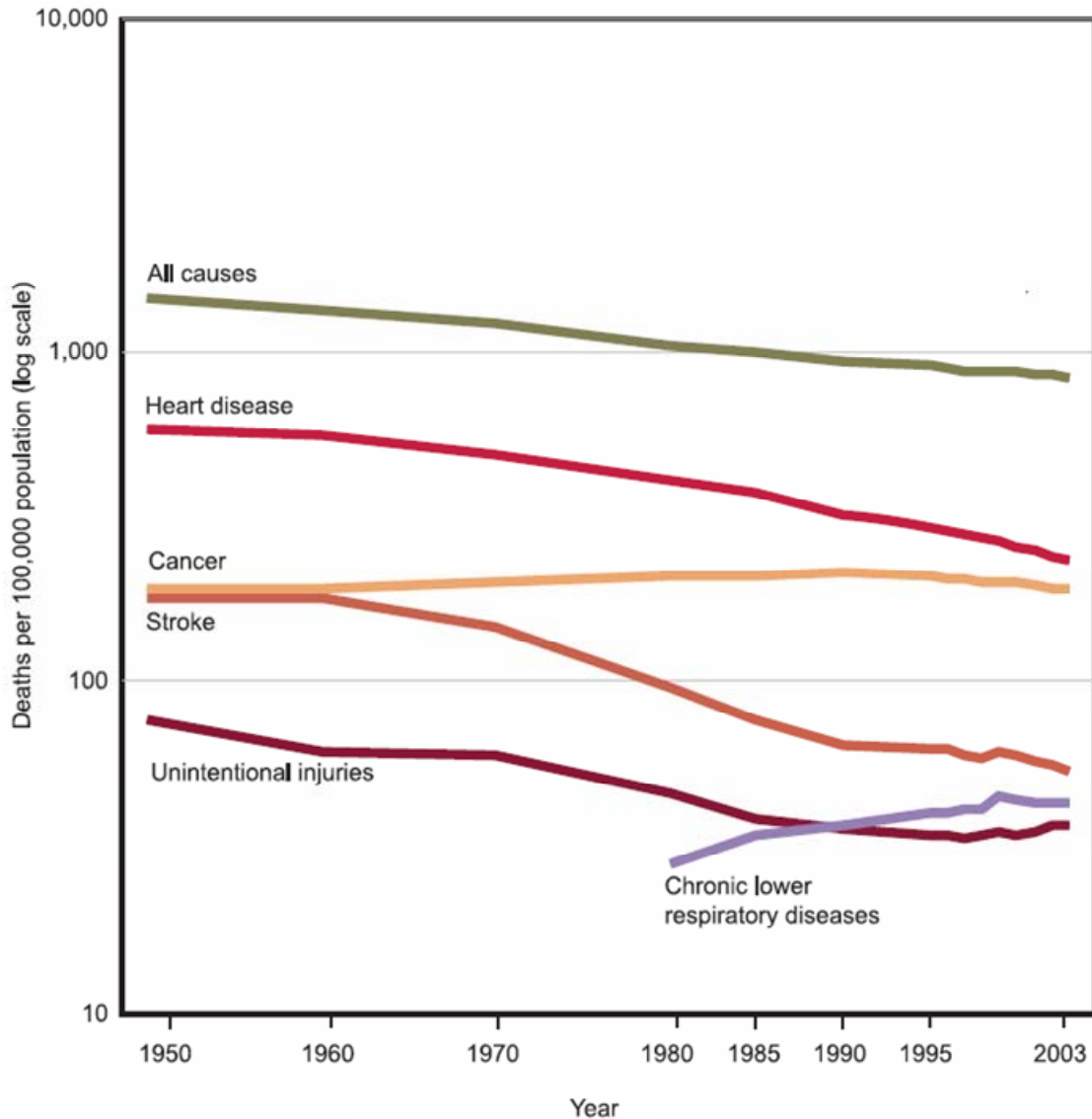


Figure 1.1: Mortality rates for leading causes of death in the United States.

Heart disease remains the leading cause of death over the past 50 years in the United States (1950-2003). Aside from deaths due to unintentional injuries, understanding how to regulate blood vessel development would largely impact therapies for other leading causes of death shown above, such as cancer, stroke and chronic lower respiratory diseases. (Image adapted from *CDC, 2003¹*)

participation of matrices that guide tissue regeneration while providing specific instructions with signaling molecules.

In order to develop functional tissue engineering constructs, an intact vasculature must be present. Overcoming this challenge is a major limitation that hinders this technology from clinical application. The goal of this thesis is to induce the formation of vascular networks within the tissue engineered constructs, by utilizing external stimuli to guide the network formation rather than utilizing artificial vascular constructs to ensure appropriate nutrient provision to all tissues. Vascularization in tissues is limited by oxygen's diffusion coefficient, where after a maximum penetration length of 200um, cells experience hypoxic conditions⁴. Therefore in order to sustain sufficient gas and exhaust exchange, to maintain cell viability within tissue engineered constructs, it is vital to understand how to control and develop new vascular networks.

Physiologically, the phenomenon of vascular remodeling occurs during embryogenesis as well as into adult life, particularly during times of physiologic change or pathological states. Understanding the factors that regulate vascular development gives insight to therapeutic approaches to blood vessel associated heart diseases that remain as one of the leading causes of death in our nation.

Mechanical signals have been identified to modulate signal transduction in vascular cells to alter gene expression^{5,6} and cell function⁷. In blood vessels, hemodynamic forces in the form of cyclic tensile strain and shear stress are known to regulate homeostasis⁸.

However, despite extensive progress in identifying the key intracellular signaling molecules that are modulated by mechanical strain, the mechanism of how cells process these mechanical signals and orchestrate physiologically relevant responses, remains unclear. Understanding the role of mechanical cues in regulating vascular remodeling can lead to broad implications for tissue engineering and to developing therapeutic approaches to heart disease.

1.2 Hypothesis

The purpose of this work is to examine whether cyclic tensile strain can regulate autocrine and paracrine signaling of vascular cells to activate sequential stages of angiogenesis.

1.3 Specific Aims

- 1. Design and construct a mechanical strain device to be used for large scale assessment of vascular cell response to cyclic tensile strain.**
- 2. Investigate the mechanism by which cyclic tensile strain regulates endothelial cell phenotypes; selective cytokine secretion, migration and *in vitro* capillary formation, associated with angiogenic activation.**
- 3. Assess role of strain gradients in modulating recruitment of smooth muscle cells towards endothelial cells under cyclic tensile strain**

1.4 Significance

Current approaches to therapeutic angiogenesis primarily rely on the delivery of exogenous growth factors to regulate the development of engineered vasculature⁹, although limitations to this approach exist. Mechanical signals are capable to regulate the development of various tissues¹⁰; but it remains unclear how cells can process these mechanical signals on the molecular scale to bring forth a physiologically relevant response. This work examines whether modulating the mechanical environment of vascular cells may be sufficient to regulating angiogenesis via autocrine and paracrine signaling. The quantitative effects of strain gradients on vascular activation and stabilization can provide parameters to model the local environment laying platform for future engineering approaches. The devices, experimental methods and model systems developed here will enable further investigation and research into how mechanical cues that initiate at local scales can activate responses critical to formation of complex vascular networks. The knowledge gained from this research can contribute to the current understanding of cues that regulate neovascularization to ultimately impact therapies for diseases associated with blood vessel dysfunction and this knowledge can also be translated to improved tissue engineering neovascularization strategies.

1.5 Outline of Thesis

A general overview of the current concepts and background that provide basis to this work is provided in Chapter 2. Specifically, a review of the role of vascular remodeling involving endothelial cells, smooth muscle engineering and mechanical signaling is

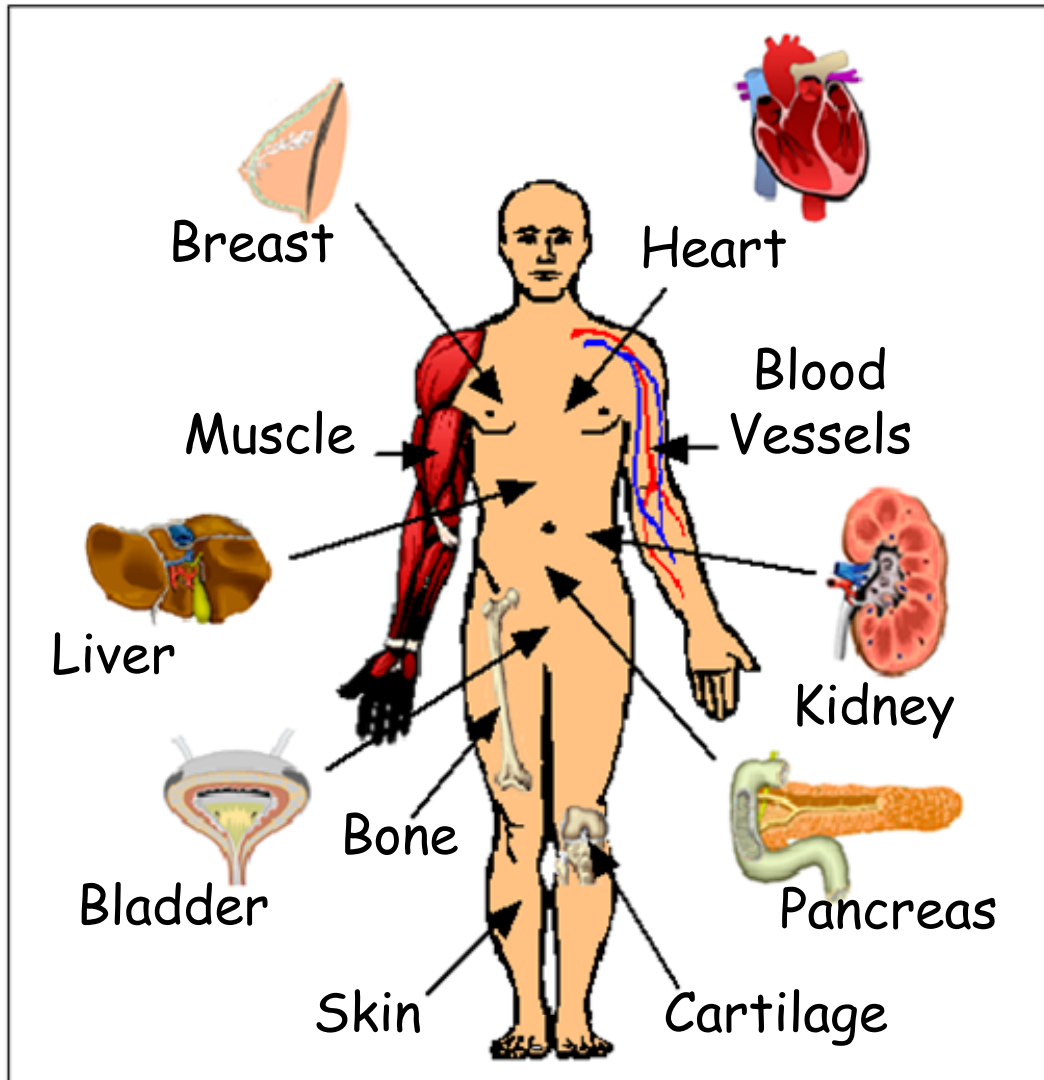


Figure 1.2: Primary areas of research in tissue engineering

Tissue engineering aims to repair or rebuild damaged tissues or organs. Organs shown illustrate several focus areas in tissue engineering. The underlying challenge remains development of an intact functional vasculature.

discussed. In Chapter 3 (Aim 1), the design criteria, motivation and construction of S.M.A.R.T (a high precision mechanical strain device) along with characterization of materials will be presented. These mechanical devices were used extensively for all cyclic strain experiments conducted in Chapter 4 and 5. In Chapter 4 (Aim 2), the mechanism of cyclic strain activated *in vitro* angiogenic processes by endothelial cells was evaluated. Following this in Chapter 5 (Aim 3), we examined whether presentation of precise strain gradients can direct vascular cell migration in the context of angiogenesis. Finally, Chapter 6 provides a critical analysis of results discussed in Chapters 4 and 5, along with implications and impact that this research will provides for future advancements.

1.6 References

1. Trends in the Health of Americans. *CDC, 2006.*
2. Langer, R. & Vacanti, J.P. Tissue engineering. *Science* **260**, 920-926 (1993).
3. Gridelli, B. & Remuzzi, G. Strategies for making more organs available for transplantation. *N Engl J Med* **343**, 404-410 (2000).
4. Folkman, J. & D'Amore, P.A. Blood vessel formation: what is its molecular basis? *Cell* **87**, 1153-1155 (1996).
5. Chien, S., Li, S. & Shyy, Y.J. Effects of mechanical forces on signal transduction and gene expression in endothelial cells. *Hypertension* **31**, 162-169 (1998).
6. Oluwole, B.O., Du, W., Mills, I. & Sumpio, B.E. Gene regulation by mechanical forces. *Endothelium* **5**, 85-93 (1997).
7. Kakisis, J.D., Liapis, C.D. & Sumpio, B.E. Effects of cyclic strain on vascular cells. *Endothelium* **11**, 17-28 (2004).
8. Lehoux, S. & Tedgui, A. Cellular mechanics and gene expression in blood vessels. *J Biomech* **36**, 631-643 (2003).
9. Gibbons, G.H. & Dzau, V.J. Molecular therapies for vascular diseases. *Science* **272**, 689-693 (1996).
10. Ingber, D.E. Mechanical signaling and the cellular response to extracellular matrix in angiogenesis and cardiovascular physiology. *Circ Res* **91**, 877-887 (2002).

CHAPTER 2

REVIEW OF MECHANOTRANSDUCTION IN VASCULAR CELLS

2.1 Introduction

In order to motivate and provide background to understand the basis for the hypothesis guiding this thesis, this chapter will review the biology and role of endothelial cells in vascular remodeling, strategies to tissue engineer smooth muscle, and extracellular signaling via mechanotransduction. Vascular remodeling is a complex process that occurs naturally during embryonic development and adult life. Dysregulation of blood vessel formation however either leads or causes pathogenesis of many disorders. The mechanisms known to activate endothelial cells during neovascularization will be reviewed. Following this, an overview of tissue engineering smooth muscle will be presented. This section will broadly discuss approaches to engineering smooth muscle, cell source, appropriate matrix, for engineering smooth muscle component in vascular grafts as well as in other physiologic tissues. In conclusion, a review of mechanotransduction will be presented, highlighting the signaling transductions pathways that govern this process in both endothelial cells and smooth muscle cells.

2.2 Role of Endothelial Cells in Vascular Remodeling

The vasculature is an active organ that responds to local cues of growth factors¹⁻⁴ intercellular communications^{5,6}, vasoactive substances⁷, and hemodynamic stimuli⁸⁻¹⁰, by altering the structure of preexisting vessels in order to deliver nutrients and gas exchange to tissues in our body. The formation of these blood vessels is mediated by distinct cellular processes that integrate endothelial, smooth muscle, and fibroblast cells into a vessel wall. Neovascularization is governed by two primary mechanisms: vasculogenesis and angiogenesis^{11,12} (Figure 2.1). In brief, vasculogenesis occurs during the development of the embryo when the early vascular plexus forms from the mesoderm to generate primitive blood vessels¹³. Angiogenesis, a mechanism that occurs both during development and in adult life, encompasses the remodeling of preexisting vessels that are sprouting as well as those that are non-sprouting¹¹. As delineated in Chapter 1, this thesis will focus on the latter process; where we will review the role of endothelial cells during neovascularization. Remodeling of the vasculature is a natural biologic process and occurs during the adult life in the reproductive organs or during pathological conditions of tumorigenesis, inflammation, or vascular diseases¹⁴.

Reorganization of the vascular network is activated by a range of stimuli from the local environment, hemodynamic conditions or circulating factors. These signals are subsequently transduced, via the extracellular matrix that supports the endothelial lining of the blood vessel, to activate a cellular response that leads to structural changes of the

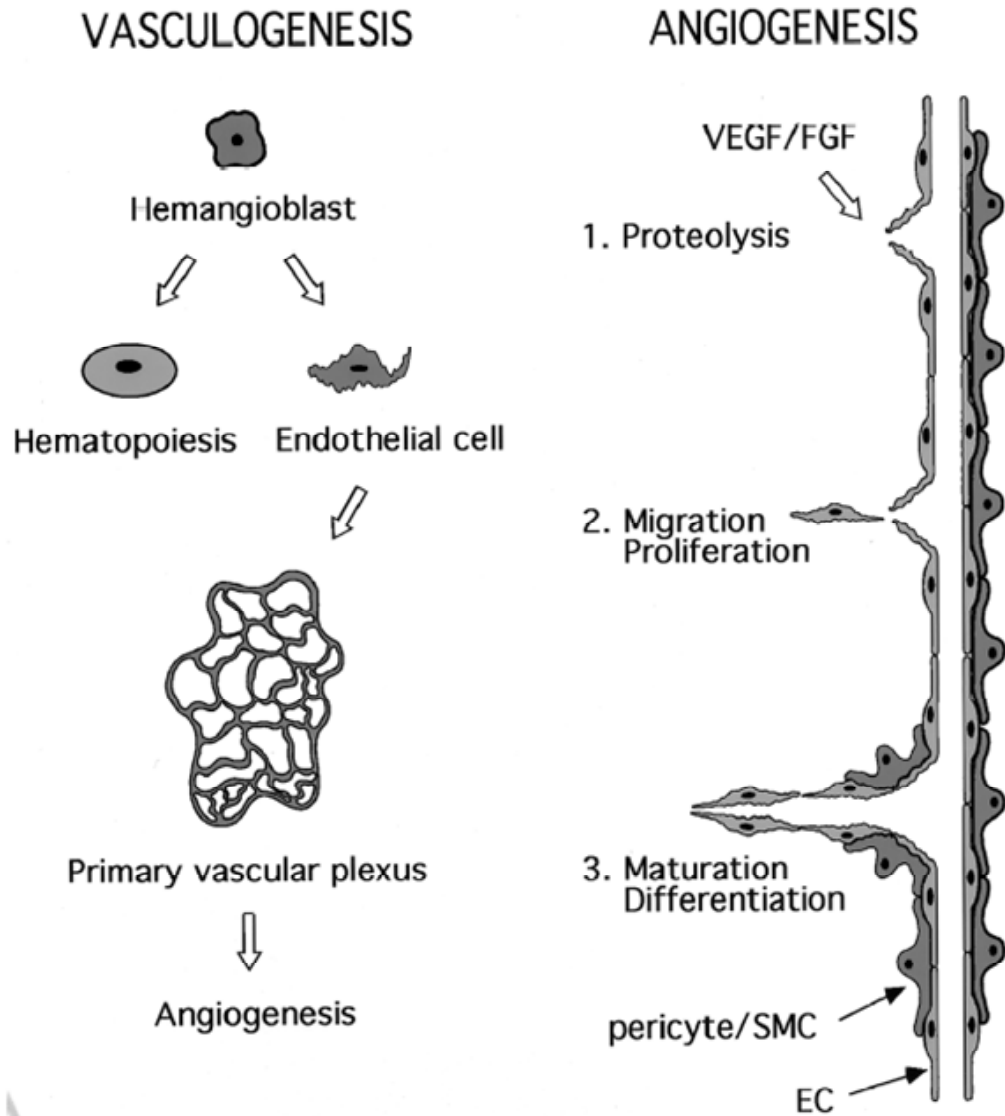


Figure 2.1: Mechanisms of blood vessel formation

Two mechanisms of blood vessel formation differentiated primarily by the cells source initiating the process. Vasculogenesis develops the vascular plexus, connecting the cardiovascular system to all tissues. Angiogenesis requires a sequence of events, activated by endothelial cell migration, differentiation, and concluding with stabilization by pericytes or smooth muscle cells. (Image adapted from Gerwins *et al.*¹²)

existing vessels. The endothelium is therefore a critical component of the remodeling process as it interfaces with blood flow and is exposed to direct contact with mechanical forces, inflammatory cytokines, and other circulating factors. Endothelial cells have been implicated to transduce chemical as well as mechanical signals¹⁵.

Angiogenesis is defined as the formation of new capillaries from existing blood vessels via sprouting. Prior to neovessel outgrowth, proteolytic degradation, via matrix metalloproteinases¹⁶ or plasminogen activators, of local extracellular matrix provides the necessary space for vascular reorganization. This is followed by migration and proliferating of endothelial cells to coalesce and form capillary structures. Endothelial cells participate directly in vascular remodeling by releasing or activating substances to influence the proliferation, migration of other cells or reorganization of the extracellular matrix. The factors that regulate endothelial cells in vascular remodeling involve VEGF-A^{17, 18}, angiopoietins and their respective Tie receptors^{2, 5, 6, 19-24} as well as several extracellular matrix components. Hypoxia has also been found to induce expression or secretion of angiogenic molecules²⁵. The endothelium is exposed to fluid forces, and the effects relayed by changes in blood flow generate a range of stresses^{26, 27} on the endothelial surface, known to activate vascular remodeling. The capacity of the endothelium to sense mechanical signals is therefore an important determinant of vascular structure. Biochemical mitogenic factors along with appropriate mechanical signals clearly regulate the neovascularization process, which relies on a precise orchestrated spatio-temporal presentation of cues to activate sequential stages of the vascular development.

2.3 Tissue Engineering of Smooth Muscle

Smooth muscle cells play an important role not only during the initial sprouting in vascular remodeling, but also for the stabilization and maturation of the vasculature. Functional vascular networks rely on its capability to allow blood perfusion²⁸. This section will provide an overview of engineering smooth muscle in a broad context, extending beyond its role in the cardiovascular system.

Smooth Muscle Cell Source

A critical question in the engineering of smooth muscle tissues is the appropriate source of the SMCs that will comprise the tissue. The majority of research to date has utilized smooth muscle procured from the tissue of interest. However, the isolation of smooth muscle progenitors may allow for a less invasive and destructive approach. In addition, it may be possible to directly recruit SMCs to the site at which one wants a tissue to form.

The most direct approach to form smooth muscle tissues is to utilize smooth muscle cells obtained from the tissue one desires to engineer. In this approach, smooth muscle containing tissue is typically explanted and dissociated into individual cells. The cells are then directly transplanted or expanded in culture, and subsequently transplanted. Direct transplantation may be advantageous as it bypasses in vitro culturing, which can alter the contractile phenotype of smooth muscle cells. In contrast, culture of smooth muscle cells prior to transplantation may lead to phenotypic changes^{29,30}, but this approach allows one to greatly expand the cell population. This may allow a relatively small explant to ultimately yield sufficient cells to engineer a large tissue. The phenotypic changes noted

in smooth muscle cells, as they revert to a synthetic phenotype³¹ may be reversed or prevented through appropriate culture conditions (i.e. cyclic mechanical loading)³².

While smooth muscle tissues characteristically contain contractile apparatus and form the muscular components of visceral structures, there are differences between SM in various tissues³³. These likely relate to the specific microenvironment and physiology of each tissue type. For this reason, SM biopsies are typically procured for the specific type of tissue being engineered. The artery is the most commonly excised tissue for vascular regeneration³⁴⁻³⁷ primarily because it is the largest blood vessel, and hence contains the thickest medial layer. Current methods for bladder replacement require a biopsy to obtain a small specimen of the donor or host bladder tissue, which is then used to expand separate cultures of urothelial and smooth muscle cells³⁸. Ureter or renal pelvis cells can be similarly harvested. Regeneration of gastrointestinal organs, specifically the stomach and the intestine, has most commonly utilized organoid units which contain smooth muscle precursors^{39,40}.

Differentiated smooth muscle cells have shown tremendous utility for the successful regeneration of smooth muscle tissues. However the invasive nature of this cell procurement, the inherent limited proliferation capability of primary cells, and maintenance of smooth muscle phenotype are all limitations to this cell source. Smooth muscle progenitors may potentially be isolated using minimally invasive techniques, and subsequently induced to differentiate down a smooth muscle lineage. Cells isolated from bone marrow are termed bone marrow stromal cells (BMSC), or

mesenchymal stem cells (MSC) depending on the mode of cell purification selection in vitro.

Bone marrow can be obtained easily from the medullary canals of long bones or the cancellous cavities⁴¹, and the resultant BMSC can be readily expanded in culture.

BMSCs have demonstrated the ability to differentiate into multiple mesenchymal cell lineages, and offer an alternative source of smooth muscle cells^{33, 42-49}. Recent studies have shown that BMSCs are inducible down a smooth muscle pathway, and this process is regulated by an interplay between stimulatory molecules^{50, 51}, with TGF- β and PDGF as the main modulators (Dennis and Charbord 2002). Mechanical stimulation has also been shown to effect differentiation of bone marrow stromal cells⁵². However, the mechanism of this effect is still unclear. Smooth muscle progenitors can also be derived from embryonic stem cells^{28, 53}, circulating blood^{54, 55}, bone marrow^{56, 57} and other tissues⁵⁸.

The recruitment of SMCs or progenitors from a surrounding tissue to an engineered tissue provides an alternative to SM transplantation. Signaling molecules such as PDGF and TGF- β have chemotactic effects on smooth muscle cells⁵⁹, and growth factors released by endothelial cells (ECs) can also induce the migration of mesenchymal stem cells and their subsequent differentiation into smooth muscle like cells^{60, 61}. Similarly, myoblast recruitment can be modulated by a gradient of a chemotactic agent⁶². This recruitment approach greatly simplifies the process of smooth muscle tissue engineering, as it eliminates the isolation and expansion of cells in vitro. In addition, this approach

could have utility in applications such as blood vessel repair where direct placement of smooth cells in the lumen could cause a thrombogenic effect. The use of signaling molecules to recruit circulating progenitor cells may provide a useful alternative in this situation.

Extracellular Matrix

Tissue engineering utilizes synthetic extracellular matrices to provide an infrastructure for the formation of tissues by providing a predefined space to localize tissue growth and the mechanical support necessary to facilitate this growth. Synthetic extracellular matrices (ECM) may also provide specific signals to the SMCs. Two general designs of synthetic extracellular matrices for smooth muscle tissue regeneration are being pursued, one involving a biological approach where the matrix is assembled by the resident cells and the other utilizing predefined polymeric structures.

SMCs maintained for extended times in culture will synthesize, secrete, and assemble an ECM with sufficient mechanical integrity to allow a sheet of confluent SMCs to be manipulated and formed into a three dimensional tissue⁶³. This technique is attractive for tissue engineering because it eliminates the need for exogenous biomaterials, and thereby eradicates any potential inflammatory issues related to the material^{64, 65}. Self assembly approaches have focused on engineering vascular grafts by individually culturing cellular sheets to model the defined layers of the blood vessel. A sheet of smooth muscle cells is used to form the medial layer, which is subsequently wrapped with a sheet composed of fibroblasts to form the adventitial layer, and finally seeded with

endothelial cells to create the lumen. Initial studies on tissues formed utilizing this approach reported poor mechanical strength^{66,67}, which is indicative of a deficient medial and, or adventitial layers. A revised approach increased the mechanical strength of tissues formed with this approach⁶³. However, a limitation to this approach is the extensive time required to form the cellular sheets.

Most approaches to engineer SM tissues have utilized three dimensional, biodegradable polymeric scaffolds. Polymeric scaffolds formed from exogenous biomaterials provide mechanical stability and can deliver signaling molecules or adhesion peptides to induce appropriate tissue development. These polymeric biomaterials are fabricated from either synthetic or naturally derived materials. Synthetic polymers typically used for engineering smooth muscle tissues include several forms of polyesters, elastomeric polymers, and hydrogels. The most common used naturally derived polymer used to engineer SMC is type I collagen.

The most prevalent synthetic polymers used to engineer smooth muscle tissues are the polyesters poly(glycolic acid) (PGA) (Fig. 2a), poly(L-lactic acid) (PLLA), and poly(lactic-co-glycolic acid) (PLGA). Advantageous features of these polymers include their reproducible and readily altered mechanical properties and degradation rates^{68,69}. These polymer scaffolds provide temporary mechanical support⁷⁰ sufficient to resist cellular contractile forces in vitro⁷¹⁻⁷⁴, and scaffolds exhibiting partial elastic properties under cyclic strain enabled induction of a more contractile, differentiated smooth muscle phenotype from attached SMCs⁷⁵. In addition to structural stability, appropriate signals

may be required to guide the development of smooth muscle tissues. Synthetic polymers can be modified to incorporate signals to alter cellular function, including cell adhesion molecules ⁷⁶⁻⁷⁸ and growth factors ^{79, 80}.

Hydrogel forming polymers have also been investigated for engineering SM tissues. Polyethylene glycol (PEG) hydrogels intrinsically resist protein adsorption and cell adhesion ⁸¹ and this characteristic offers advantages for studying the effects of specific bioactive ligands or peptides presented from the scaffold ^{82, 83}. Studies utilizing surface modified PEGs have demonstrated that a number of cellular functions, including adhesion ⁸², migration ⁸⁴, and matrix production ⁸⁵ can be regulated by ligand presentation. In general, hydrogels are an appealing scaffold material because they are structurally similar to the highly hydrated extracellular matrix of many tissues ⁸⁶. However, the use of hydrogels is often constrained by their limited range of mechanical properties.

The elasticity provided by elastin in SM tissues has motivated the development of elastomeric scaffolds that can similarly provide this property to engineered SM. Elastomeric polymers can recover from extensive deformation ⁸⁷⁻⁸⁹ and are designed to resemble the incompressible nature of the ECM ⁹⁰. This property of biomaterials may be ideal to engineer functional SM tissues that require transduction of mechanical signals from the extracellular environment in order to elicit and activate key cellular functions ⁹¹⁻⁹³. This type of biomaterial resolves the limitations of lack of pliancy that limits many synthetic polymer scaffolds (i.e., poly(lactic acid) (PLA)).

Type I collagen (Fig. 2b) has been frequently used to create polymer scaffolds for engineering SM tissues^{71, 75, 94, 95}. Naturally derived collagen is an attractive biologic material because collagen is the primary constituent of the ECM⁹⁶, and contains adhesion ligands that facilitate cell attachment. Although type I collagen does not require additional surface modification to promote tissue formation, glycosaminoglycans (GAGs)⁹⁷ and growth factors⁹⁸ can be incorporated to improve mechanical properties and to induce specific cellular functions. Type I collagen matrices used to engineer SM tissues have demonstrated partial elasticity and are capable of withstanding cyclic strain⁷⁵. The high tensile strength of type I collagen can be attributed to its molecular structure, while the elasticity is conferred by the intermolecular cross-linking. The degradation of type I collagen scaffolds is dependent on the extent of cross-linking, pore structure and the apparent density, which are variables that can be readily altered to meet a desired target. Although type I collagen is typically extracted from xenogeneic sources, it is considered biocompatible and exhibits low immunogenic responses, likely due to the similarity of this molecule between species⁹⁹. However, naturally derived materials may suffer from batch to batch variations.

Another collagen based biomaterial, small intestinal submucosa (SIS), has also been widely used in tissue engineering research¹⁰⁰⁻¹⁰². This xenogeneic matrix is harvested from the submucosal layer of the intestine. SIS may provide functional growth factors¹⁰³ that contribute to SM tissue formation. In addition, SIS matrices maintain elasticity and high strength¹⁰⁴. SIS has typically been obtained from porcine sources, but isolation from rats¹⁰⁵ and canines¹⁰⁶ has also been attempted. SIS has been used to promote

regeneration of several SM tissues, in the blood vessels^{107, 108} and in the bladder^{104, 106,}
¹⁰⁹.

Engineered Smooth Muscle Tissues

A number of studies to date have utilized a combination of scaffolding technologies and cells to reconstruct the smooth muscle component of cardiovascular, gastrointestinal and urinary tissues. The two primary tissue engineering approaches used to regenerate tissues are cell transplantation and cell recruitment from surrounding tissue. Cell transplantation requires an initial step of procuring cells, often via biopsy from the host, followed by dissociation and expansion in vitro. The cells are then seeded onto a scaffold and implanted as a cell-matrix construct. Alternatively, an implanted acellular matrix may be implanted to promote the recruitment of neighboring SMCs and possibly other cell types of interest (e.g., ECs, urothelial cells). Work to date in engineering SM tissues is briefly summarized in this section.

A great deal of research has been performed with the goal of developing blood vessel substitutes, due to the large impact this advance would have on the millions of patients that annually suffer from diseases of blood vessels¹¹⁰. Strategies to engineer blood vessel must provide adequate mechanical properties, to avoid catastrophic failure in this mechanically demanding site, and appropriate cellular components to form the complex vascular wall. An early approach to engineer the blood vessels involved the culture of different vascular cell populations in collagen gels to form three distinct layers, resembling the three layers of native blood vessel⁶⁶. However, this model did not lead to

tissues with adequate mechanical strength. A later approach exploited the ability of fibroblasts and SM cells to synthesize and secrete their own ECM and form self assembled sheets. These sheets were subsequently wrapped around a mandrel to form distinct layers of the native vessels⁶³. This method led to tissues with much greater mechanical strength, comparable to that of human vessels⁶⁷. The increased mechanical strength of these tissues may be partially attributed to paracrine effects between ECs and SMCs^{5, 60, 111} that contribute to the stability of nascent blood vessels by increasing matrix production. Also, implantation of a decellularized SIS with additional type I bovine collagen into a rabbit artery led to the formation of a blood vessel characterized by reasonable burst strength, cell and matrix organization¹⁰⁷.

Several groups have utilized externally applied mechanical stimulation to improve the mechanical integrity of engineered SM tissues (Fig. 4b). Blood vessel substitutes formed from allogeneic vascular SMCs and ECs cultured on biodegradable PGA scaffolds were maintained under pulsatile stress, and this resulted in an increased matrix production¹¹². These engineered constructs were subsequently implanted into swine for seven weeks and the explanted vessels exhibited adequate burst pressures and histology. Several studies document that one can improve the properties of constructs engineered using collagen through the use of mechanical stimulation^{113, 114}. The significance of mechanical stimulation was also demonstrated by studies where synthetic SMCs cultured with ECs on collagen gels were found to undergo a phenotypic reversion under contractile forces^{31, 115}.

2.4 Mechanotransduction and Extracellular Signaling

Blood vessels are physiologically exposed to hemodynamic forces in the form of cyclic tensile strain and shear stress due to the pulsatile nature of blood flow. Vascular endothelial and smooth muscle cells are exposed to both types of mechanical forces, where predominantly only endothelial cells are subject to shear stress. Extensive research demonstrates that mechanical signals modulate cell functions of vascular endothelial¹¹⁶ and smooth muscle cells⁹¹⁻⁹³. This section will review the mechanosensors on vascular endothelial and smooth muscle cell membranes used to detect signals. This is followed by a comprehensive overview of the various intracellular signaling pathways, where an enormous number of studies have documented signaling molecules implicated responsive to mechanical stimuli. A brief review of chemical signals is discussed at the end, as vascular remodeling is likely a process involving the interplay of extracellular signals.

Endothelial cells (ECs) act as mechanosensors and detect changes in the mechanical environment through various sensing mechanisms. Intracellular signaling pathways have been documented to initiate via cell adhesion molecules (CAMs), receptor tyrosine kinases (RTKs), ion channels, and G-protein coupled receptors (GPCRs), and likely, the interplay of these sensing mechanisms.

Mechanosensors: cell adhesion molecules (CAMs)

Integrins (a member of the heterophilic CAM subfamily), link the immunoglobulin superfamily or the extracellular matrix (ECM) to the cell cytoskeleton¹¹⁷ and provide for

a method to anchor the cell to the substratum or to other cells. Integrins are composed of transmembrane α and β subunits that simultaneously bind to extracellular proteins (collagen, fibronectin, and laminin) and intracellular anchor proteins at focal adhesion sites e.g. focal adhesion kinase (FAK) and c-Src, and cytoskeletal proteins e.g., talin, α -actinin, filamin, vinculin, via the cytoplasmic tail of the β subunit⁹⁶. The intracellular proteins at focal contacts can directly link to the cytoskeleton by binding to actin filaments and through this, provide a bridge by which mechanical strain can be transduced from the ECM to the cytoskeleton. Cyclic strain modulates the directional organization of EC integrins^{118, 119} cultured on surfaces treated with fibronectin and collagen. Reorganization of integrins resulting in clustering, activates tyrosine phosphorylation^{120, 121} to initiate downstream signaling pathways. Exposure of ECs to shear stress induce clustering^{122, 123} of integrins, association with adaptor proteins¹²² and activation of focal adhesion kinases¹²³. Recent studies suggest that integrins can associate with adaptor proteins that link to transmembrane growth factor receptors (GFRs)¹²⁴, where a majority are receptor tyrosine kinases (RTKs). Cyclic mechanical strain of SMCs increases levels of focal contact components¹²⁵, integrin clustering¹²⁴, and provide a potential mechanism for the role of mechanical signals in activation of FAKs. Shear stress has been documented to enhance the expression of several immunoglobulin superfamily, primarily PECAM-1^{126, 127}, a molecule located at the junction sites of confluent EC monolayers, ICAM-1¹²⁸ and VCAM^{129, 130}, intercellular molecules linking ECs to SMCs.

Mechanosensors: RTK (receptor tyrosine kinases)

Receptor tyrosine kinases (RTKs) include a transmembrane spanning domain, an extracellular N-terminal region and an intracellular C-terminal region. The extracellular N-terminal region is composed of large protein domains that bind to extracellular ligands while the intracellular C-terminal region is primarily responsible for signal transduction and kinase activity. Shear stress have been demonstrated to activate VEGF receptor, Flk-1¹²², of ECs, independent of VEGF ligand binding¹³¹. While Tie-2, an endothelial cell specific receptor to ligand Angiopoietin 1 and 2, was also shown to upregulate in response to shear forces. Cyclic strain has been shown to stimulate tyrosine phosphorylation of PDGFR- α ¹³² and increase PDGR- β in aortic SMCs¹³³.

Modulation of signaling pathways

Cyclic strain and shear stress can activate a number of mechanosensors that result in activation and propagation of signals through a network of pathways. A great deal of research has reported the activation of multiple signaling molecules in response to mechanical signals, including FAK, Rho family GTPases, PI3K, protein kinase C (PKC), Notch, and most widely studied, MAPKs. Signaling via Akt in response to shear stress has been implicated to maintain endothelial survival and integrity in blood vessels¹³⁴, a downstream target of Phosphoinositide 3-kinases (PI3K)¹³⁵, also known to exhibit enhanced activation in response to cyclic strain. Exposure of SMCs to cyclic strain also induces the phosphorylation and activation of pro-survival Akt protein kinase¹³⁶, and ECs exposed to shear stress similarly exhibit activation of the Akt pathway¹³⁷. Akt is activated in response to a number of growth factor stimuli, including PDGF, VEGF, EGF, insulin, and thrombin in ECs^{138, 139} and has been implicated in cell functions such as

proliferation and anti-apoptosis. Rho family GTPases serve as convergence points for actin cytoskeleton signals and acts as molecular switches to control cellular processes. The Rho family members, Cdc42, Rac, and Rho have different functions in regulating the actin cytoskeleton structure and intracellular signaling. Shear stress has been shown to induce a transient activation of Cdc42¹⁴⁰, while sustained activation¹⁴⁰ and decreased activity of RhoA¹⁴¹ have both been documented. Generally, Cdc42 and Rac regulates filopodia and lamellipodia formation, while RhoA increases cell contractility¹⁴². Mitogen-activated protein kinases (MAPKs) are a group of serine/threonine kinases that activate in response to dual phosphorylation at conserved threonine and tyrosine residues to extracellular stimuli and regulate various cellular functions. There are 3 distinct MAPK modules in mammalian cells, the extracellular signal regulated protein kinases 1 and 2 (ERK1/2)^{143, 144}, the JNK/SAPK¹⁴⁵, and the p38¹⁴⁶ pathways, where activation of these molecules in ECs have been reported in response to cyclic strain. However, the cyclic strain induced activation of JNK in SMCs has been documented to be integrin independent, occurring in cultures treated with proectin and laminin¹⁴⁷. Protein kinase C (PKC) is a crucial serine/threonine kinase that is co-activated by membrane bound diacylglycerols (DAG) and Ca²⁺ and phospholipid phosphatidylserine at the plasma membrane¹⁴⁸. PKC is known to activate various target proteins to alter cellular function and exposure of vascular endothelial and smooth muscle cells to cyclic strain leads to activation of the PKC pathway¹⁴⁹⁻¹⁵¹. Focal adhesion kinase (FAK) binds to the cytosolic tail of one of the integrin subunits and can cross phosphorylate when triggered by integrin clustering and documented above to reorganize in response to mechanical stimuli. Recent studies have also shown that cyclic strain can mediate the upregulation of

Notch¹⁵², a signaling pathway important for neuronal development and endothelial fate in angiogenesis.

Mechanical signal effects of cell function

Mechanical forces regulate a number of physiologic tissues that are normally exposed to loading or compressive forces. Extensive studies have been conducted on a number of cell and tissue types to investigate regulatory effects by mechanical stimuli. Several tissues commonly reported to respond to mechanical forces is listed here, whereas more relevant literature on vascular remodeling is discussed within each specific aim of this thesis. Cyclic uniaxial loading has been reported to regulate vascular endothelial cell patterning¹⁵³, skeletal muscle growth¹⁵⁴, osteogenic growth^{155, 156}, cardiomyocyte contractility¹⁵⁷, and extracellular matrix production¹⁵⁸⁻¹⁶⁰. Early studies focused largely on bone and found that physical strain held a role in regulating differentiation^{161, 162}, remodeling^{163, 164} and regenerative of bone tissue. Application of biaxial strain have been reported to enhance smooth muscle development^{75, 93} and organization¹⁶⁵, activate endothelial cell gene expression¹¹⁶, osteogenic differentiation^{32, 166}, and cell adhesion¹²⁵.

Extracellular Signaling: paracrine, autocrine signaling and vascular mitogens

Several mechanisms exist to enable one cell to influence the behavior of other cells via extracellular signal molecules. Contact dependent (Figure 2.2A) signaling occur when signaling molecules remain bound to the signaling cell surface and influence only other cells that come in direct contact with the signaling cell (e.g. PECAM/CD31 expressed on EC membranes regulate adhesion with to other ECs and activate downstream signaling

pathways when bound)¹⁶⁷. However, most signaling molecules are secreted. Paracrine signaling (Figure 2.2B) occurs when secreted molecules act as local mediators and affect only cells in the immediate environment of the signaling cell. Paracrine signaling molecules are often rapidly taken up target cells, or degraded over large distances (e.g. PDGF secreted by ECs to induce chemotactic effects on SMCs^{168, 169}).

Cells can also send signals to self regulate via autocrine signaling (Figure 2.2C). This process occurs when a cell secretes signaling molecules into the local environment to bind to the surface receptors of cells identical to the original signaling cell. This signaling mechanism is particularly prevalent during embryogenesis to reinforce a developmental decision (e.g. after a cell has initiated differentiation down a specific path). Autocrine signaling is most effective when performed simultaneously by neighboring cells of the same type (e.g. Angiopoietin 2 secreted by ECs)^{22, 23, 170}, and it is likely to be used to self activate a group of cells to perform a concerted response. Thus, autocrine signaling is thought to be one possible mechanism underlying the community effect that is observed in early development, during which a group of identical cells can respond to a differentiation-inducing signal but a single isolated cell of the same type cannot⁹⁶. Many diseased states similarly utilize autocrine signaling to overcome the normal controls on cell proliferation and survival. By secreting signals that act back on the cell's own receptors, autocrine signaling allows cancer cells to activate anti-apoptotic pathways¹⁷¹ in locations normal functioning cells would not be able to survive.

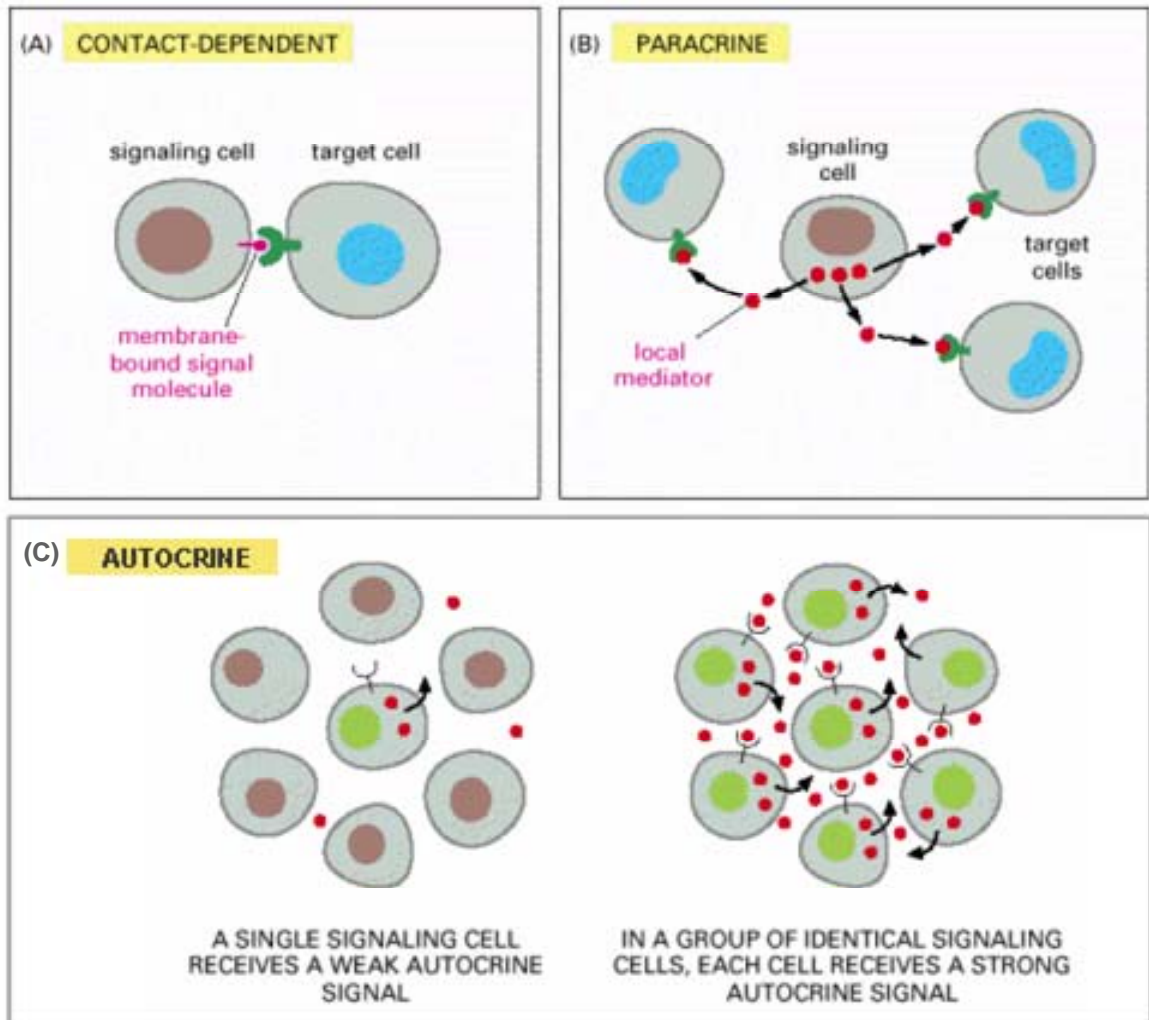


Figure 2.2A-C Mechanisms of Extracellular Signaling

(A) Contact-dependent signaling requires cells to be in direct membrane contact. (B) Paracrine signaling relies on signaling molecules secreted by one cell into the extracellular space to effect local target cells. (C) Autocrine signaling is a mechanism by which one cells secretes signaling molecules into the extracellular space to return and bind to its own surface receptors, essentially acting as a positive feedback regulator.

(Image adapted from Alberts *et al.*⁹⁶)

The extracellular environment scaffolds and serves as a temporary holding ground for these autocrine and paracrine that play a pivotal role in vascular remodeling by providing instructions to endothelial and smooth muscle cells. Mitogenic factors have shown to possess a significant effect on of both endothelial cells and smooth muscle cells in culture include vascular endothelial growth factor (VEGF), angiopoietins (ANG), platelet derived growth factor (PDGF), transforming growth factor- β (TGF- β), and to a lesser extent, heparin binding-epidermal growth factor (HB-EGF) and fibroblast growth factor-2 (FGF-2)^{5, 172}. PDGF has been shown to have potent effects on proliferation, migration, and matrix production by smooth muscle cells^{28, 53, 59, 60, 62, 92, 173, 174}. An increase in the synthesis of SM extracellular proteins is stimulated by TGF- β and these matrix components provide mechanical integrity to engineered smooth muscle tissues^{59, 61, 85, 98, 175-178}. Particularly in strategies where smooth muscle recruitment is important, angiopoietin and HB-EGF have both shown to mediate endothelial and smooth muscle cell interactions^{5, 20, 111, 179}. However, SM tissue engineering strategies that utilize growth factors must consider the mode of delivery. Polymeric encapsulation of growth factors is a common approach to deliver the molecules to the developing smooth muscle tissues in a controlled and sustained manner¹⁸⁰.

2.5 Summary

Vascular remodeling is a process critical to tissue engineering and for developing therapies associated with neovascularization. Cytokines, circulating factors and hemodynamic stimuli play a key role in this process due to their ability to direct the activation of the endothelial cells that line the endothelium. Equally important is to

understand the cues that regulate the recruitment of smooth muscle cells to neovessels and approaches to engineer smooth muscle in culture, in order to develop stable mature vascular networks. Understanding how these vascular cells together are regulated by local mechanical stimuli together with biochemical cues would enable improved regulation of vascular remodeling.

2.6 References

1. Carmeliet, P. & Jain, R.K. Angiogenesis in cancer and other diseases. *Nature* **407**, 249-257 (2000).
2. Fiedler, U. & Augustin, H.G. Angiopoietins: a link between angiogenesis and inflammation. *Trends Immunol* **27**, 552-558 (2006).
3. Montesano, R., Vassalli, J.D., Baird, A., Guillemin, R. & Orci, L. Basic fibroblast growth factor induces angiogenesis in vitro. *Proc Natl Acad Sci U S A* **83**, 7297-7301 (1986).
4. Risau, W. Angiogenic growth factors. *Prog Growth Factor Res* **2**, 71-79 (1990).
5. Iivanainen, E. et al. Angiopoietin-regulated recruitment of vascular smooth muscle cells by endothelial-derived heparin binding EGF-like growth factor. *Faseb J* **17**, 1609-1621 (2003).
6. Daly, C. et al. Angiopoietin-2 functions as an autocrine protective factor in stressed endothelial cells. *Proc Natl Acad Sci U S A* **103**, 15491-15496 (2006).
7. BATEGAY, E.J. Angiogenesis: mechanistic insights, neovascular diseases, and therapeutic prospects. *J Mol Med* **73**, 333-346 (1995).
8. Conway, E.M., Collen, D. & Carmeliet, P. Molecular mechanisms of blood vessel growth. *Cardiovasc Res* **49**, 507-521 (2001).
9. Li, S., Huang, N.F. & Hsu, S. Mechanotransduction in endothelial cell migration. *J Cell Biochem* **96**, 1110-1126 (2005).
10. Ingber, D.E. Mechanical signaling and the cellular response to extracellular matrix in angiogenesis and cardiovascular physiology. *Circ Res* **91**, 877-887 (2002).

11. Risau, W. Mechanisms of angiogenesis. *Nature* **386**, 671-674 (1997).
12. Gerwins, P., Skoldenberg, E. & Claesson-Welsh, L. Function of fibroblast growth factors and vascular endothelial growth factors and their receptors in angiogenesis. *Crit Rev Oncol Hematol* **34**, 185-194 (2000).
13. Risau, W. & Flamme, I. Vasculogenesis. *Annu Rev Cell Dev Biol* **11**, 73-91 (1995).
14. Carmeliet, P. Angiogenesis in health and disease. *Nat Med* **9**, 653-660 (2003).
15. Oluwole, B.O., Du, W., Mills, I. & Sumpio, B.E. Gene regulation by mechanical forces. *Endothelium* **5**, 85-93 (1997).
16. Carmeliet, P. & Collen, D. Gene manipulation and transfer of the plasminogen and coagulation system in mice. *Semin Thromb Hemost* **22**, 525-542 (1996).
17. Carmeliet, P. et al. Abnormal blood vessel development and lethality in embryos lacking a single VEGF allele. *Nature* **380**, 435-439 (1996).
18. Ferrara, N. et al. Heterozygous embryonic lethality induced by targeted inactivation of the VEGF gene. *Nature* **380**, 439-442 (1996).
19. Maisonpierre, P.C. et al. Angiopoietin-2, a natural antagonist for Tie2 that disrupts in vivo angiogenesis. *Science* **277**, 55-60 (1997).
20. Lobov, I.B., Brooks, P.C. & Lang, R.A. Angiopoietin-2 displays VEGF-dependent modulation of capillary structure and endothelial cell survival in vivo. *Proc Natl Acad Sci U S A* **99**, 11205-11210 (2002).
21. Asahara, T. et al. Tie2 receptor ligands, angiopoietin-1 and angiopoietin-2, modulate VEGF-induced postnatal neovascularization. *Circ Res* **83**, 233-240 (1998).

22. Fiedler, U. et al. The Tie-2 ligand angiopoietin-2 is stored in and rapidly released upon stimulation from endothelial cell Weibel-Palade bodies. *Blood* **103**, 4150-4156 (2004).
23. Fiedler, U. et al. Angiopoietin-2 sensitizes endothelial cells to TNF-alpha and has a crucial role in the induction of inflammation. *Nat Med* **12**, 235-239 (2006).
24. Stratmann, A., Risau, W. & Plate, K.H. Cell type-specific expression of angiopoietin-1 and angiopoietin-2 suggests a role in glioblastoma angiogenesis. *Am J Pathol* **153**, 1459-1466 (1998).
25. Miller, J.W. et al. Vascular endothelial growth factor/vascular permeability factor is temporally and spatially correlated with ocular angiogenesis in a primate model. *Am J Pathol* **145**, 574-584 (1994).
26. LoGerfo, F.W., Soncrant, T., Teel, T. & Dewey, C.F., Jr. Boundary layer separation in models of side-to-end arterial anastomoses. *Arch Surg* **114**, 1369-1373 (1979).
27. Ojha, M. Spatial and temporal variations of wall shear stress within an end-to-side arterial anastomosis model. *J Biomech* **26**, 1377-1388 (1993).
28. Koike, N. et al. Tissue engineering: creation of long-lasting blood vessels. *Nature* **428**, 138-139 (2004).
29. Owens, G.K. Regulation of differentiation of vascular smooth muscle cells. *Physiol Rev* **75**, 487-517 (1995).
30. Campbell, J.H. & Campbell, G.R. Vascular smooth muscle in culture. (CRC Press, Boca Raton, Fla.; 1987).

31. Kanda, K., Miwa, H. & Matsuda, T. Phenotypic reversion of smooth muscle cells in hybrid vascular prostheses. *Cell Transplant* **4**, 587-595 (1995).
32. Nikolovski, J., Kim, B.S. & Mooney, D.J. Cyclic strain inhibits switching of smooth muscle cells to an osteoblast-like phenotype. *Faseb J* **17**, 455-457 (2003).
33. Young, B. et al. (Churchill Livingstone, Edinburgh ; New York; 2000).
34. Stegemann, J.P. & Nerem, R.M. Altered response of vascular smooth muscle cells to exogenous biochemical stimulation in two- and three-dimensional culture. *Exp Cell Res* **283**, 146-155 (2003).
35. McKee, J.A. et al. Human arteries engineered in vitro. *EMBO Rep* **4**, 633-638 (2003).
36. Stock, U.A., Vacanti, J.P., Mayer Jr, J.E. & Wahlers, T. Tissue engineering of heart valves -- current aspects. *Thorac Cardiovasc Surg* **50**, 184-193 (2002).
37. Shinoka, T. et al. Creation of viable pulmonary artery autografts through tissue engineering. *J Thorac Cardiovasc Surg* **115**, 536-545; discussion 545-536 (1998).
38. Oberpenning, F., Meng, J., Yoo, J.J. & Atala, A. De novo reconstitution of a functional mammalian urinary bladder by tissue engineering. *Nat Biotechnol* **17**, 149-155 (1999).
39. Maemura, T., Shin, M., Sato, M., Mochizuki, H. & Vacanti, J.P. A tissue-engineered stomach as a replacement of the native stomach. *Transplantation* **76**, 61-65 (2003).
40. Kaihara, S. et al. Long-term follow-up of tissue-engineered intestine after anastomosis to native small bowel. *Transplantation* **69**, 1927-1932 (2000).

41. Junqueira, L.C.U. & Carneiro, J. Basic histology : text & atlas, Edn. 10th. (Lange Medical Books McGraw-Hill Medical Pub. Division, New York; 2003).
42. Pittenger, M.F. et al. Multilineage potential of adult human mesenchymal stem cells. *Science* **284**, 143-147 (1999).
43. Bianco, P. & Robey, P.G. Stem cells in tissue engineering. *Nature* **414**, 118-121 (2001).
44. Bianco, P., Riminucci, M., Gronthos, S. & Robey, P.G. Bone marrow stromal stem cells: nature, biology, and potential applications. *Stem Cells* **19**, 180-192 (2001).
45. Krebsbach, P.H., Kuznetsov, S.A., Bianco, P. & Robey, P.G. Bone marrow stromal cells: characterization and clinical application. *Crit Rev Oral Biol Med* **10**, 165-181 (1999).
46. Ferrari, G. et al. Muscle regeneration by bone marrow-derived myogenic progenitors. *Science* **279**, 1528-1530 (1998).
47. Ferrari, G. & Mavilio, F. Myogenic stem cells from the bone marrow: a therapeutic alternative for muscular dystrophy? *Neuromuscul Disord* **12 Suppl 1**, S7-10 (2002).
48. Hirschi, K.K. & Goodell, M.A. Hematopoietic, vascular and cardiac fates of bone marrow-derived stem cells. *Gene Ther* **9**, 648-652 (2002).
49. Kadner, A. et al. A new source for cardiovascular tissue engineering: human bone marrow stromal cells. *Eur J Cardiothorac Surg* **21**, 1055-1060 (2002).
50. Dennis, J.E. & Charbord, P. Origin and differentiation of human and murine stroma. *Stem Cells* **20**, 205-214 (2002).

51. Kinner, B., Zaleskas, J.M. & Spector, M. Regulation of smooth muscle actin expression and contraction in adult human mesenchymal stem cells. *Exp Cell Res* **278**, 72-83 (2002).
52. Altman, G.H. et al. Cell differentiation by mechanical stress. *Faseb J* **16**, 270-272 (2002).
53. Yamashita, J. et al. Flk1-positive cells derived from embryonic stem cells serve as vascular progenitors. *Nature* **408**, 92-96 (2000).
54. Han, C.I., Campbell, G.R. & Campbell, J.H. Circulating bone marrow cells can contribute to neointimal formation. *J Vasc Res* **38**, 113-119 (2001).
55. Simper, D., Stalboerger, P.G., Panetta, C.J., Wang, S. & Caplice, N.M. Smooth muscle progenitor cells in human blood. *Circulation* **106**, 1199-1204 (2002).
56. Sata, M. et al. Hematopoietic stem cells differentiate into vascular cells that participate in the pathogenesis of atherosclerosis. *Nat Med* **8**, 403-409 (2002).
57. Shimizu, K. et al. Host bone-marrow cells are a source of donor intimal smooth-muscle-like cells in murine aortic transplant arteriopathy. *Nat Med* **7**, 738-741 (2001).
58. Majka, S.M. et al. Distinct progenitor populations in skeletal muscle are bone marrow derived and exhibit different cell fates during vascular regeneration. *J Clin Invest* **111**, 71-79 (2003).
59. Hirschi, K.K., Rohovsky, S.A. & D'Amore, P.A. PDGF, TGF-beta, and heterotypic cell-cell interactions mediate endothelial cell-induced recruitment of 10T1/2 cells and their differentiation to a smooth muscle fate. *J Cell Biol* **141**, 805-814 (1998).

60. Hirschi, K.K., Rohovsky, S.A., Beck, L.H., Smith, S.R. & D'Amore, P.A. Endothelial cells modulate the proliferation of mural cell precursors via platelet-derived growth factor-BB and heterotypic cell contact. *Circ Res* **84**, 298-305 (1999).
61. Darland, D.C. & D'Amore, P.A. TGF beta is required for the formation of capillary-like structures in three-dimensional cocultures of 10T1/2 and endothelial cells. *Angiogenesis* **4**, 11-20 (2001).
62. Corti, S. et al. Chemotactic factors enhance myogenic cell migration across an endothelial monolayer. *Exp Cell Res* **268**, 36-44 (2001).
63. L'Heureux, N., Paquet, S., Labbe, R., Germain, L. & Auger, F.A. A completely biological tissue-engineered human blood vessel. *Faseb J* **12**, 47-56 (1998).
64. Shin, H., Quinten Ruhe, P., Mikos, A.G. & Jansen, J.A. In vivo bone and soft tissue response to injectable, biodegradable oligo(poly(ethylene glycol) fumarate) hydrogels. *Biomaterials* **24**, 3201-3211 (2003).
65. Cao, Y. et al. Comparative study of the use of poly(glycolic acid), calcium alginate and pluronics in the engineering of autologous porcine cartilage. *J Biomater Sci Polym Ed* **9**, 475-487 (1998).
66. Weinberg, C.B. & Bell, E. A blood vessel model constructed from collagen and cultured vascular cells. *Science* **231**, 397-400 (1986).
67. L'Heureux, N., Germain, L., Labbe, R. & Auger, F.A. In vitro construction of a human blood vessel from cultured vascular cells: a morphologic study. *J Vasc Surg* **17**, 499-509 (1993).

68. Thomson, R.C., Yaszemski, M.J., Powers, J.M. & Mikos, A.G. Fabrication of biodegradable polymer scaffolds to engineer trabecular bone. *J Biomater Sci Polym Ed* **7**, 23-38 (1995).
69. Wong, W. & Mooney, D. in Synthetic biodegradable polymer scaffolds. (ed. M.D. Atala A, eds.) 51-84 (Birkhäuser, Boston; 1997).
70. Mikos, A.G., Sarakinos, G., Leite, S.M., Vacanti, J.P. & Langer, R. Laminated three-dimensional biodegradable foams for use in tissue engineering. *Biomaterials* **14**, 323-330 (1993).
71. Kim, B.S. & Mooney, D.J. Engineering smooth muscle tissue with a predefined structure. *J Biomed Mater Res* **41**, 322-332 (1998).
72. Peter, S.J., Miller, M.J., Yasko, A.W., Yaszemski, M.J. & Mikos, A.G. Polymer concepts in tissue engineering. *J Biomed Mater Res* **43**, 422-427 (1998).
73. Niklason, L.E. & Langer, R.S. Advances in tissue engineering of blood vessels and other tissues. *Transpl Immunol* **5**, 303-306 (1997).
74. Mooney, D.J. et al. Stabilized polyglycolic acid fibre-based tubes for tissue engineering. *Biomaterials* **17**, 115-124 (1996).
75. Kim, B.S. & Mooney, D.J. Scaffolds for engineering smooth muscle under cyclic mechanical strain conditions. *J Biomech Eng* **122**, 210-215 (2000).
76. Nikolovski, J. & Mooney, D.J. Smooth muscle cell adhesion to tissue engineering scaffolds. *Biomaterials* **21**, 2025-2032 (2000).
77. Mann, B.K., Tsai, A.T., Scott-Burden, T. & West, J.L. Modification of surfaces with cell adhesion peptides alters extracellular matrix deposition. *Biomaterials* **20**, 2281-2286 (1999).

78. Gao, J., Niklason, L. & Langer, R. Surface hydrolysis of poly(glycolic acid) meshes increases the seeding density of vascular smooth muscle cells. *J Biomed Mater Res* **42**, 417-424 (1998).
79. Mooney, D.J., Baldwin, D.F., Suh, N.P., Vacanti, J.P. & Langer, R. Novel approach to fabricate porous sponges of poly(D,L-lactic-co-glycolic acid) without the use of organic solvents. *Biomaterials* **17**, 1417-1422 (1996).
80. Richardson, T.P., Peters, M.C., Ennett, A.B. & Mooney, D.J. Polymeric system for dual growth factor delivery. *Nat Biotechnol* **19**, 1029-1034 (2001).
81. Gombotz, W.R., Wang, G.H., Horbett, T.A. & Hoffman, A.S. Protein adsorption to poly(ethylene oxide) surfaces. *J Biomed Mater Res* **25**, 1547-1562 (1991).
82. Mann, B.K. & West, J.L. Cell adhesion peptides alter smooth muscle cell adhesion, proliferation, migration, and matrix protein synthesis on modified surfaces and in polymer scaffolds. *J Biomed Mater Res* **60**, 86-93 (2002).
83. Tulis, D.A. et al. YC-1-mediated vascular protection through inhibition of smooth muscle cell proliferation and platelet function. *Biochem Biophys Res Commun* **291**, 1014-1021 (2002).
84. Gobin, A.S. & West, J.L. Cell migration through defined, synthetic ECM analogs. *Faseb J* **16**, 751-753 (2002).
85. Mann, B.K., Schmedlen, R.H. & West, J.L. Tethered-TGF-beta increases extracellular matrix production of vascular smooth muscle cells. *Biomaterials* **22**, 439-444 (2001).
86. Drury, J.L. & Mooney, D.J. Hydrogels for tissue engineering: scaffold design variables and applications. *Biomaterials* **24**, 4337-4351 (2003).

87. Guan, J., Sacks, M.S., Beckman, E.J. & Wagner, W.R. Synthesis, characterization, and cytocompatibility of elastomeric, biodegradable poly(ester-urethane)ureas based on poly(caprolactone) and putrescine. *J Biomed Mater Res* **61**, 493-503 (2002).
88. Lee, S.H. et al. Elastic biodegradable poly(glycolide-co-caprolactone) scaffold for tissue engineering. *J Biomed Mater Res* **66A**, 29-37 (2003).
89. Fromstein, J.D. & Woodhouse, K.A. Elastomeric biodegradable polyurethane blends for soft tissue applications. *J Biomater Sci Polym Ed* **13**, 391-406 (2002).
90. Wang, Y., Ameer, G.A., Sheppard, B.J. & Langer, R. A tough biodegradable elastomer. *Nat Biotechnol* **20**, 602-606 (2002).
91. Owens, G.K. Role of mechanical strain in regulation of differentiation of vascular smooth muscle cells. *Circ Res* **79**, 1054-1055 (1996).
92. Stegemann, J.P. & Nerem, R.M. Phenotype modulation in vascular tissue engineering using biochemical and mechanical stimulation. *Ann Biomed Eng* **31**, 391-402 (2003).
93. Kim, B.S., Nikolovski, J., Bonadio, J. & Mooney, D.J. Cyclic mechanical strain regulates the development of engineered smooth muscle tissue. *Nat Biotechnol* **17**, 979-983 (1999).
94. Nakanishi, Y. et al. Tissue-engineered urinary bladder wall using PLGA mesh-collagen hybrid scaffolds: a comparison study of collagen sponge and gel as a scaffold. *J Pediatr Surg* **38**, 1781-1784 (2003).

95. Pariente, J.L., Kim, B.S. & Atala, A. In vitro biocompatibility evaluation of naturally derived and synthetic biomaterials using normal human bladder smooth muscle cells. *J Urol* **167**, 1867-1871 (2002).
96. Alberts, B. Molecular biology of the cell. (Garland Science, New York; 2002).
97. Cavallaro, J.F., Kemp, P.D. & Kraus, K.H. Collagen Fabrics as Biomaterials. *Biotechnol Bioeng* **43**, 781-791 (1994).
98. Vaughan, M.B., Howard, E.W. & Tomasek, J.J. Transforming growth factor-beta1 promotes the morphological and functional differentiation of the myofibroblast. *Exp Cell Res* **257**, 180-189 (2000).
99. Li, S.T. Biologic Biomaterials: Tissue-Derived Biomaterials (Collagen). In: Brozino JD, editor. The Biomedical Engineering Handbook. (CRC Press, Boca Raton, FL; 1995).
100. Kropp, B.P. et al. Regenerative urinary bladder augmentation using small intestinal submucosa: urodynamic and histopathologic assessment in long-term canine bladder augmentations. *J Urol* **155**, 2098-2104 (1996).
101. Badylak, S.F., Coffey, A.C., Lantz, G.C., Tacker, W.A. & Geddes, L.A. Comparison of the resistance to infection of intestinal submucosa arterial autografts versus polytetrafluoroethylene arterial prostheses in a dog model. *J Vasc Surg* **19**, 465-472 (1994).
102. Zhang, Y. et al. Coculture of bladder urothelial and smooth muscle cells on small intestinal submucosa: potential applications for tissue engineering technology. *J Urol* **164**, 928-934; discussion 934-925 (2000).

103. Voytik-Harbin, S.L., Brightman, A.O., Kraine, M.R., Waisner, B. & Badylak, S.F. Identification of extractable growth factors from small intestinal submucosa. *J Cell Biochem* **67**, 478-491 (1997).
104. Chen, M.K. & Badylak, S.F. Small bowel tissue engineering using small intestinal submucosa as a scaffold. *J Surg Res* **99**, 352-358 (2001).
105. Wang, Z.Q., Watanabe, Y. & Toki, A. Experimental assessment of small intestinal submucosa as a small bowel graft in a rat model. *J Pediatr Surg* **38**, 1596-1601 (2003).
106. Yoo, J.J., Meng, J., Oberpenning, F. & Atala, A. Bladder augmentation using allogenic bladder submucosa seeded with cells. *Urology* **51**, 221-225 (1998).
107. Huynh, T. et al. Remodeling of an acellular collagen graft into a physiologically responsive neovessel. *Nat Biotechnol* **17**, 1083-1086 (1999).
108. Badylak, S.F., Lantz, G.C., Coffey, A. & Geddes, L.A. Small intestinal submucosa as a large diameter vascular graft in the dog. *J Surg Res* **47**, 74-80 (1989).
109. Falke, G., Caffaratti, J. & Atala, A. Tissue engineering of the bladder. *World J Urol* **18**, 36-43 (2000).
110. Tu, J.V. et al. Use of cardiac procedures and outcomes in elderly patients with myocardial infarction in the United States and Canada. *N Engl J Med* **336**, 1500-1505 (1997).
111. Nishishita, T. & Lin, P.C. Angiopoietin 1, PDGF-B, and TGF-beta gene regulation in endothelial cell and smooth muscle cell interaction. *J Cell Biochem* **91**, 584-593 (2004).

112. Niklason, L.E. et al. Functional arteries grown in vitro. *Science* **284**, 489-493 (1999).
113. Seliktar, D., Black, R.A., Vito, R.P. & Nerem, R.M. Dynamic mechanical conditioning of collagen-gel blood vessel constructs induces remodeling in vitro. *Ann Biomed Eng* **28**, 351-362 (2000).
114. Seliktar, D., Nerem, R.M. & Galis, Z.S. Mechanical strain-stimulated remodeling of tissue-engineered blood vessel constructs. *Tissue Eng* **9**, 657-666 (2003).
115. Reusch, P., Wagdy, H., Reusch, R., Wilson, E. & Ives, H.E. Mechanical strain increases smooth muscle and decreases nonmuscle myosin expression in rat vascular smooth muscle cells. *Circ Res* **79**, 1046-1053 (1996).
116. Chien, S., Li, S. & Shyy, Y.J. Effects of mechanical forces on signal transduction and gene expression in endothelial cells. *Hypertension* **31**, 162-169 (1998).
117. Assoian, R.K. & Schwartz, M.A. Coordinate signaling by integrins and receptor tyrosine kinases in the regulation of G1 phase cell-cycle progression. *Curr Opin Genet Dev* **11**, 48-53 (2001).
118. Yano, Y., Geibel, J. & Sumpio, B.E. Cyclic strain induces reorganization of integrin alpha 5 beta 1 and alpha 2 beta 1 in human umbilical vein endothelial cells. *J Cell Biochem* **64**, 505-513 (1997).
119. Frangos, S.G. et al. The integrin-mediated cyclic strain-induced signaling pathway in vascular endothelial cells. *Endothelium* **8**, 1-10 (2001).
120. Kornberg, L.J., Earp, H.S., Turner, C.E., Prockop, C. & Juliano, R.L. Signal transduction by integrins: increased protein tyrosine phosphorylation caused by clustering of beta 1 integrins. *Proc Natl Acad Sci U S A* **88**, 8392-8396 (1991).

121. Lipfert, L. et al. Integrin-dependent phosphorylation and activation of the protein tyrosine kinase pp125FAK in platelets. *J Cell Biol* **119**, 905-912 (1992).
122. Chen, K.D. et al. Mechanotransduction in response to shear stress. Roles of receptor tyrosine kinases, integrins, and Shc. *J Biol Chem* **274**, 18393-18400 (1999).
123. Wang, Y. et al. Interplay between integrins and FLK-1 in shear stress-induced signaling. *Am J Physiol Cell Physiol* **283**, C1540-1547 (2002).
124. Giancotti, F.G. & Ruoslahti, E. Integrin signaling. *Science* **285**, 1028-1032 (1999).
125. Cunningham, J.J., Linderman, J.J. & Mooney, D.J. Externally applied cyclic strain regulates localization of focal contact components in cultured smooth muscle cells. *Ann Biomed Eng* **30**, 927-935 (2002).
126. Tzima, E. et al. A mechanosensory complex that mediates the endothelial cell response to fluid shear stress. *Nature* **437**, 426-431 (2005).
127. Newman, P.J. & Newman, D.K. Signal transduction pathways mediated by PECAM-1: new roles for an old molecule in platelet and vascular cell biology. *Arterioscler Thromb Vasc Biol* **23**, 953-964 (2003).
128. Cheng, J.J., Wung, B.S., Chao, Y.J. & Wang, D.L. Cyclic strain enhances adhesion of monocytes to endothelial cells by increasing intercellular adhesion molecule-1 expression. *Hypertension* **28**, 386-391 (1996).
129. Nagel, T., Resnick, N., Atkinson, W.J., Dewey, C.F., Jr. & Gimbrone, M.A., Jr. Shear stress selectively upregulates intercellular adhesion molecule-1 expression in cultured human vascular endothelial cells. *J Clin Invest* **94**, 885-891 (1994).

130. Tsuboi, H., Ando, J., Korenaga, R., Takada, Y. & Kamiya, A. Flow stimulates ICAM-1 expression time and shear stress dependently in cultured human endothelial cells. *Biochem Biophys Res Commun* **206**, 988-996 (1995).
131. Wang, Y. et al. Shear stress and VEGF activate IKK via the Flk-1/Cbl/Akt signaling pathway. *Am J Physiol Heart Circ Physiol* **286**, H685-692 (2004).
132. Hu, Y., Bock, G., Wick, G. & Xu, Q. Activation of PDGF receptor alpha in vascular smooth muscle cells by mechanical stress. *Faseb J* **12**, 1135-1142 (1998).
133. Ma, Y.H., Ling, S. & Ives, H.E. Mechanical strain increases PDGF-B and PDGF beta receptor expression in vascular smooth muscle cells. *Biochem Biophys Res Commun* **265**, 606-610 (1999).
134. Lee, H.J. & Koh, G.Y. Shear stress activates Tie2 receptor tyrosine kinase in human endothelial cells. *Biochem Biophys Res Commun* **304**, 399-404 (2003).
135. Ikeda, M., Kito, H. & Sumpio, B.E. Phosphatidylinositol-3 kinase dependent MAP kinase activation via p21ras in endothelial cells exposed to cyclic strain. *Biochem Biophys Res Commun* **257**, 668-671 (1999).
136. Chen, A.H. et al. Cyclic strain activates the pro-survival Akt protein kinase in bovine aortic smooth muscle cells. *Surgery* **130**, 378-381 (2001).
137. Go, Y.M. et al. Phosphatidylinositol 3-kinase gamma mediates shear stress-dependent activation of JNK in endothelial cells. *Am J Physiol* **275**, H1898-1904 (1998).
138. Downward, J. Mechanisms and consequences of activation of protein kinase B/Akt. *Curr Opin Cell Biol* **10**, 262-267 (1998).

139. Coffey, P.J., Jin, J. & Woodgett, J.R. Protein kinase B (c-Akt): a multifunctional mediator of phosphatidylinositol 3-kinase activation. *Biochem J* **335** (Pt 1), 1-13 (1998).
140. Li, S. et al. Distinct roles for the small GTPases Cdc42 and Rho in endothelial responses to shear stress. *J Clin Invest* **103**, 1141-1150 (1999).
141. Tzima, E., del Pozo, M.A., Shattil, S.J., Chien, S. & Schwartz, M.A. Activation of integrins in endothelial cells by fluid shear stress mediates Rho-dependent cytoskeletal alignment. *Embo J* **20**, 4639-4647 (2001).
142. Van Aelst, L. & D'Souza-Schorey, C. Rho GTPases and signaling networks. *Genes Dev* **11**, 2295-2322 (1997).
143. Ikeda, M., Takei, T., Mills, I., Kito, H. & Sumpio, B.E. Extracellular signal-regulated kinases 1 and 2 activation in endothelial cells exposed to cyclic strain. *Am J Physiol* **276**, H614-622 (1999).
144. Kito, H. et al. Role of mitogen-activated protein kinases in pulmonary endothelial cells exposed to cyclic strain. *J Appl Physiol* **89**, 2391-2400 (2000).
145. Wung, B.S., Cheng, J.J., Chao, Y.J., Hsieh, H.J. & Wang, D.L. Modulation of Ras/Raf/extracellular signal-regulated kinase pathway by reactive oxygen species is involved in cyclic strain-induced early growth response-1 gene expression in endothelial cells. *Circ Res* **84**, 804-812 (1999).
146. Azuma, N. et al. Endothelial cell response to different mechanical forces. *J Vasc Surg* **32**, 789-794 (2000).
147. Reusch, H.P., Chan, G., Ives, H.E. & Nemenoff, R.A. Activation of JNK/SAPK and ERK by mechanical strain in vascular smooth muscle cells depends on

- extracellular matrix composition. *Biochem Biophys Res Commun* **237**, 239-244 (1997).
148. Aberts, B., Johnson, A., Lewis, J., Raff, M., Robers, K., Walter, P. Molecular Biology of the Cell, Edn. 4th. (Garland Science, New York, NY; 2002).
149. Rosales, O.R. & Sumpio, B.E. Protein kinase C is a mediator of the adaptation of vascular endothelial cells to cyclic strain in vitro. *Surgery* **112**, 459-466 (1992).
150. Rosales, O.R. & Sumpio, B.E. Changes in cyclic strain increase inositol trisphosphate and diacylglycerol in endothelial cells. *Am J Physiol* **262**, C956-962 (1992).
151. Cheng, J.J., Chao, Y.J. & Wang, D.L. Cyclic strain activates redox-sensitive proline-rich tyrosine kinase 2 (PYK2) in endothelial cells. *J Biol Chem* **277**, 48152-48157 (2002).
152. Morrow, D., Cullen, J.P., Cahill, P.A. & Redmond, E.M. Cyclic strain regulates the Notch/CBF-1 signaling pathway in endothelial cells: role in angiogenic activity. *Arterioscler Thromb Vasc Biol* **27**, 1289-1296 (2007).
153. Matsumoto, T. et al. Mechanical Strain Regulates Endothelial Cell Patterning in Vitro. *Tissue Eng* (2006).
154. Vandeburgh, H.H. & Karlisch, P. Longitudinal growth of skeletal myotubes in vitro in a new horizontal mechanical cell stimulator. *In Vitro Cell Dev Biol* **25**, 607-616 (1989).
155. Murray, D.W. & Rushton, N. The effect of strain on bone cell prostaglandin E2 release: a new experimental method. *Calcif Tissue Int* **47**, 35-39 (1990).

156. Neidlinger-Wilke, C., Wilke, H.J. & Claes, L. Cyclic stretching of human osteoblasts affects proliferation and metabolism: a new experimental method and its application. *J Orthop Res* **12**, 70-78 (1994).
157. Decker, M.L., Janes, D.M., Barclay, M.M., Harger, L. & Decker, R.S. Regulation of adult cardiocyte growth: effects of active and passive mechanical loading. *Am J Physiol* **272**, H2902-2918 (1997).
158. Jones, D.B., Nolte, H., Scholubbers, J.G., Turner, E. & Veltel, D. Biochemical signal transduction of mechanical strain in osteoblast-like cells. *Biomaterials* **12**, 101-110 (1991).
159. Carano, A. & Siciliani, G. Effects of continuous and intermittent forces on human fibroblasts in vitro. *Eur J Orthod* **18**, 19-26 (1996).
160. Xu, J., Liu, M., Liu, J., Caniggia, I. & Post, M. Mechanical strain induces constitutive and regulated secretion of glycosaminoglycans and proteoglycans in fetal lung cells. *J Cell Sci* **109** (Pt 6), 1605-1613 (1996).
161. Lanyon, L.E. & Rubin, C.T. Static vs dynamic loads as an influence on bone remodelling. *J Biomech* **17**, 897-905 (1984).
162. Carter, D.R., Orr, T.E., Fyhrie, D.P. & Schurman, D.J. Influences of mechanical stress on prenatal and postnatal skeletal development. *Clin Orthop Relat Res*, 237-250 (1987).
163. O'Connor, J.A., Lanyon, L.E. & MacFie, H. The influence of strain rate on adaptive bone remodelling. *J Biomech* **15**, 767-781 (1982).
164. Rubin, C.T. & Lanyon, L.E. Regulation of bone mass by mechanical strain magnitude. *Calcif Tissue Int* **37**, 411-417 (1985).

165. Putnam, A.J., Schultz, K. & Mooney, D.J. Control of microtubule assembly by extracellular matrix and externally applied strain. *Am J Physiol Cell Physiol* **280**, C556-564 (2001).
166. Simmons, C.A. et al. Cyclic strain enhances matrix mineralization by adult human mesenchymal stem cells via the extracellular signal-regulated kinase (ERK1/2) signaling pathway. *J Biomech* **36**, 1087-1096 (2003).
167. Masuda, M., Osawa, M., Shigematsu, H., Harada, N. & Fujiwara, K. Platelet endothelial cell adhesion molecule-1 is a major SH-PTP2 binding protein in vascular endothelial cells. *FEBS Lett* **408**, 331-336 (1997).
168. Jain, R.K. & Booth, M.F. What brings pericytes to tumor vessels? *J Clin Invest* **112**, 1134-1136 (2003).
169. Lindahl, P. et al. Paracrine PDGF-B/PDGF-Rbeta signaling controls mesangial cell development in kidney glomeruli. *Development* **125**, 3313-3322 (1998).
170. Scharpfenecker, M., Fiedler, U., Reiss, Y. & Augustin, H.G. The Tie-2 ligand angiopoietin-2 destabilizes quiescent endothelium through an internal autocrine loop mechanism. *J Cell Sci* **118**, 771-780 (2005).
171. Hennessy, B.T. & Mills, G.B. Ovarian cancer: homeobox genes, autocrine/paracrine growth, and kinase signaling. *Int J Biochem Cell Biol* **38**, 1450-1456 (2006).
172. Adam, R.M. et al. Signaling through PI3K/Akt mediates stretch and PDGF-BB-dependent DNA synthesis in bladder smooth muscle cells. *J Urol* **169**, 2388-2393 (2003).

173. Hellstrom, M., Kalen, M., Lindahl, P., Abramsson, A. & Betsholtz, C. Role of PDGF-B and PDGFR-beta in recruitment of vascular smooth muscle cells and pericytes during embryonic blood vessel formation in the mouse. *Development* **126**, 3047-3055 (1999).
174. Stringa, E., Knauper, V., Murphy, G. & Gavrilovic, J. Collagen degradation and platelet-derived growth factor stimulate the migration of vascular smooth muscle cells. *J Cell Sci* **113** (Pt 11), 2055-2064 (2000).
175. Wrenn, R.W., Raeuber, C.L., Herman, L.E., Walton, W.J. & Rosenquist, T.H. Transforming growth factor-beta: signal transduction via protein kinase C in cultured embryonic vascular smooth muscle cells. *In Vitro Cell Dev Biol* **29A**, 73-78 (1993).
176. Desmouliere, A., Geinoz, A., Gabbiani, F. & Gabbiani, G. Transforming growth factor-beta 1 induces alpha-smooth muscle actin expression in granulation tissue myofibroblasts and in quiescent and growing cultured fibroblasts. *J Cell Biol* **122**, 103-111 (1993).
177. Hirschi, K.K. et al. Transforming growth factor-beta induction of smooth muscle cell phenotype requires transcriptional and post-transcriptional control of serum response factor. *J Biol Chem* **277**, 6287-6295 (2002).
178. Cutroneo, K.R. Gene therapy for tissue regeneration. *J Cell Biochem* **88**, 418-425 (2003).
179. Du, L. et al. Signaling molecules in nonfamilial pulmonary hypertension. *N Engl J Med* **348**, 500-509 (2003).

180. Holland, T.A., Tessmar, J.K., Tabata, Y. & Mikos, A.G. Transforming growth factor-beta1 release from oligo(poly(ethylene glycol) fumarate) hydrogels in conditions that model the cartilage wound healing environment. *J Control Release* **94**, 101-114 (2004).

CHAPTER 3

DESIGN AND CONSTRUCTION OF A COMPUTER CONTROLLED STRAIN MECHANICS ASSESSING RESEARCH TOOL (SMART)

3.1 Introduction

In order to address the hypothesis that cyclic strain can play a role in regulating vascular cells during angiogenic activation, I needed to develop a strain device that allowed me to systematically assess strain effects at high precision and in a higher throughput method. This new device was designed to deliver uniaxial tensile strain, as it is most physiologically relevant to the forces experienced by vascular cells that comprise the walls of blood vessels during cyclic distension caused by blood flow.

Cells throughout our body are exposed to various forms of mechanical stimuli. Studies have reported that mechanical stretch signals play a role in maintaining homeostasis in vascular tissues^{1,2}. Long bones of the musculoskeletal system undergo compressive loading from vertical impact, as opposed to the tensile forces translated through skeletal muscles to which they are connected³. The respiratory system, lined by epithelial cells⁴, experiences tensile forces purely through the mechanics of breathing, similar to gastrointestinal tissues which expand cyclically due to peristaltic movement. Healthy

tissues under normal function are capable to withstand persistent loads, but the question remains whether mechanical signals can alone regulate cell processes. The desire to replicate these signals in order to understand the mechanisms that underlie cellular responses to strain has led to the development of numerous mechanical strain devices used for *in vitro* studies.

To date, the majority of *in vitro* mechanostimulatory devices used to examine effects of mechanical cyclic strain on vascular cells mainly focus on the use of uniaxial and biaxial tensile applications. The fundamental difference between uniaxial and biaxial tensile strain resides in the boundary conditions that characterize each strain regime. Several types of biaxial strain devices have been developed, and the methods of force application range from use of a dynamic indenter⁵ to using vacuum pressures (both positive⁶ or negative^{7, 8}) to stretch the bottom surface of the elastic substrate to which the cells are cultured. One main advantage of using biaxial strain devices is the availability of commercial devices (Flexercell machine⁹) and associated consumables for experimental operations. However, most biaxial strain devices present non homogeneous strain fields within each culture surface⁸, where a radial strain gradient is introduced from the source of strain. However, a region of equi-biaxial stretch exists in the center^{10, 11} of each well. A number of custom uniaxial strain devices have been developed to examine cells that are normally exposed to lateral stresses¹²⁻¹⁶. However, a limitation of most uniaxial strain devices is the capability to assess only a the limited number of samples^{11, 13-16} at one time. Most devices also lack the platform to perform consistent clamping and loading of

samples, which can significantly alter substrate strain^{13, 14, 17} and ultimately, introduce large variations between experiments.

Presented here are the design criteria for several devices: a novel large scale uniaxial **Strain Mechanics Assessing Research Tool (S.M.A.R.T)**, a mini S.M.A.R.T. for microscope image documentation, and custom elastomeric culture plates designed specifically for these strain devices. The design criteria of each are listed as follows:

Design Criteria of large scale S.M.A.R.T.

- simultaneously strain 48 wells (12 conditions, n = 4)
- programmable strain regimen via a computer interface (amplitude, frequency, and or alternations with time)
- precision application of repeatable cyclic strain (repeatability and error ~1um)
- each condition capable to be individually loaded and removed
- strains 2D and 3D materials
- entire device able to be dismantled and parts autoclavable
- device construction material: strong, light, does not pit, wear.

Design Criteria of mini S.M.A.R.T.

- Easily loads device clamps from large scale S.M.A.R.T.
- Fits onto inverted microscope (Olympus IX81) stage for image documentation and live cell imaging.

Design Criteria of Device Clamps

- Alignment marker for consistent clamping locale to PDMS plates.
- Allows individual culture of each condition and ease of loading onto device.

Design Criteria of Elastomeric culture wells (PDMS)

- Surface area for culture adaptable to various sizes: 1cm², 5cm², 35cm²
- 2D plates : homogeneous strain and adaptable to create strain gradients
- 2D plates: 4 wells per plate (for statistical analysis)
- 2D plates : mold contains alignment holes for consistent clamping
- 2D plates : walls reinforced at based to secure attachment
- 3D plates: homogeneous strain and adaptable to create strain gradients
- 3D plates: adaptable for microfluidic delivery of drugs

3.2 Materials and Methods

Design of S.M.A.R.T

The design chart of operating the large scale S.M.A.R.T. (Figure 3.1) consists of a linear motor (Newmark, Mission Viejo, CA), a NSC stepper motor controller (Newmark, Mission Viejo, CA) with an open loop feedback, a power supply, and a computer interface. The computer interfaces with the controller to communicate input values of displacement, frequency, and length of run time. The SMART apparatus consists of several main components: The linear motor, the moving stage, stationary stage, the base, and the device cover (Figure 3.2A-B).

Principle of Straining

The apparatus is designed to apply a dynamic uniaxial stretch to a maximum of 48 elastomeric wells (12 conditions) simultaneously. The principle of strain applied to each square PDMS elastomeric well, clamped by Aluminum plates to align and fit onto the

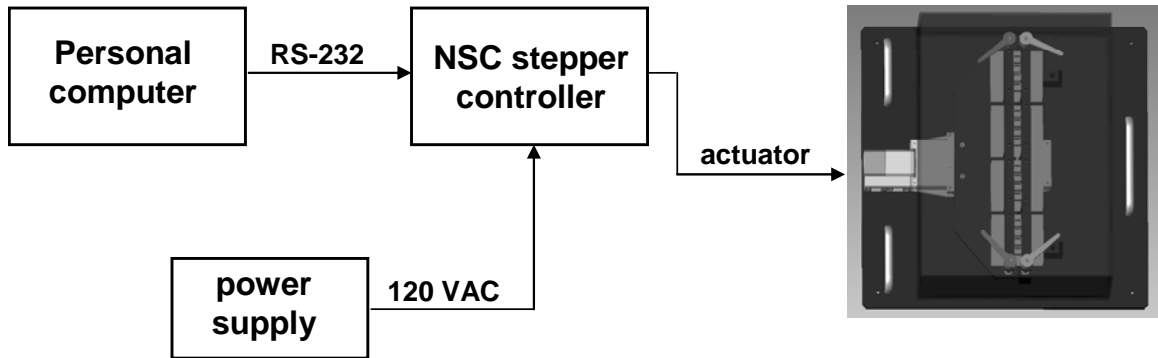


Figure 3.1: Design chart of S.M.A.R.T system

The device is regulated by a controller that is programmable using a computer interface to alter displacement, frequency, and time.

S.M.A.R.T. is based on distension that is driven by a linear motor in a uniaxial direction (Figure 3.2C).

Linear motor

Power requirement for the linear motor was assessed in order to select an appropriate linear motor. The minimum motor power required to strain the maximum load of 12 PDMS plates was determined using an Instron material tester (Instron, Norwood, MA). The force required to stretch one PDMS well to 110% was measured and scaled up (by 48 wells) to measure the minimum total force required to distend all plates by 10% strain.

Moving and Stationary stage platform and alignment bar

The moving plate (15" x 3.9") was constructed using a 0.375" thick Aluminum plate. The plate was positioned by placing the longer side perpendicular to the direction of strain in order to allow loading of numerous samples. The moving plate had 4 tapped holes in the center to allow fixture to the linear motor using screws. The edge of the plate (along 15" side) had 8 blind holes to allow insertion of 8 alignment pins. Alignment pins were inserted along the edge of both the moving plate and the stationary plate in order to precisely but quickly fasten 4 sets of PDMS clamps (2 alignment pins per each side of clamp).

The stationary plate was constructed using a 0.75" thick Aluminum plate, and stood at a height of 2.159" over the linear motor device. The stationary plate had 4 tapped holes on the side in order to fix 2 support knees, an added design to eliminate any possible

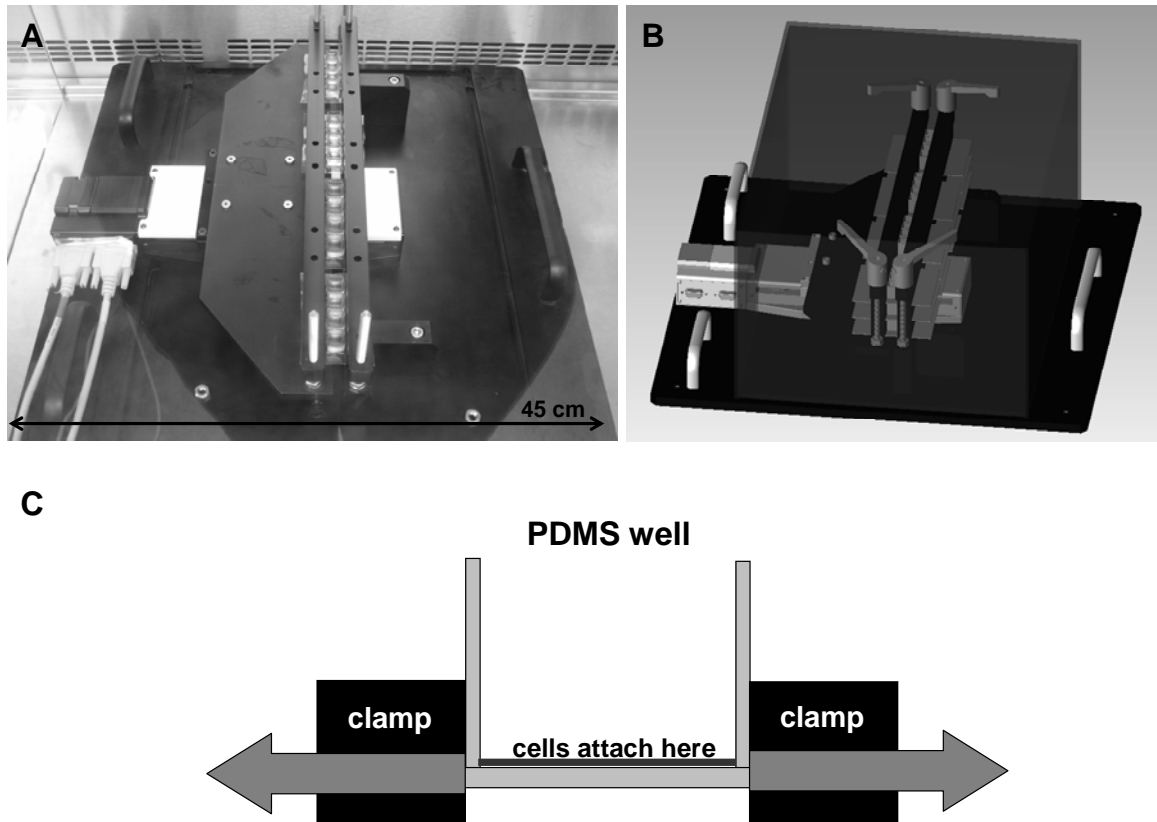


Figure 3.2A-C: Large scale S.M.A.R.T. device and principle of straining

(A) Photograph of completed S.M.A.R.T. Shown loaded are 4 sets of PDMS plates, (16 wells). (B) 3D render of AUTOCAD design of large scale S.M.A.R.T. Shown here is the device with a Lexan cover over the strain device to provide a contained sterile environment. (C) A cross sectional view of a PDMS well where device clamps are shown on the left and right immediate exterior of the PDMS well, along with the direction of uniaxial tensile strain.

torquing caused by strain forces applied on the PDMS plates that may cause arching of the standing stationary plate. Finally, the stationary plate had 8 blind holes on the top face, for the aforementioned alignment pins. Along the furthest edge of the moving and stationary plates, 2 long (4" threaded) rods protruded to fix a master alignment bar. This alignment bar was to secure all PDMS clamps maintained seated and to eliminate any torquing movements, to ultimately ensure that samples on the third level experienced equal strain as samples on the bottom, first level.

SMART base plate and Lexan cover

The base plate (18" x 18") was constructed of a 0.38" Aluminum plate, capable to withstand a minimum of 40lbs, exceeding the weight of all device components. The bottom surface of the base was tapped with 4 holes to attach leveling mounts with dampening pads onto the device which serve two purposes (1) to dampen any vibrational motion to not affect other cell cultures in the incubator and (2) to allow easy lifting of device off other metal surfaces (in incubator). The top surface of the base was tapped with 14 tapped holes (4 screws to fix the linear motor, 2 screws to fix the stationary stage platform, 2 screws to fix the support beam to the stationary stage platform, and finally 6 screws to fix three handles to lift device). A method to enclose the straining samples from the surrounding incubator environment was developed by designing a Lexan cover, machined (Altec Plastics, MA) with dimensions: (12 x 13 x 8) in³. The material, polycarbonate lexan was selected for its temperature resistance (up to T=250°F), and therefore would be autoclavable. In order to secure a location for placement of the Lexan cover, a groove was machined into the base plate to enclose cell culture samples, as well

as a portion of the linear motor. However, in order to allow gas exchange into the cell cultures (region enclosed by the lexan cover), it was necessary to develop a 2 step groove. In order to achieve this, a region at the 4 corners was machined by only 0.13” (where the lexan cover would sit within the groove, however slightly lifted), while the entire perimeter was machined to a deeper 0.25” groove (to allow gas exchange into the cell culture strain area). The entire base plate, constructed of Aluminum was anodized to avoid pitting over continuous use.

Design of mini S.M.A.R.T

The mini SMART is a small scale strain device that loads 2 PDMS plates (one for strain application and one for non strained culture) and designed to fit precisely onto an inverted microscope stage (Olympus IX81). This device was designed to supplement the large scale SMART device and serves three main purposes: (1) for quick, high resolution, image documentation of cultures removed temporarily from the large scale SMART, (2) for live cell imaging of cells under strained conditions and (3) for 2D or 3D material characterization in response to strain. The strained PDMS plate is loaded by clamping one side to a linear stage motion controller (Newport, Irvine, CA) that is driven by a digital manual actuator (Newport, Irvine, CA) (Figure 3.3A-B), that can be replaced with a motorized actuator. The static condition is loaded by screwing clamps onto a fixed overhead bar onto the microscope stage adaptor.

PDMS clamps

The clamps were composed of 2 sets of top and bottom clamps (Figure 3.4A). Each

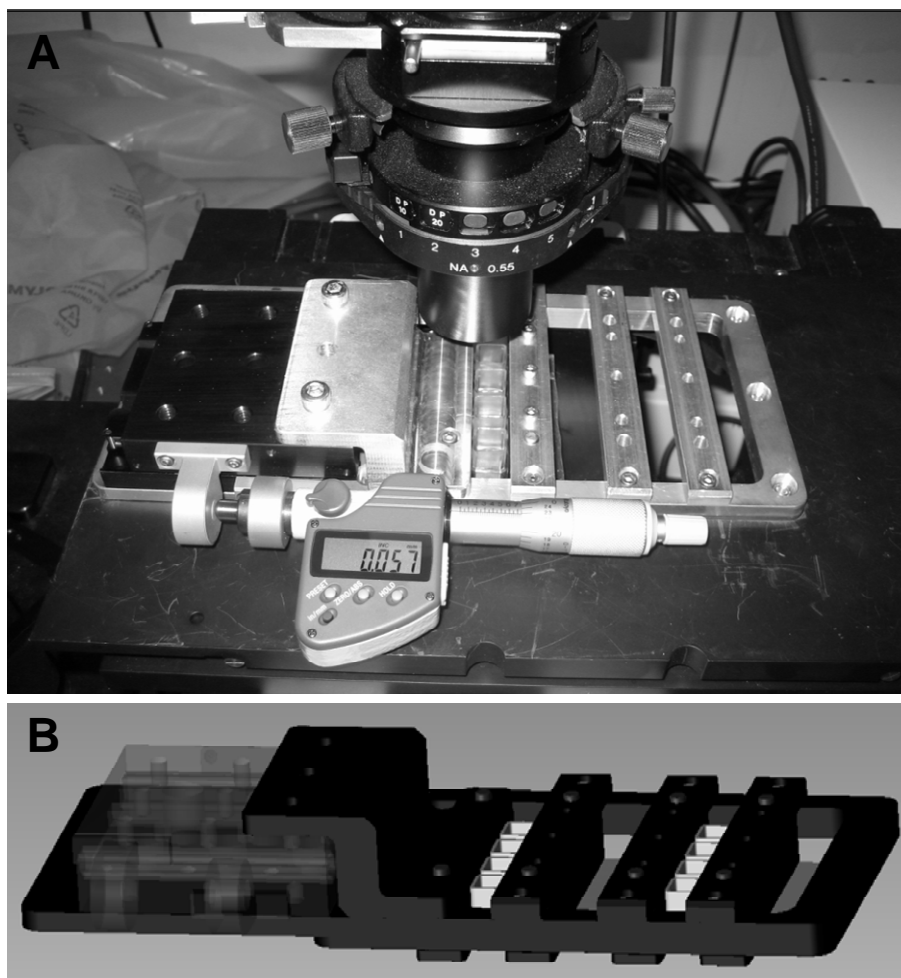


Figure 3.3A-B: Microscope adaptable mini S.M.A.R.T.

(A) Image of completed mini-SMART sitting on the microscope stage with one PDMS plate loaded onto straining arm. (B) 3D render of mini SMART AUTOCAD drawing with both PDMS plates loaded.

top clamp had 3 tapped holes (to screw and secure clamping of PDMS between top and bottom clamp). Additionally, 2 through holes (0.187") were machined in the top clamps to insert alignment pins. The bottom clamp also had 2 through holes (though slightly larger). Alignment pins served the purpose of fast and precise, loading and unloading. In addition, it allowed for precision stacking of the PDMS clamps to 3 levels.

Design of PDMS culture plates and molds

Elastomeric culture wells were developed (1) to be able to quantify protein secretion levels normalized to cell count, (2) to conserve media use, and (3) to develop a method that was more sterile and did not require regular contact with sample culture medium. The elastomeric PDMS plates were generated using Sylgard 184 (Dow Corning, Midland, MI) to form three sizes of culture wells surface areas (1cm², 5cm², and 35cm²). Culture wells of different sizes were designed in order to satisfy needs for various types in order to satisfy needs for various types of analysis (ranging from: image documentation or large cell numbers for RNA isolation). The plate design (SA = 1cm²) contained alignment markers to ensure consistent clamping from sample to sample.

Mold for PDMS culture plates

In order to create culture wells, with walls and base constructed of elastomeric PDMS material, it was necessary to design a PDMS mold to provide confined structure until the viscous unpolymerized PDMS cured into solid elastomeric wells (Figure 3.4B). The mold for 1cm² surface area well plates included 6 separate Aluminum parts. The outer mold (3.5 x 3.5 x 0.6in) was an Aluminum block with 4 square through holes machined

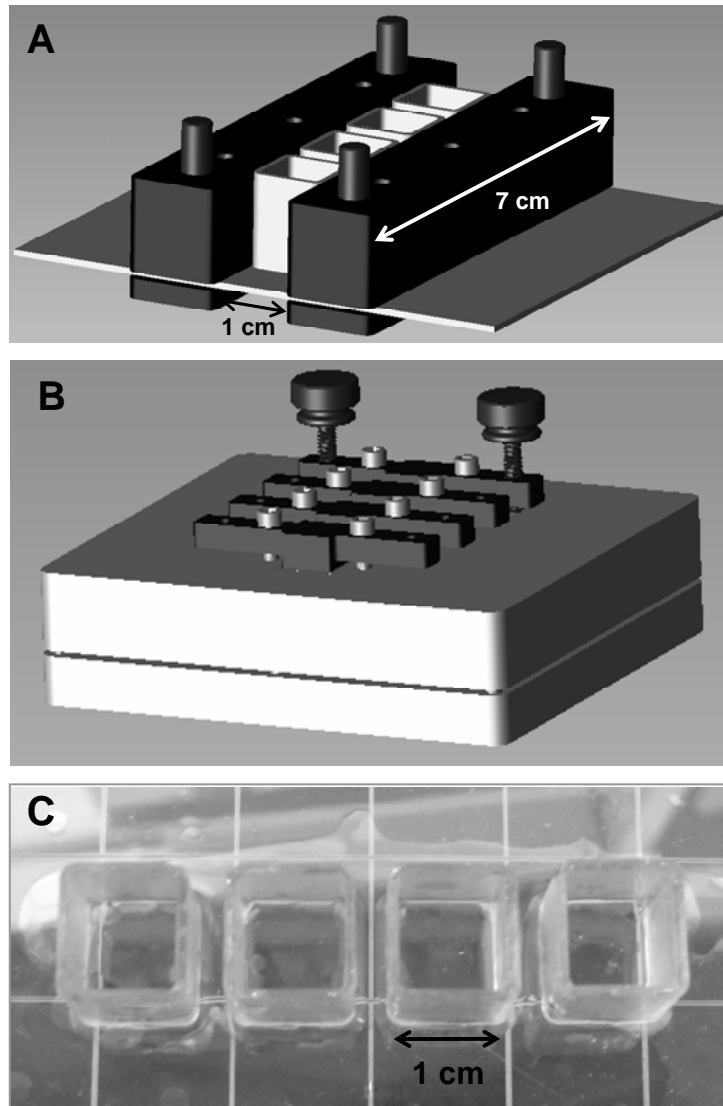


Figure 3.4: PDMS clamp unit, mold, and plate.

(A) 3D angled render of AUTOCAD drawing of PDMS plate-clamp unit. (B) PDMS plate mold. (C) Photograph of PDMS plate (4 wells, surface area/well = 1 cm^2).

in the center to provide outer shape for 4 wells. The bottom mold (mirror finished, to ensure optical clarity for image documentation) was attached using 4 screws to the outer mold to clamp a 0.02" PDMS sheet. Lastly, 4 inner mold pieces (also mirror finished) were inserted and screwed into the outer mold, to provide inner shape for the well walls. The placement of the 4 inserts onto the outer mold was designed to provide support with venting to allow flow of unpolymerized PDMS to conform to the well shape. After placing all mold components together, the unpolymerized PDMS mixture was made (at a 1:10 ratio of the Sylgard 184 mix) and pipetted into the crevice between the outer mold and 4 inserts. The entire mold was then placed into an oven set at $T=60^{\circ}\text{C}$ and cured for 2 hrs to allow time for polymerization, where after removal of mold reveals a cured PDMS culture plate (Figure 3.4C). In order to ensure consistent clamping of the PDMS plates, through holes were machined into the bottom mold to fit punches that created alignment holes in reference to wells for placement of screws when clamping.

Creating PDMS wells with surface a strain gradient

PDMS wells presenting a surface strain gradient, only under application of tensile strain, were created by using O_2 plasma to covalently bond a (width = 8mm) strip of micromachined glass ($t=1 \times w=8 \times l=7$) mm^3 to the center bottom surface of a PDMS well (Figure 3.5).

Quantification of surface strain of 2D culture

Internal 2D surface strain in PDMS wells was measured by drawing gridlines onto the culture surface of the PDMS wells and measuring the distance of displacement of

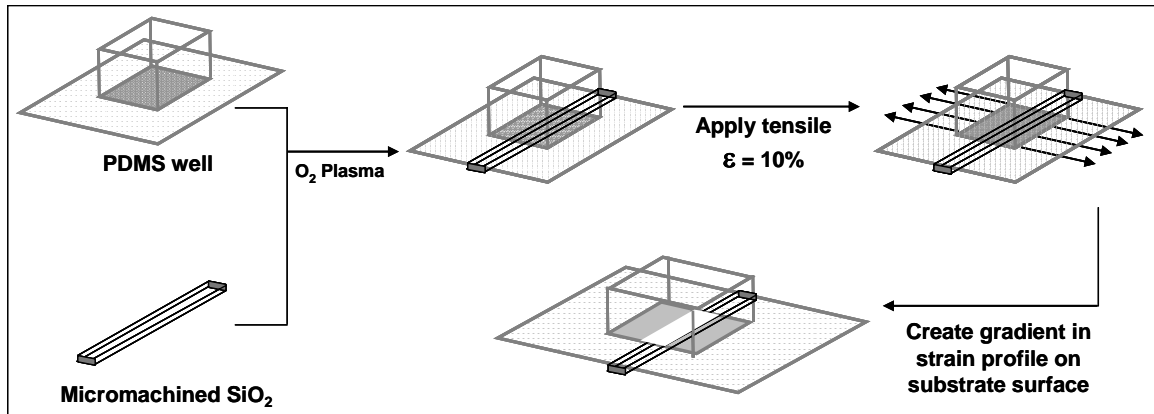


Figure 3.5: Method to create PDMS wells with strain gradient

Micromachined SiO₂ is covalently bound to the bottom surface of a PDMS well using O₂ plasma. Application of tensile strain reveals a culture surface with regions of low or no strain (region directly above micromachined SiO₂) in contrast to regions of higher strain (region away from center, near edge).

gridlines in response to applied strain. The micrometer fixed to the moving plate of the mini S.M.A.R.T device distends the well at a precise distance, and the resultant internal strain (surface displacement) was digitally measured using IPLAB 4.0, imaging software (BD Biosciences, Rockville, MD). To assess homogeneity of unaltered 2D wells, data points were sampled from different locations (n=3) on the culture surface for statistical analysis. For strain gradient measurements, internal strain was assessed at various specified locations (n=3) at each applied displacement throughout the PDMS well at each strain level.

Quantification of surface strain of 3D fibrin gels

Internal strain within 3D fibrin gels cultured in PDMS wells was characterized by measuring the distance of displacement between microcarrier beads (center to center) in response to applied displacement. A micrometer fixed to the moving plate of the mini SMART device was used to displace the material and microscopic image measurements were gathered using IPLAB 4.0 imaging software (BD Biosciences, Rockville, MD). Cytodex 3 microcarriers (GE Healthcare, Piscataway, NJ) with diameter ~200um were uniformly embedded at 600 microcarriers/mL into a fibrin gel, constituted of fibrinogen (4 mg/mL; Sigma), aprotinin (500ng/mL; Sigma), and thrombin (25 units/mL). In order to confer uniform strain throughout the gel, a thick PDMS plate (slab of PDMS ~1cm thick, with 4 wells created using 1x1cm² square molds) containing wall reinforcements was developed to deliver a flat strain profile.

3.3 Results

Measuring minimum power requirement

The minimum power requirement was examined and the force required to distend one PDMS well with walls by 110% was calculated to be 1.35N (Figure 3.6). Force required to distend PDMS with no walls was measured as a control, to validate PDMS elastic modulus. In order to determine the design rule required for the linear motor, we assessed the force needed to distend the maximum load (scaled up to 48 PDMS wells) by 110%. This calculation yielded the minimum motor power required to be 65N, substantially under the 220N load potential of the linear motor used.

Applied strain is conferred and internal 2D strain profile is homogeneous

The correlation of applied strain to resultant measured internal strain was assessed. Stretching 2D PDMS wells using mini SMART and measuring the distance of displacement between gridlines demonstrated a linear relationship between applied strain and measured internal strain (Figure 3.7). The strain field was also found to be fairly homogeneous within the culture area, as represented by the small variance within each data set.

Characterizing surface presentation of a strain gradient (2D)

To determine whether a surface strain gradient can be achieved by bonding a much stiffer (glass) material onto the bottom surface of an elastomeric material (PDMS well) under an applied strain of 10% (Figure 3.8A), the displacement of gridlines on the PDMS culture surface was measured. Applying 10% strain resulted in enhanced levels of strain at the edge of the wells, while the center of the PDMS well (where the stiff glass surface was

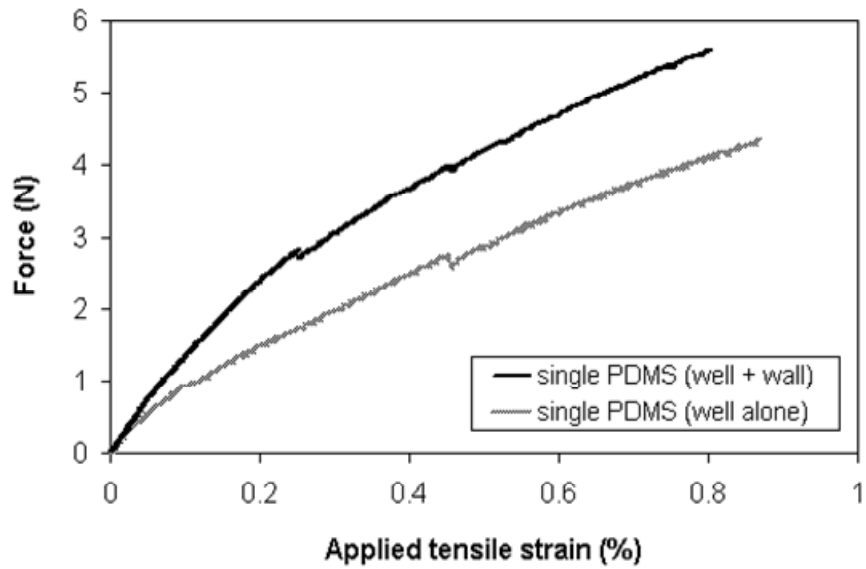


Figure 3.6: Force Profile per PDMS well

Force required to strain one PDMS well by 10% is significantly increased with PDMS well walls. Measurement of force was quantified by incrementally straining substrates at precise displacements.

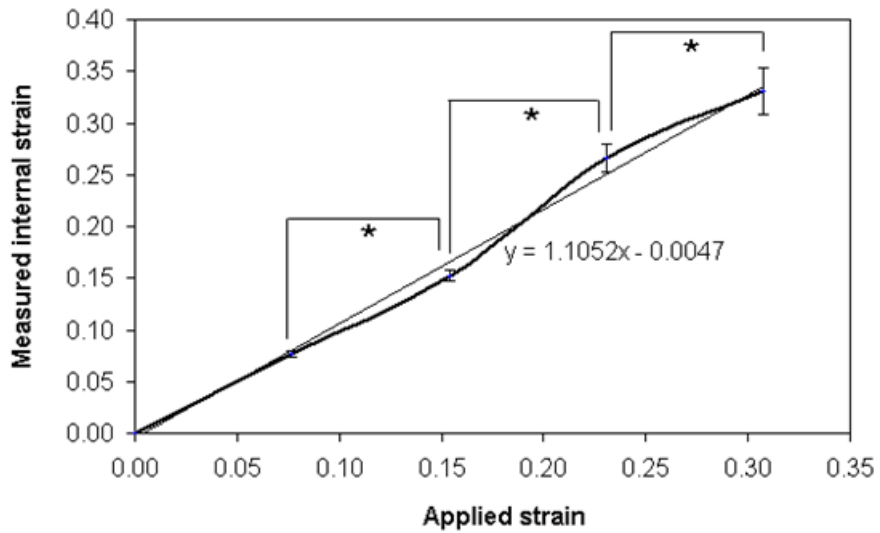


Figure 3.7: Applied strain is directly conferred in 2D.

Linear correlation between applied strain and measured surface strain within PDMS wells.

Strain field is relatively homogeneous within PDMS well, as shown by the small error

variation within each data set. (n=3)

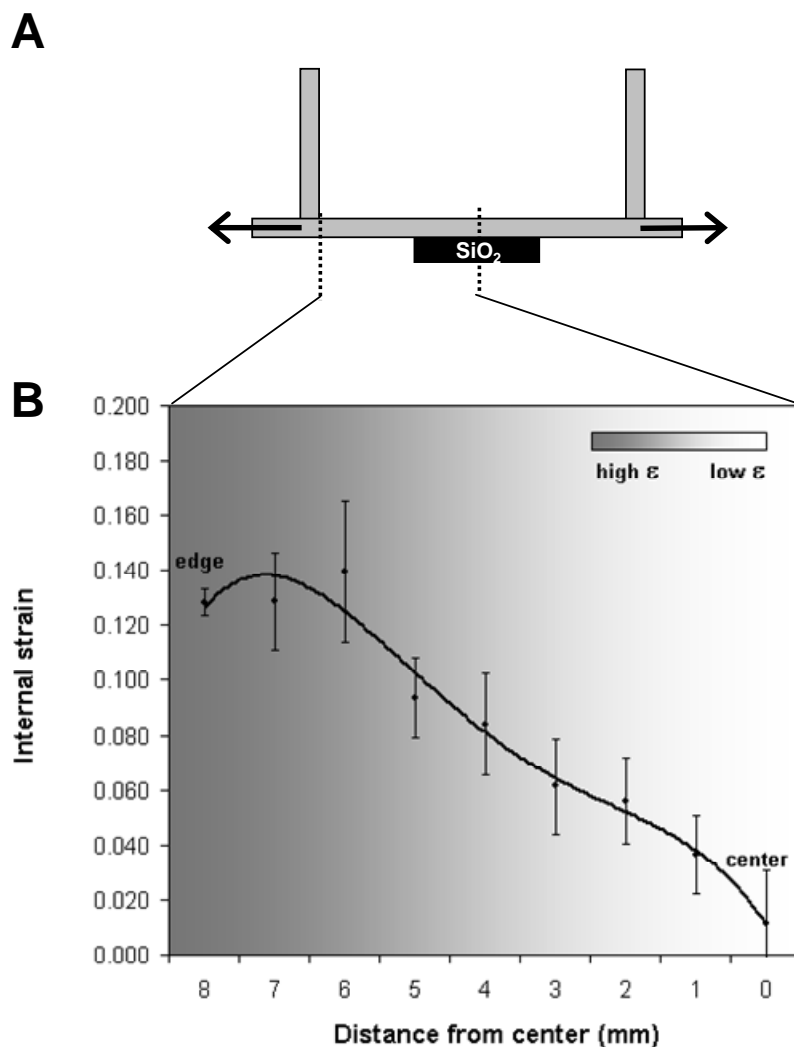


Figure 3.8: Strain gradient within PDMS well for 2D cultures

(A) A cross sectional profile of a PDMS well with a glass strip covalently bonded to the bottom surface of well creates a culture region that is less elastomeric (surface above the glass) and regions that experience high internal strain (to the right and left regions of glass strip) under application of tensile strain. (B) Internal 2D strain profile was quantified by measuring the displacement between gridlines, drawn throughout the culture surface of PDMS well, in response to applied incremental displacements using the mini S.M.A.R.T. (n=3).

bonded to the bottom side) experienced minimal strain. This gradient in strain was characterized (Figure 3.8B) within the culture surface of one PDMS well.

Internal 3D strain and integrity

The correlation of applied strain to resultant measured internal strain within 3D fibrin gels, contained within PDMS plates was examined. Microcarrier Cytodex beads embedded within fibrin gels strained in a linear pattern compared to that of applied strain (Figure 3.9A). The integrity of fibrin gels under cyclic tensile loading was measured over a duration of 5 days to examine the extent of gel degradation. Results (Figure 3.9B) indicate that only slight levels of in measured fibrin gel degradation occur at day 4 of loading.

3.4 Discussion

The design and construction of S.M.A.R.T. and mini S.M.A.R.T., and the associated components demonstrated through characterization studies that these devices can be effectively used to systematically examine cellular responses on a micron scale to cyclic uniaxial strain. In particular, these devices will be particularly useful for studies that require straining of 2D and 3D constructs an in studying migration or capillary formation processes of vascular remodeling.

Measured internal strain was directly correlated with the applied tensile strain in both 2D and 3D samples using the custom developed PDMS wells and fibrin gels in PDMS wells, respectively. The custom PDMS wells provided a homogeneous strain field and were

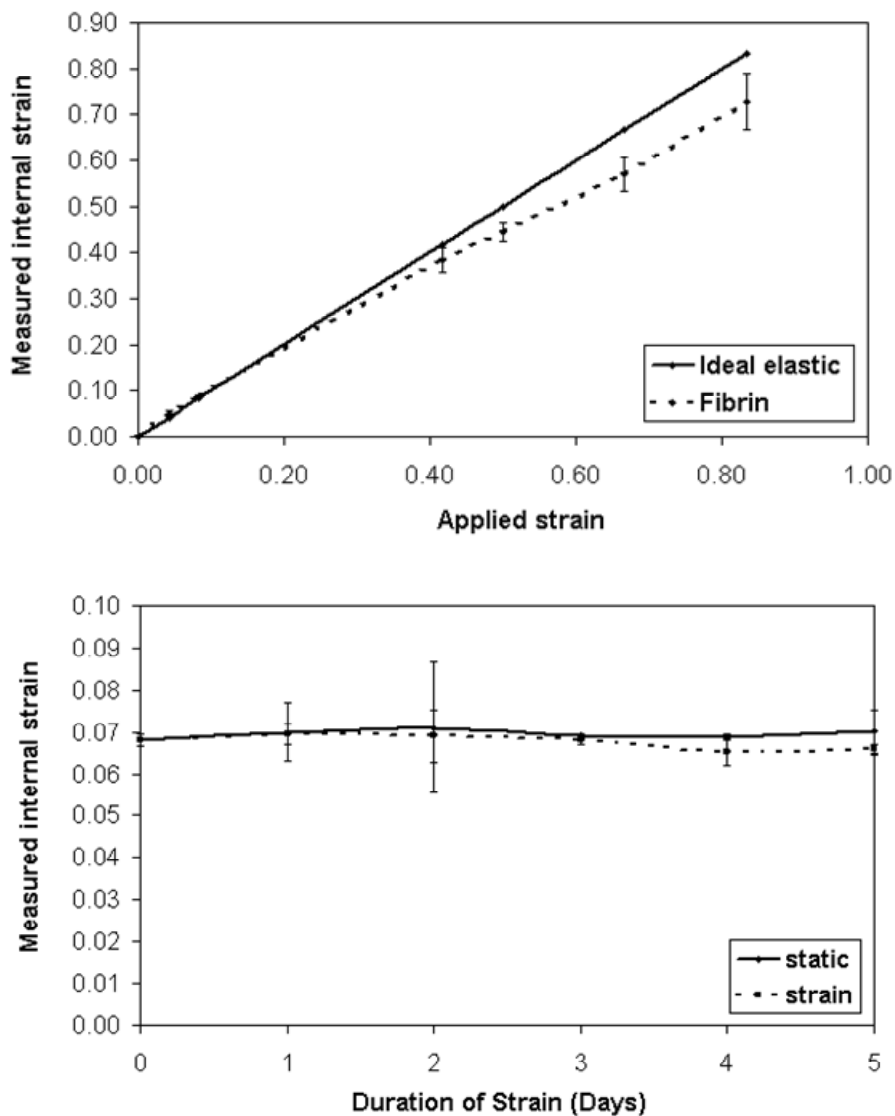


Figure 3.9: Applied strain is conferred, integrity maintained in 3D gels

(A) The homogeneity of internal strain in 3D fibrin gels was evaluated by measuring the displacement between microcarrier beads (diameter ~200um) that were embedded into the fibrin gel using the mini S.M.A.R.T. (B) Integrity of fibrin gel was determined by cyclically loading gels and measuring the displacement between beads in response to cyclic loading over a 5 day timecourse in comparison to non strained gels (n=3).

successfully adaptable to also present a gradient in surface strain. A novel technique to strain 3D gels in custom PDMS chambers with wall supports yielded a uniform strain throughout the entire sample. SMART overcomes the limitations of most designs to provide the following features: (1) it can deliver high precision consistent strain (2) all strained samples can be image documented (3) various sizes of culture wells are available to allow for various forms of analysis (4) various sizes of culture wells are available to allow for various forms of analysis. For future studies, the mini S.M.A.R.T can be used for live cells image documentation of cell response to strain and the 3D PDMS plates can be adaptable for microfluidic applications.

3.5 References

1. Smith, J.J. & Kampine, J.P. Circulatory Physiology, Edn. Third Edition. (Williams & Wilkins, Baltimore; 1990).
2. O'Rourke, M., Kelly, R. & Arolio, A. The Arterial Pulse. (Lea & Febiger, Philadelphia; 1992).
3. Biewener, A.A. Biomechanical consequences of scaling. *J Exp Biol* **208**, 1665-1676 (2005).
4. Xu, J., Liu, M., Liu, J., Caniggia, I. & Post, M. Mechanical strain induces constitutive and regulated secretion of glycosaminoglycans and proteoglycans in fetal lung cells. *J Cell Sci* **109** (Pt 6), 1605-1613 (1996).
5. Vandeburgh, H.H. A computerized mechanical cell stimulator for tissue culture: effects on skeletal muscle organogenesis. *In Vitro Cell Dev Biol* **24**, 609-619 (1988).
6. Winston, F.K., Macarak, E.J., Gorfien, S.F. & Thibault, L.E. A system to reproduce and quantify the biomechanical environment of the cell. *J Appl Physiol* **67**, 397-405 (1989).
7. Banes, A.J., Gilbert, J., Taylor, D. & Monbureau, O. A new vacuum-operated stress-providing instrument that applies static or variable duration cyclic tension or compression to cells in vitro. *J Cell Sci* **75**, 35-42 (1985).
8. Gilbert, J.A., Weinhold, P.S., Banes, A.J., Link, G.W. & Jones, G.L. Strain profiles for circular cell culture plates containing flexible surfaces employed to mechanically deform cells in vitro. *J Biomech* **27**, 1169-1177 (1994).
9. <http://www.flexcellint.com/index.html>.

10. Sotoudeh, M., Jalali, S., Usami, S., Shyy, J.Y. & Chien, S. A strain device imposing dynamic and uniform equi-biaxial strain to cultured cells. *Ann Biomed Eng* **26**, 181-189 (1998).
11. Waters, C.M. et al. A system to impose prescribed homogenous strains on cultured cells. *J Appl Physiol* **91**, 1600-1610 (2001).
12. Vandeburgh, H.H. & Karlisch, P. Longitudinal growth of skeletal myotubes in vitro in a new horizontal mechanical cell stimulator. *In Vitro Cell Dev Biol* **25**, 607-616 (1989).
13. Murray, D.W. & Rushton, N. The effect of strain on bone cell prostaglandin E2 release: a new experimental method. *Calcif Tissue Int* **47**, 35-39 (1990).
14. Neidlinger-Wilke, C., Wilke, H.J. & Claes, L. Cyclic stretching of human osteoblasts affects proliferation and metabolism: a new experimental method and its application. *J Orthop Res* **12**, 70-78 (1994).
15. Pfister, B.J., Weihs, T.P., Betenbaugh, M. & Bao, G. An in vitro uniaxial stretch model for axonal injury. *Ann Biomed Eng* **31**, 589-598 (2003).
16. Carano, A. & Siciliani, G. Effects of continuous and intermittent forces on human fibroblasts in vitro. *Eur J Orthod* **18**, 19-26 (1996).
17. Jones, D.B., Nolte, H., Scholubbers, J.G., Turner, E. & Veltel, D. Biochemical signal transduction of mechanical strain in osteoblast-like cells. *Biomaterials* **12**, 101-110 (1991).
18. Matsumoto, T. et al. Mechanical Strain Regulates Endothelial Cell Patterning in Vitro. *Tissue Eng* (2006).

19. Decker, M.L., Janes, D.M., Barclay, M.M., Harger, L. & Decker, R.S. Regulation of adult cardiocyte growth: effects of active and passive mechanical loading. *Am J Physiol* **272**, H2902-2918 (1997).
20. Lanyon, L.E. & Rubin, C.T. Static vs dynamic loads as an influence on bone remodelling. *J Biomech* **17**, 897-905 (1984).
21. Carter, D.R., Orr, T.E., Fyhrie, D.P. & Schurman, D.J. Influences of mechanical stress on prenatal and postnatal skeletal development. *Clin Orthop Relat Res*, 237-250 (1987).
22. O'Connor, J.A., Lanyon, L.E. & MacFie, H. The influence of strain rate on adaptive bone remodelling. *J Biomech* **15**, 767-781 (1982).
23. Rubin, C.T. & Lanyon, L.E. Regulation of bone mass by mechanical strain magnitude. *Calcif Tissue Int* **37**, 411-417 (1985).
24. Kim, B.S., Nikolovski, J., Bonadio, J. & Mooney, D.J. Cyclic mechanical strain regulates the development of engineered smooth muscle tissue. *Nat Biotechnol* **17**, 979-983 (1999).
25. Kim, B.S. & Mooney, D.J. Scaffolds for engineering smooth muscle under cyclic mechanical strain conditions. *J Biomech Eng* **122**, 210-215 (2000).
26. Putnam, A.J., Schultz, K. & Mooney, D.J. Control of microtubule assembly by extracellular matrix and externally applied strain. *Am J Physiol Cell Physiol* **280**, C556-564 (2001).
27. Chien, S., Li, S. & Shyy, Y.J. Effects of mechanical forces on signal transduction and gene expression in endothelial cells. *Hypertension* **31**, 162-169 (1998).

28. Simmons, C.A. et al. Cyclic strain enhances matrix mineralization by adult human mesenchymal stem cells via the extracellular signal-regulated kinase (ERK1/2) signaling pathway. *J Biomech* **36**, 1087-1096 (2003).
29. Nikolovski, J., Kim, B.S. & Mooney, D.J. Cyclic strain inhibits switching of smooth muscle cells to an osteoblast-like phenotype. *Faseb J* **17**, 455-457 (2003).
30. Cunningham, J.J., Linderman, J.J. & Mooney, D.J. Externally applied cyclic strain regulates localization of focal contact components in cultured smooth muscle cells. *Ann Biomed Eng* **30**, 927-935 (2002).

CHAPTER 4

MECHANISM OF CYCLIC TENSILE STRAIN REGULATION OF ENDOTHELIAL CELL ANGIOGENIC PROCESSES

4.1 Introduction

Mapping the cues that regulate angiogenesis, the formation of nascent vessels, gives insight to the development of therapies for diseases such as peripheral ischemia and cancer¹. Angiogenesis requires an orchestrated presentation of cues in a specific spatial and temporal sequence². Much research in this field has focused on documenting cell response to exogenous biochemical cues, and vascular endothelial growth factor (VEGF) has been identified as one of the most potent factors during the early stages of angiogenesis, activating migration and sprout formation. Angiopoietin-1 (Ang-1), a cytokine that mediates the interactions formed between endothelial cells (ECs) and smooth muscle cells (SMCs), and Angiopoietin-2 (Ang-2), an early angiogenic factor that inversely acts to disrupt and dissociate these bonds, are both ligands expressed by vascular cells that competitively bind to the membrane receptor Tie-2. Platelet derived growth factor- $\beta\beta$ (PDGF- $\beta\beta$), a chemotactant released by ECs, is a late stage cytokine that recruits SMCs to stabilize the nascent EC sprouts. Understanding the effects of soluble factors alone however, is likely insufficient to fully understand the angiogenic

process. Blood vessels are exposed to cyclic tensile strain resulting from blood hemodynamic forces, and mechanical signals have been implicated in the modulation of EC functions. Mechanical strain has been reported to alter EC proliferation^{3,4}, alignment^{5,6}, migration^{7,8} and *in vitro* sprout formations^{9,10}, likely through activating various intracellular signaling pathways¹¹⁻¹⁷. Altogether, past works suggests that the angiogenic process is governed by an interplay between chemical and mechanical signals.

The effects of cyclic tensile strain on the secretion of angiogenic factors, and the role of these factors in strain-mediated alterations in endothelial cell phenotype were analyzed in this study. Human umbilical vein endothelial cells (HUVECs) and human aortic smooth muscle cells (HASMCs)¹⁸, were used here as model cell types representing the vascular endothelium and supportive elastic layer, respectively. Vascular cells were cultured in 2D directly on elastomeric poly(dimethylsiloxane) (PDMS) substrates and in fibrin 3D cultures, as an *in vitro* model for angiogenesis, and both types of culture were exposed to cyclic tensile strain at physiologic levels. Cyclic tensile strain was demonstrated to alter EC phenotype and Ang-2 expression, and the alterations in Ang-2 mediated changes in EC migration, and *in vitro* capillary formation.

4.2 Materials and Methods

Cell Culture

Human umbilical vein endothelial cells (HUVECs, Cambrex, Walkersville, MD) and human aortic smooth muscle cells (HASMCs, Cambrex, Walkersville, MD), were cultured at 37°C, 5% CO₂ in endothelial growth medium (EGM-2) and smooth muscle cell growth medium (SmGm-2), respectively (Cambrex, Walkersville, MD), containing

2% FBS. HUVECs were used between passages 3 and 6 and HASMCs were used between passages 3 and 7.

Quantification of migration in response to chemotactic gradients

HUVECS were seeded (1×10^4 cells/well) in basal media (EBM-2) into the upper reservoir of a transwell chemotaxis insert (Corning Life Sciences) and exposed to a range of specific growth factors concentrations presented in the lower reservoir. The bottom surface of the transwell inserts were coated with 2 μ g/mL of fibronectin (Sigma) for 24 hr and rinsed in PBS prior to use. Cells were allowed to migrate across a (3 μ m pore) polycarbonate porous membrane for 12 hr in a humidified incubator with 5% CO₂ at 37°C. After 12 hrs, all cells that did not migrate were removed by PBS rinsing and gentle cotton swabbing. Migrated cells on the bottom surface of the filter were subsequently fixed in 3.7% formaldehyde (Electron Microscopy Sciences, Hatfield, PA) for 15 minute. The membrane was then rinsed in PBS and stained using DAPI (300nM) (Molecular Probes, Eugene, OR) for 15 min, cut and placed onto a microscope slide for fluorescent microscope imaging (Olympus IX81). Cells in five random fields (at 100x magnification) were counted to quantify average number of migrated cells per insert. Data represent means of the number of migrating cells per condition normalized to the negative control (no growth factor).

Quantification of migration in response to cyclic strain

Custom polydimethylsiloxane (PDMS) elastomeric wells were prepared for cell culture by activating their surface through ultraviolet irradiation for 10 min, followed by coating

the surface with fibronectin (2ug/mL) for 2 hrs⁴⁰ to enhance cell adhesion. Cells were seeded in 2 mm diameter circular activated regions created by placing a non-coated silicon sheet, containing a 2 mm diameter hole, onto the bottom sheet prior to cell seeding, and seeding cells into the resultant well formed by the top sheet¹⁰. HUVECs were statically cultured in the 2mm diameter region for 24 hrs and subsequently, the PDMS mask was removed, and samples were loaded onto strain device and cells were allowed to migrate from the confluent circular 2 mm diameter population under cyclic strain loading for a duration of 2 days. All PDMS plates were strained using a custom built linear motor that was computer controlled. Cells were all strained at a frequency of 1Hz and at strain amplitude of 7%. Distance of cell migration in response to strain was normalized to cells experiencing no application of strain.

***In vitro* angiogenesis: sprouting assay**

HUVECs were dynamically seeded, using spinner flasks, onto cytodex-3 microcarriers (GE Healthcare, Piscataway, NJ) over a 24 hr incubation at 37°C (Figure 4.1). The cell coated microcarriers were then maintained under agitated culture to prevent aggregation between microcarriers or attachment to culture flask. Cell coated microcarriers were embedded at 600 microcarriers/mL into a fibrin gel, constituted of fibrinogen (4 mg/mL; Sigma), aprotinin (500ng/mL; Sigma), and thrombin (25 units/mL). A range of exogenous recombinant human growth factors: vascular endothelial growth factor (rhVEGF, R&D systems, Minneapolis, MN) at 1-50 ng/mL, angiopoietin-2 (rhAng-2, R&D systems, Minneapolis, MN) at 1-200 ng/mL, angiopoietin-1 (rhAng-1, R&D systems, Minneapolis, MN) at 1-50 ng/mL, rhPDGF, R&D systems, Minneapolis, MN) at

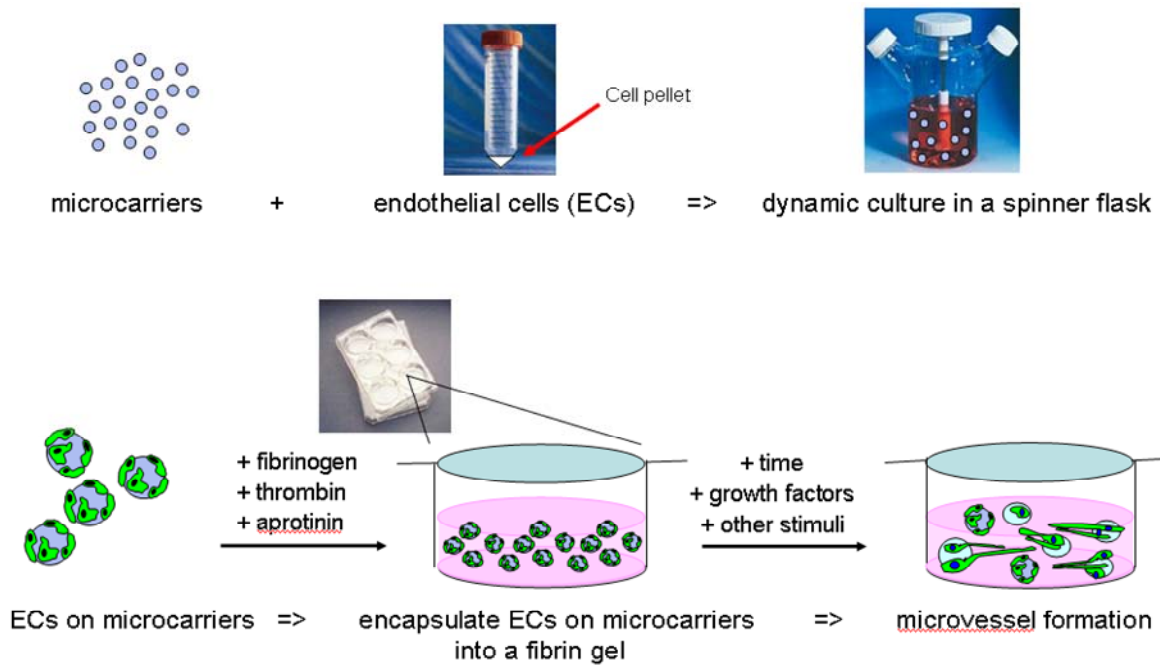


Figure 4.1: Method to *in vitro* angiogenesis: sprouting assay.

Microcarriers and ECs were dynamically cultured in a spinner flask overnight to allow adhesion of ECs onto the microcarriers. Microcarriers seeded with ECs were then embedded into a fibrin gel and stimulated with external factors (cytokines or cyclic strain) to induce formation of *in vitro* capillary or sprouts.

1-50 ng/mL and hepatocyte growth factor (rhHGF, Chemicon) at 20ng/mL were added to the culture media, and medium was exchanged every 24 hours. All static sprouting assays were assayed after 5 days and all cyclically strained samples, after 48 hours. Following the culture period, samples were immediately fixed in 4% paraformaldehyde (EMS, Hatfield, PA). Data shown represents the average number of sprouts, where the total sprouts per a well were normalized to the total beads per well. High resolution images (100x) of sprouts were captured using an inverted fluorescent microscope (Olympus IX81). A sprout is defined as a structure protruding from a microcarrier that is composed of more than one cell (Figure 4.2).

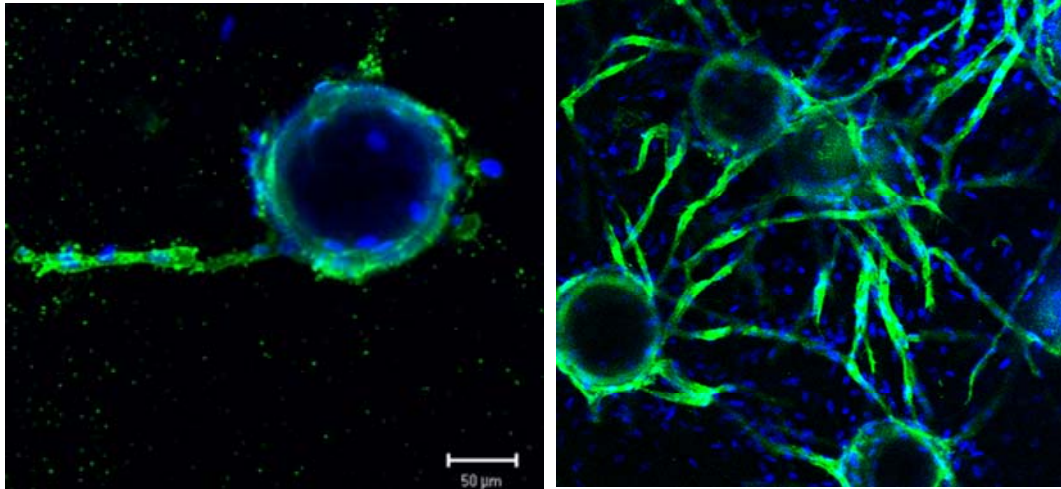
Quantification of angiogenic protein secretion

HUVECs were seeded into treated PDMS elastomeric wells at confluence (4×10^5 cells/cm²), and statically cultured for 24 hrs at 37°C prior to loading onto the mechanical tensile strain device. Cytokine secretion by HUVECs and HASMCs into the culture medium was analyzed by collecting the medium and employing commercial, quantitative sandwich enzyme immunoassay techniques (R&D Systems, Minneapolis, MN).

Real-time RT-PCR

Extraction of total HUVEC RNA was performed using RNeasy Mini Kit (Qiagen, Valencia, CA). cDNA was generated from 200ng of total RNA using Thermoscript cDNA synthesis kit (Invitrogen) according to manufacturer specifications. Amplification of target cDNA sequences using gene specific primers (hAng-2, Qiagen) was performed by using DNA Engine Opticon2 (Bio-Rad). PCR mixtures were used as follows: 12.5 uL

A Confocal (100x) / FITC-CD31 / DAPI



B Photomicrographs Brightfield (100x)



Figure 4.2: Sprout formations by HUVECs.

HUVECs seeded on microcarriers embedded into fibrin gels were stimulated (either by varying cytokine concentration, conditioned media, or cyclic strain) to form in vitro sprouts. Image documentation of sprouts were observed after 5 days of external stimulation through use of (A) confocal microscopy, immunostaining for CD31 membrane receptors (FITC/green) and nucleus (DAPI/blue) or (B) brightfield/DIC microscopy.

SYBR-greenMM (Qiagen), 5uL DEPC water, 5uL sample cDNA, and 2.5uL of primer (Qiagen). Settings for PCR reaction were as follows: denaturing phase = 95°C for 15 sec, annealing phase = 50°C for 15 sec, and elongation phase = 72°C for 15 sec (39 cycles). Each cDNA test sample was assayed in technical duplicates, from triplicate biological samples. Expression results were normalized to that of glyceraldehydephosphate dehydrogenase (GAPDH).

Vector construction and synthesis

The short hairpin RNA (shRNA) sequence was designed and cloned into pSilencer 2.1-neo vector (Ambion). Briefly, the shRNA 63mer oligonucleotide (IDTDNA) containing the sense strand, loop, antisense strand, and pol III terminator were annealed, and inserted via ligating into flanked BamHI and Hind III sites, following a U6 human promoter.

Plasmids were transformed into E.coli-DH5 α competent cells (Invitrogen) as per manufacturer instructions. DNA sequencing (using ABI3730xl Genetic Analyzers) was performed to confirm propagation and purification of product using Plasmid Maxi Kit (Qiagen). Oligonucleotide for shRNA (Ang-2) used was as follows 5'-

GATCCGCAACGCTATGTGCTTAAATTCAAGAGATTTAAGCAC

ATAGCGTTGCTTTTTTGGAAA-3'. A scrambled shRNA sequence containing a random oligonucleotide sequence that was BLAST⁴¹ against the human genome was simultaneously transfected in all experiments as a negative control.

Plasmid transfection and FACS

HUVECs were cultured to 90% confluence, trypsinized and centrifuged to pellet. Cells

(2×10^6 cells/100 μ L), shRNA plasmid, and pmaxGFP were then resuspended in a transfection medium (AMAXA, Cologne, Germany) and electroporated using the Amaxa nucleofactor device. After exposure, cells were cultured in EGM-2 with a basal level (10 μ g/mL) of geneticin for selective pressure. Positive cells were selected using FACS (BD Biosciences LSRII flow cytometer) and subsequently used for experiments. To validate effective inhibition of Ang-2, FACS sorted cells were cultured in 96 well plates (2×10^4 cells/well) in EGM-2 with 10 μ g/mL geneticin and protein secretion levels were measure daily over a time-course of 5 days using a quantitative sandwich enzyme immunoassay technique for Ang-2 (R&D Systems, Minneapolis, MN).

Statistical Analysis

Statistical comparison of two samples was performed using a two-tailed Student *t*-test when applicable. $P < 0.05$ was considered as statistically significant.

4.3 Results

Cyclic tensile strain alters endothelial phenotype and angiogenic factor secretion

The effects of cyclic strain on EC migration and *in vitro* sprout formation were first confirmed. Cyclic tensile strain (7%, 1 Hz) enhanced, by 1.6 fold, the directional migration of HUVECs in 2D culture (Figure 4.3A), as expected¹⁹. Two days of cyclic tensile strain also enhanced sprout formation by HUVECs in fibrin gels by 4 fold, compared to static culture (Figure 1B), again in agreement with earlier investigations⁹. Addition of recombinant human VEGF-165, a known stimulant to capillary formation²⁰,²¹, also increased sprout formation both under static and strained conditions (Figure 4.3B),

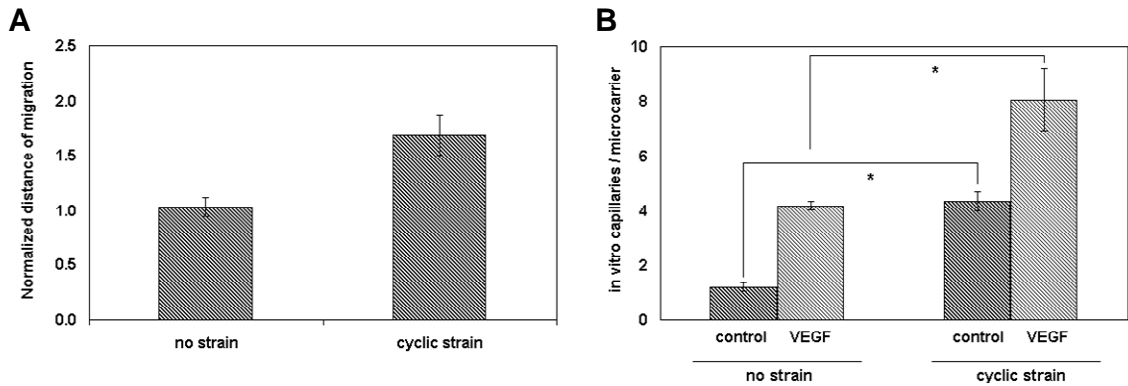


Figure 4.3A-B: Cyclic strain enhanced EC migration and sprout formation

Cyclic tensile strain at a frequency of 1Hz and $\epsilon = 7\%$ for a duration of 2 days enhanced directed EC migration and sprout formation. (A) Directed migration of HUVECs on PDMS with no strain and application of strain was quantified by measuring the distance on the culture surface to which the edge of the cell population migrated in the direction normal to strain direction, normalized to the extent of cell migration parallel to strain application. (B) Formation of sprouts by endothelial cells in 3D culture, as a function of static culture (no strain) or application of cyclic strain. Sprouting was analyzed in the absence (control) or presence (VEGF) of exogenous VEGF in the medium. Values represent mean (n = 4), * indicative of $P < 0.05$.

confirming the expected biological responsiveness of the cells used in these studies.

To examine whether cyclic strain upregulated genes involved in angiogenesis, the levels of angiogenic proteins secreted by vascular cells were quantified over a 5 day time-course of cyclic strain. Cyclic strain of HUVECs led to a 5-fold upregulation in the secretion of PDGF- $\beta\beta$ (Figure 4.4A), and a 4.8-fold upregulation of Ang-2 (Figure 4.4B). In contrast, cyclic strain of HASMCs resulted only in a slight enhancement of Ang-1 (Figure 4.4C), while secretion of VEGF did not appear to be effected by strain (Figure 4.4D). In both strained and non-strained conditions, the secretion of PDGF- $\beta\beta$ and Ang-2 by HASMC, and Ang-1 and VEGF by HUVECS, respectively, was minimal. The time course of upregulation of PDGF- $\beta\beta$ and Ang-2 secretion by HUVECs was next investigated. Ang-2 expression was increased 3-fold by day 1 and then slowly subsided over the ongoing 13 days to control levels (Figure 4.4E). PDGF secretion, in contrast, did not rise until 2 days of cyclic stretch, and then quickly returned to baseline control levels (Figure 4.4F). As minimal effects of cyclic strain on angiogenic factor secretion by HASMC were noted, all subsequent studies focused on HUVECs.

Role of Ang-2 in endothelial cell migration and sprout formation

To determine if the levels of altered angiogenic factors resulting from cyclic strain were capable of altering EC phenotype, HUVECs in fibrin gels were exposed to exogenous recombinant human Ang-2, Ang-1, PDGF and VEGF, at levels corresponding to those produced by cells under strained conditions. Ang-2 and VEGF enhanced the formation of sprouts (Figure 4.5A-B), while PDGF (Figure 4.5C) and Ang-1 (Figure 4.5D) had no

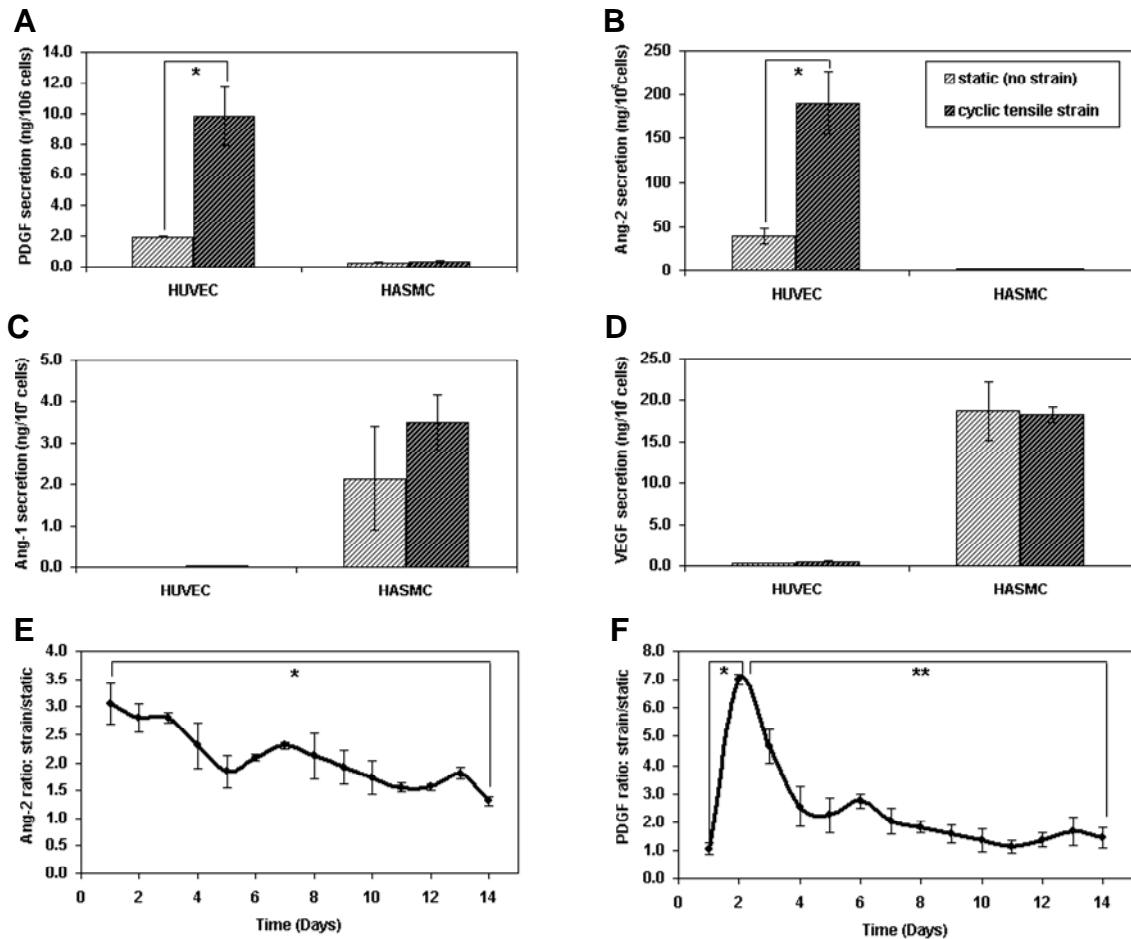


Figure 4.4A-F: Cyclic strain regulates temporal secretion of angiogenic factors

Cyclic tensile strain upregulated secretion of angiogenic factors by vascular cells, in a temporal manner. (A-D) Secretion of PDGF, Ang-2, Ang-1 and VEGF by HUVECs and HASMCs was quantified after exposure to 5 days of cyclic strain. Protein levels were quantified using enzyme immunoassays and values (n=3) were normalized to total cell number per well. (E) Expression profiles of HUVECs secretion of Ang-2 and PDGF in response to 14 days of cyclic strain. Values represent normalized protein levels (n=3) under strain to protein levels secreted under static (no strain) conditions. * indicative of $P < 0.05$ and ** indicative of $P < 0.005$.

discernible effects. The effects of these factors on HUVEC migration across porous transwell membranes was next examined, and VEGF was found to enhance HUVEC migration (Figure 4.5E), concurring with known effects of this cytokine²². Ang-2 similarly enhanced HUVEC migration, while Ang-1 had no effect (Figure 4.5E). To test whether cyclic strain-induced upregulation of Ang-2 was causative for the strain induced increase in EC migration and sprouting, RNAi was used to knockdown the endogenous expression of Ang-2 in HUVECs. HUVECs were transfected with a plasmid that was designed and constructed to release a 63mer silencing hairpin ribonucleic acid (shRNA) that binds specifically to the intracellular mRNA of Ang-2 and blocks the translation of this protein. Examination of Ang-2 secretion by cells positively transfected with shRNA (Ang-2) confirmed a dramatic inhibition of Ang-2 expression for 4 days following treatment (Figure 4.6A). The baseline (no cyclic strain) migration of ECs with shRNA (Ang-2), was decreased by approximately by 1.6 fold (Figure 4.6B), while cells subjected to strain exhibited a 2-fold decrease in migration with shRNA treatment (Figure 4.6C). Inhibiting Ang-2 also resulted in a 2.2 fold decrease in sprouting with exposure to cyclic strain, in both the absence and presence of exogenous VEGF in the culture medium (Figure 4.6D). Finally, gene expression levels of Ang-2 and its receptor (Tie-2) in HUVECs were analyzed using real time RT-PCR, and cyclic strain for 5 days resulted in 1.5-fold and 2-fold increases in mRNA levels for Ang-2 and Tie-2, respectively (Figure 4.6E).

4.4 Discussion

The results of these studies indicate that Ang-2 can activate ECs to migrate and form

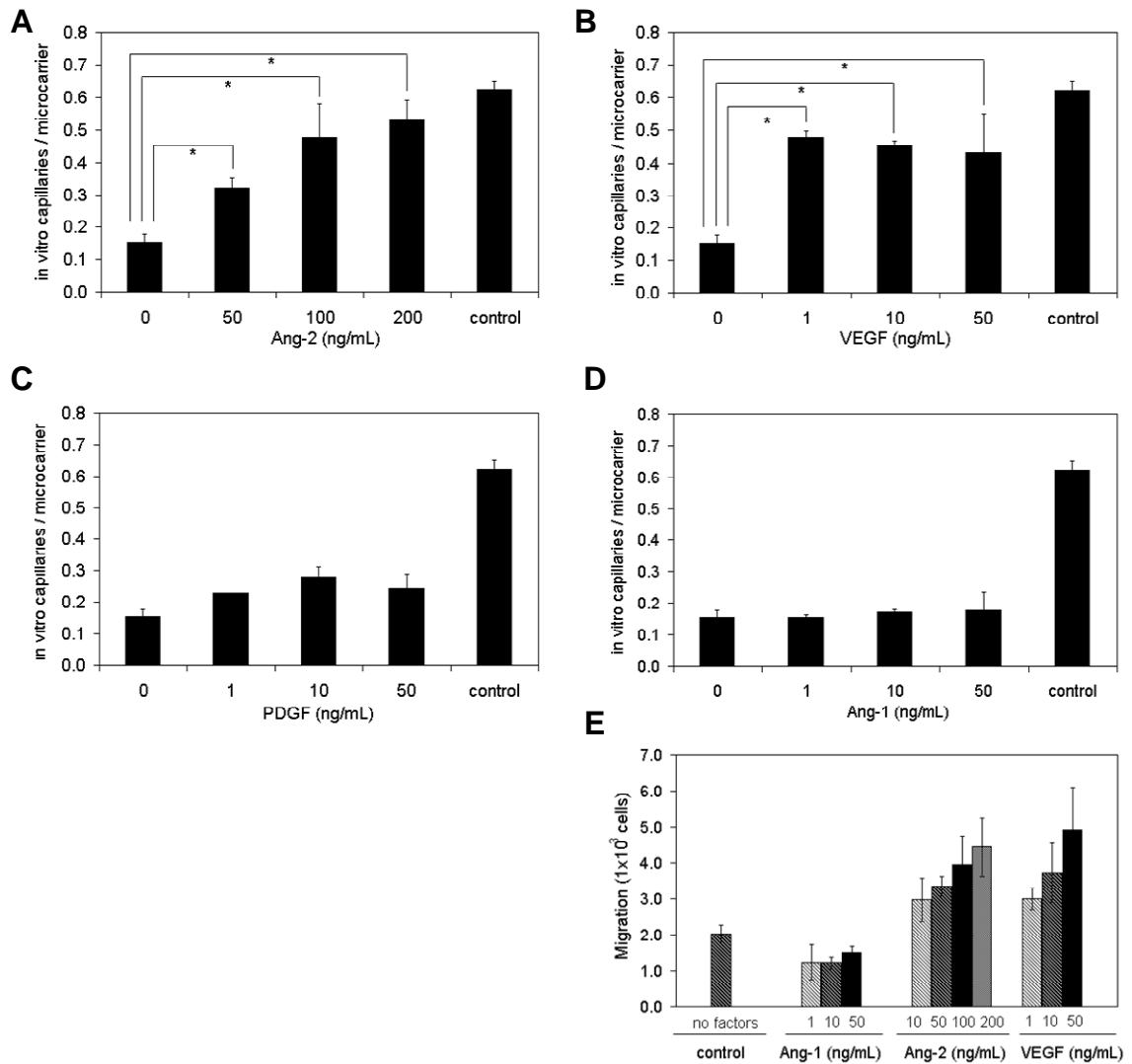


Figure 4.5A-E: Ang-2 and VEGF enhance HUVEC migration and sprout formation

Exogenous application of Ang-2 and VEGF enhanced sprout formation and migration of HUVECs. Sprout formation in response to recombinant (A) Ang-2, (B) VEGF, (C) PDGF, and (D) Ang-1 was quantified (n=4). (E) 2D migration of HUVECs across transwell inserts after 12 hrs in static culture with exposure increasing concentrations of various cytokines (n=4). * indicative of $P < 0.05$.

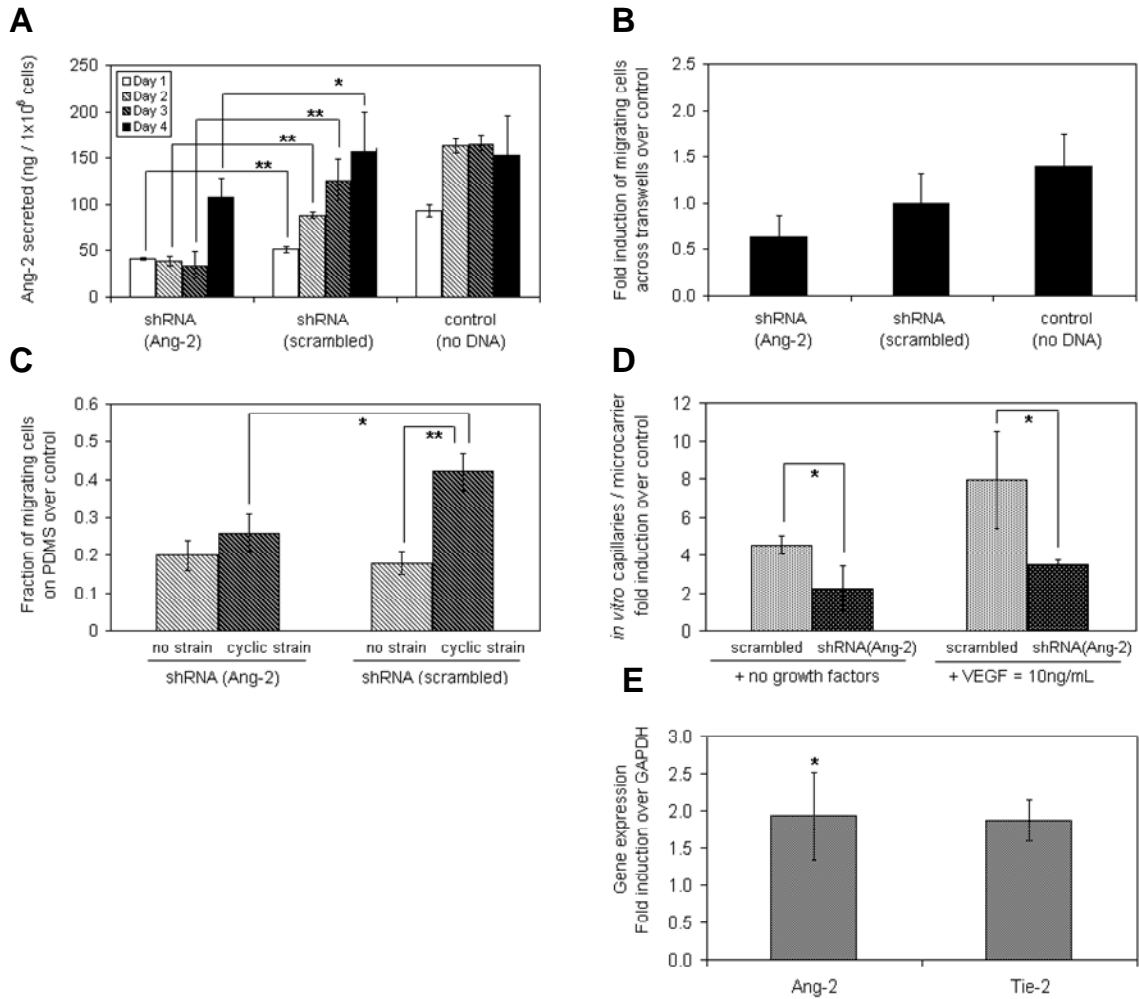


Figure 4.6A-E: Knockdown of Ang-2 decrease EC responsiveness to strain

RNAi was utilized to determine the role of Ang-2 in HUVEC response to cyclic strain.

(A) Effectiveness of shRNA knockdown of endogenous Ang-2 secretion by HUVECs transfected with shRNA to Ang-2 (Ang-2), a control shRNA (scrambled sequence), and control untreated cells was quantified using enzyme immunoassays, daily (n=5) over 4 days. Values represent mass of protein secreted, normalized to total cell phenotype of endothelial cells, characterized here by directed cell migration and in vitro

number per well (B) Level of static HUVEC migration, over 24 hrs, across transwell inserts, normalized to untreated control cells, with either shRNA to Ang-2 (Ang-2) or

scrambled shRNA control (scrambled) (n=4) (C) Level of HUVEC migration in response to 48hrs cyclic strain on PDMS. Values represent number of cells under cyclic strain that migrated out of original confined circular region, d=2mm, normalized to static, non-strained conditions (n=3). (D) Formation of sprouts under application of strain was quantified using HUVECs with and without Ang-2 shRNA treatment, in culture medium with or without added VEGF. Values (n=3) are normalized to a non-strained, no growth factors control. (E) Cyclic strain effect on gene expression of Ang-2 and Tie-2 mRNA levels was quantified by real time RT –PCR, normalizing all values (n=6) to GAPDH levels.* indicative of $P < 0.05$ and ** indicative of $P < 0.005$.

sprouts, processes important to the early stages of angiogenesis. The angiogenic sprout formation was also enhanced in response to cyclic uniaxial strain. Cyclic strain increased expression of both Ang-2 and its receptor, Tie-2, in ECs, and this increased Ang-2 expression mediated the cyclic strain induced alterations in EC angiogenic phenotype.

Cyclic strain upregulated EC secretion of angiogenic cytokines, specifically, PDGF- $\beta\beta$ and Ang-2. Previous studies reported that cyclic strain enhanced the expression of PDGF-R^{8, 23}, and shear stress enhanced gene expression of PDGF- $\beta\beta$ ^{24, 25} and Tie-2²⁶. However, upregulation of PDGF- $\beta\beta$ and Ang-2 in response to cyclic strain has, to our knowledge, not been previously documented. Interestingly, VEGF, a potent factor in angiogenic activation was not affected by strain, although regulation of this cytokine is governed by other local cues²⁷. The temporal profile of increased angiogenic cytokine secretion by ECs in response to cyclic strain was striking, as Ang-2, a factor important to the initiation of angiogenesis² was upregulated early, followed by later expression of PDGF, which plays important roles in later stages of angiogenesis^{2, 28}. This data suggests that cyclic strain modulates angiogenesis by altering the balance of angiogenic factors, and by temporally mediating the upregulation of factors driving activation versus those promoting vessel stabilization.

Ang-2 was found in this study, even in the absence of mechanical stimulation, to enhance sprout formation and migration of endothelial cells. The role of angiopoietins in vascular development has been the subject of active investigation, and until recently it was

believed that Ang-1 played solely a stabilizing role via activation of the tyrosine kinase receptor Tie-2²⁹ while Ang-2, the antagonist to Ang-1, was believed to play more of a facilitative role³⁰. For example, expression of Ang-2 was identified primarily at sites of active vessel remodeling³⁰⁻³³. However, recent studies demonstrate that there may exist a contextual role to Ang-2's functions, as it serves in some instances to inhibit vascular leakage³⁴ while in other situations it may function as a proinflammatory cytokine³⁵. Increased secretion of Ang-2 in response to biochemical stimulants has also been documented, supporting the suggestion³⁶ that Ang-2 function is more complex than initially identified³⁷. Although VEGF-A and angiopoietins play distinct roles in vascular development, they also have complementary and coordinated roles. VEGF-A, has been shown to modulate migration²² and in vitro capillary formation³⁸ of ECs and Ang-2, at levels secreted in response to cyclic strain signals, appears to have similar effects on ECs. While the molecular mechanisms linking cyclic strain to Ang-2 expression are not clear, they likely involve the various intracellular signaling pathways previously documented to mediate mechanical effects on ECs^{12, 39} that induce local differentiation and the formation of nascent blood vessels.

The findings of this study provide a specific example of how localized mechanical signals can be translated into biochemical cues capable of signaling over physiologic relevant distances via chemical gradients. While not addressed in this report, this coupled mechanism may provide new points to intervene and regulate the angiogenic process, and may also improve the current understanding of various vascular diseases.

4.5 References

1. Carmeliet, P. Angiogenesis in health and disease. *Nat Med* **9**, 653-660 (2003).
2. Jain, R.K. Molecular regulation of vessel maturation. *Nat Med* **9**, 685-693 (2003).
3. Upchurch, G.R., Jr., Leopold, J.A., Welch, G.N. & Loscalzo, J. Nitric Oxide Alters Human Microvascular Endothelial Cell Response to Cyclic Strain. *J Cardiovasc Pharmacol Ther* **3**, 135-142 (1998).
4. Woodell, J.E., LaBerge, M., Langan, E.M., 3rd & Hilderman, R.H. In vitro strain-induced endothelial cell dysfunction determined by DNA synthesis. *Proc Inst Mech Eng [H]* **217**, 13-20 (2003).
5. Naruse, K., Sai, X., Yokoyama, N. & Sokabe, M. Uni-axial cyclic stretch induces c-src activation and translocation in human endothelial cells via SA channel activation. *FEBS Lett* **441**, 111-115 (1998).
6. Girard, P.R. & Nerem, R.M. Shear stress modulates endothelial cell morphology and F-actin organization through the regulation of focal adhesion-associated proteins. *J Cell Physiol* **163**, 179-193 (1995).
7. Li, S. Analysis of endothelial cell migration under flow. *Methods Mol Biol* **294**, 107-121 (2005).
8. Kakisis, J.D., Liapis, C.D. & Sumpio, B.E. Effects of cyclic strain on vascular cells. *Endothelium* **11**, 17-28 (2004).
9. Von Offenberg Sweeney, N. et al. Cyclic strain-mediated regulation of vascular endothelial cell migration and tube formation. *Biochem Biophys Res Commun* **329**, 573-582 (2005).

10. Matsumoto, T. et al. Mechanical Strain Regulates Endothelial Cell Patterning in Vitro. *Tissue Eng* (2006).
11. Wang, Y. et al. Visualizing the mechanical activation of Src. *Nature* **434**, 1040-1045 (2005).
12. Giancotti, F.G. & Ruoslahti, E. Integrin signaling. *Science* **285**, 1028-1032 (1999).
13. Shyy, J.Y. & Chien, S. Role of integrins in cellular responses to mechanical stress and adhesion. *Curr Opin Cell Biol* **9**, 707-713 (1997).
14. Wang, N., Butler, J.P. & Ingber, D.E. Mechanotransduction across the cell surface and through the cytoskeleton. *Science* **260**, 1124-1127 (1993).
15. Li, C., Hu, Y., Mayr, M. & Xu, Q. Cyclic strain stress-induced mitogen-activated protein kinase (MAPK) phosphatase 1 expression in vascular smooth muscle cells is regulated by Ras/Rac-MAPK pathways. *J Biol Chem* **274**, 25273-25280 (1999).
16. Tzima, E. et al. A mechanosensory complex that mediates the endothelial cell response to fluid shear stress. *Nature* **437**, 426-431 (2005).
17. Zheng, W., Christensen, L.P. & Tomanek, R.J. Stretch induces upregulation of key tyrosine kinase receptors in microvascular endothelial cells. *Am J Physiol Heart Circ Physiol* **287**, H2739-2745 (2004).
18. Folkman, J. & D'Amore, P.A. Blood vessel formation: what is its molecular basis? *Cell* **87**, 1153-1155 (1996).
19. Wang, J.H., Goldschmidt-Clermont, P., Wille, J. & Yin, F.C. Specificity of endothelial cell reorientation in response to cyclic mechanical stretching. *J Biomech* **34**, 1563-1572 (2001).

20. Carmeliet, P. Mechanisms of angiogenesis and arteriogenesis. *Nat Med* **6**, 389-395 (2000).
21. Gerhardt, H. et al. VEGF guides angiogenic sprouting utilizing endothelial tip cell filopodia. *J Cell Biol* **161**, 1163-1177 (2003).
22. Koch, A.E. et al. Vascular endothelial growth factor. A cytokine modulating endothelial function in rheumatoid arthritis. *J Immunol* **152**, 4149-4156 (1994).
23. Resnick, N. et al. Platelet-derived growth factor B chain promoter contains a cis-acting fluid shear-stress-responsive element. *Proc Natl Acad Sci U S A* **90**, 4591-4595 (1993).
24. Malek, A.M., Gibbons, G.H., Dzau, V.J. & Izumo, S. Fluid Shear-Stress Differentially Modulates Expression of Genes Encoding Basic Fibroblast Growth-Factor and Platelet-Derived Growth Factor-B Chain in Vascular Endothelium. *Journal of Clinical Investigation* **92**, 2013-2021 (1993).
25. Hsieh, H.J., Li, N.Q. & Frangos, J.A. Shear-Stress Increases Endothelial Platelet-Derived Growth-Factor Messenger-Rna Levels. *American Journal of Physiology* **260**, H642-H646 (1991).
26. Lee, H.J. & Koh, G.Y. Shear stress activates Tie2 receptor tyrosine kinase in human endothelial cells. *Biochemical and Biophysical Research Communications* **304**, 399-404 (2003).
27. Enholm, B. et al. Comparison of VEGF, VEGF-B, VEGF-C and Ang-1 mRNA regulation by serum, growth factors, oncoproteins and hypoxia. *Oncogene* **14**, 2475-2483 (1997).
28. Risau, W. Mechanisms of angiogenesis. *Nature* **386**, 671-674 (1997).

29. Asahara, T. et al. Tie2 receptor ligands, angiopoietin-1 and angiopoietin-2, modulate VEGF-induced postnatal neovascularization. *Circ Res* **83**, 233-240 (1998).
30. Holash, J., Wiegand, S.J. & Yancopoulos, G.D. New model of tumor angiogenesis: dynamic balance between vessel regression and growth mediated by angiopoietins and VEGF. *Oncogene* **18**, 5356-5362 (1999).
31. Maisonpierre, P.C. et al. Angiopoietin-2, a natural antagonist for Tie2 that disrupts in vivo angiogenesis. *Science* **277**, 55-60 (1997).
32. Stratmann, A., Risau, W. & Plate, K.H. Cell type-specific expression of angiopoietin-1 and angiopoietin-2 suggests a role in glioblastoma angiogenesis. *Am J Pathol* **153**, 1459-1466 (1998).
33. Fiedler, U. & Augustin, H.G. Angiopoietins: a link between angiogenesis and inflammation. *Trends Immunol* **27**, 552-558 (2006).
34. Daly, C. et al. Angiopoietin-2 functions as an autocrine protective factor in stressed endothelial cells. *Proc Natl Acad Sci U S A* **103**, 15491-15496 (2006).
35. Fiedler, U. et al. Angiopoietin-2 sensitizes endothelial cells to TNF-alpha and has a crucial role in the induction of inflammation. *Nat Med* **12**, 235-239 (2006).
36. Fiedler, U. et al. The Tie-2 ligand angiopoietin-2 is stored in and rapidly released upon stimulation from endothelial cell Weibel-Palade bodies. *Blood* **103**, 4150-4156 (2004).
37. Holash, J. et al. Vessel cooption, regression, and growth in tumors mediated by angiopoietins and VEGF. *Science* **284**, 1994-1998 (1999).

38. Tonnesen, M.G., Feng, X. & Clark, R.A. Angiogenesis in wound healing. *J Investig Dermatol Symp Proc* **5**, 40-46 (2000).
39. Li, C., Hu, Y., Sturm, G., Wick, G. & Xu, Q. Ras/Rac-Dependent activation of p38 mitogen-activated protein kinases in smooth muscle cells stimulated by cyclic strain stress. *Arterioscler Thromb Vasc Biol* **20**, E1-9 (2000).
40. Cunningham, J.J., Nikolovski, J., Linderman, J.J. & Mooney, D.J. Quantification of fibronectin adsorption to silicone-rubber cell culture substrates. *Biotechniques* **32**, 876, 878, 880 passim (2002).

CHAPTER 5

ROLE OF CYCLIC STRAIN IN MODULATING RECRUITMENT OF SMOOTH MUSCLE CELLS TOWARDS MIGRATING ENDOTHELIAL CELLS

5.1 Introduction

The recruitment of smooth muscle cells (SMCs), critical to blood vessel function and maturation¹⁻³, comprises the medial layer that stabilizes neovessels formed from endothelial cells (ECs) during angiogenesis. Understanding the cues that regulate SMC migration gives insight to vascular diseases⁴ associated with abnormal states, as in atherosclerosis⁵ and cancer^{6,7}. A number of proximal environmental cues that control SM migration have been investigated, and platelet-derived growth factor (PDGF-BB), has been identified as the most potent chemoattractant for cultured vascular SMCs⁸⁻¹². Other soluble factors secreted by ECs, with lesser chemotactic effect on SM migration, include basic fibroblast growth factor (bFGF)¹³ and heparin-binding epidermal growth factor (HB-EGF)¹⁴. Physiologically relevant hemodynamic forces have also demonstrated to modulate SM migration¹⁵⁻¹⁷, phenotype¹⁸⁻²¹, and intracellular signaling molecules²²⁻²⁴. *In vitro* techniques used to assess SM migration traditionally employ the use of the Boyden chamber, or a similar type of device, to measure cell migration across porous membranes²⁵. Alternative methods using radiolabeled SMCs infiltration into

amniotic membrane in response to have been quantitatively analyzed in response to chemotactic cues²⁶. Novel methods utilizing nanoparticles bound to SMC surface epitopes²⁷, have been used to quantify proliferation and can likely be adapted to studying migration of SMCs.

The effect of cyclic tensile strain on EC secretion of paracrine factors, and the role of these factors in mediating SMC migration were analyzed in this study. Isolated colonies of human umbilical vein endothelial cells (HUVECs) and human aortic smooth muscle cells (HASMCs) were seeded in co-culture and at physiologically relevant distances as an *in vitro* model for neovessel development, specifically to assess strain regulated chemotactic effects of PDGF. An elastomeric homogeneous PDMS culture well that presented regions of high and low surface strain (Chapter 3) was used in combination with a precise seeding method to pattern (each colony = 1mm in diameter) and expose ECs and SMCs to individual levels of cyclic tensile strain. The magnitude of cyclic tensile strain was shown to enhance the number, but not directionality of migrating SMCs. In the co-culture system, PDGF secreted by strain-mediated migrating ECs demonstrated to provide the directional cues for SMCs recruitment towards these EC colonies.

5.2 Materials and Methods

Vascular Cell Culture

Human umbilical vein endothelial cells (HUVECs, Cambrex, Walkersville, MD) and human aortic smooth muscle cells (HASMCs, Cambrex, Walkersville, MD), were

cultured in a humidified incubator at 37°C, 5% CO₂, in endothelial growth medium (EGM-2) and smooth muscle cell growth medium (SmGm-2), respectively (Cambrex, Walkersville, MD), containing 2% FBS. HUVECs were used between passages 3 and 6 and HASMCs were used between passages 3 and 7. Co-cultures of HUVECs and HASMCs were maintained in culture medium that constituted of 1:1, EGM-2 and SmGm-2.

Creating an array of isolated cell cultures (each colony diameter = 1mm)

Custom polydimethylsiloxane (PDMS) elastomeric wells were prepared for cell culture by activating their surface through ultraviolet irradiation for 10 min, followed by coating the surface with fibronectin (2ug/mL) for 2 hrs^{28, 29} to enhance cell adhesion.

Cell colonies grown in 1 mm diameter regions were patterned (Figure 5.1) to form a rectangular array of (4 x 3) colonies on a PDMS substrate with strain gradients (Figure 5.2). This modified masking technique utilizes a coated silicon sheet, containing an array of 1 mm diameter holes and was placed directly onto the bottom sheet prior to cell seeding. Individually, HUVECs and HASMCs were suspended into a fibrin solution constituted of fibrinogen (4 mg/mL; Sigma) and thrombin (25 units/mL) and were precisely seeded (250 cells/well) into the resultant (1mm diameter) wells formed by the top sheet. After fibrin gelation, cells were statically cultured in the 1mm diameter regions in designated medium with Plasmin (10ug/mL) for 24 hrs. Subsequently, the PDMS mask was removed, and samples were loaded onto the strain device and cells were allowed to migrate from the confluent circular 1 mm diameter population under cyclic strain loading for a duration of 2 days.

Quantification of Vascular Cell Migration: Number, Rate, and Directionality in response to cyclic tensile strain

All PDMS wells were strained using a custom built linear motor that was computer controlled. Cells were strained at a frequency of 1Hz and at strain amplitude of 7%. To detect and document coculture migration in response to strain, vascular cells were fixed in 3.7% formaldehyde (Electron Microscopy Sciences, Hatfield, PA) for 15 minutes and rinsed in PBS. Expression of CD31, an endothelial-specific membrane marker, was detected using a mouse antibody against human CD31 (1:20 dilution; Dako Cytomation) followed by a secondary Rhodamine conjugated goat-anti-mouse IgG antibody (1:50 dilution, Jackson ImmunoResearch, West Grove, PA). A nuclear stain DAPI (300nM) (Molecular Probes, Eugene, OR), was also applied onto the samples for 15 min to detect the location of all cells. The base of the PDMS wells were then cut and placed onto a microscope slide for fluorescent microscope imaging (Olympus IX81) for quantification. Refer to Appendix B for scripts to run automated large mosaic image capture. Fraction of cell migration and proliferation in response to strain was normalized to cells experiencing no application of strain. The average velocity was quantified by measuring the change in distance of the cell colony periphery (y-axis) from the original 1mm diameter culture, over 48hrs. SMC migration in response to a PDGF source or an EC source was quantified by measuring the fraction of cells that migrated outside of the original 1mm-diameter circular region. Directionality of SMC migration was assessed by first quantifying the number of cells that migrated outside of the original 1mm-diameter circular region, then by measuring the fraction that preferentially migrated either to the left or right hemisphere based on the original seeding circular region.

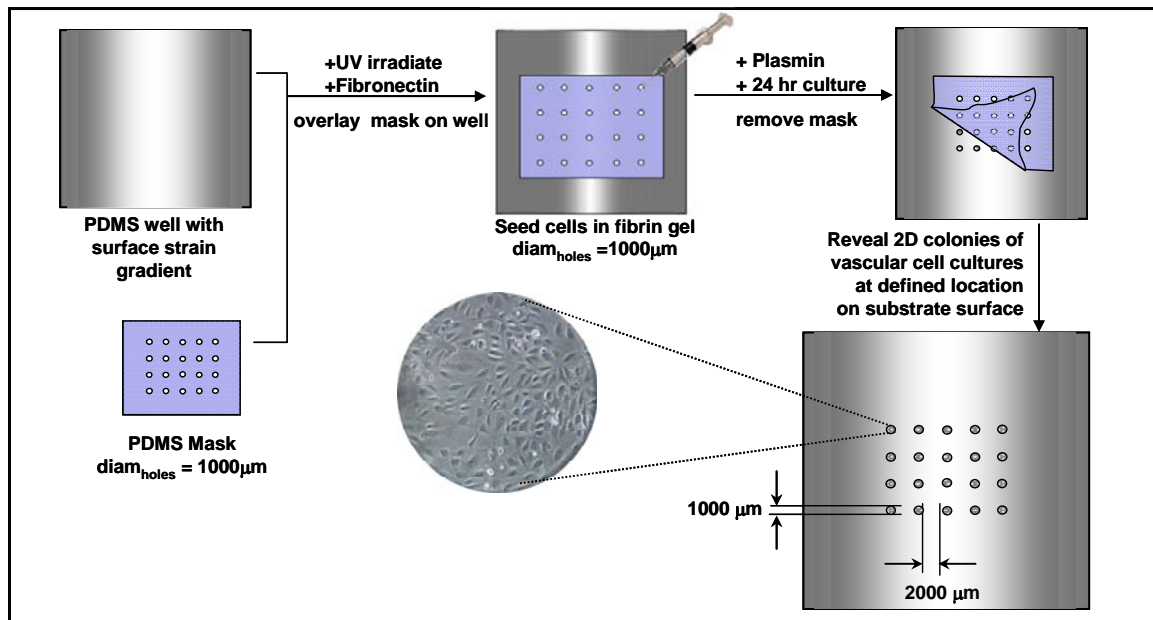


Figure 5.1: Method to culture a precise array of ECs and SMCs

Culturing isolated colonies of human vascular cells in PDMS wells enabled quantitative analysis of cell migration in response to cyclic tensile strain. PDMS wells that present a gradient in surface strain, when under application of strain, were overlaid with a PDMS mask with holes used to confine cell culture into discrete colonies. Cells in fibrin gel solution were seeded into each hole and culture medium with Plasmin was added to slowly degrade the gel and to form a monolayer culture. Mask was removed to reveal an array of vascular cell colonies.

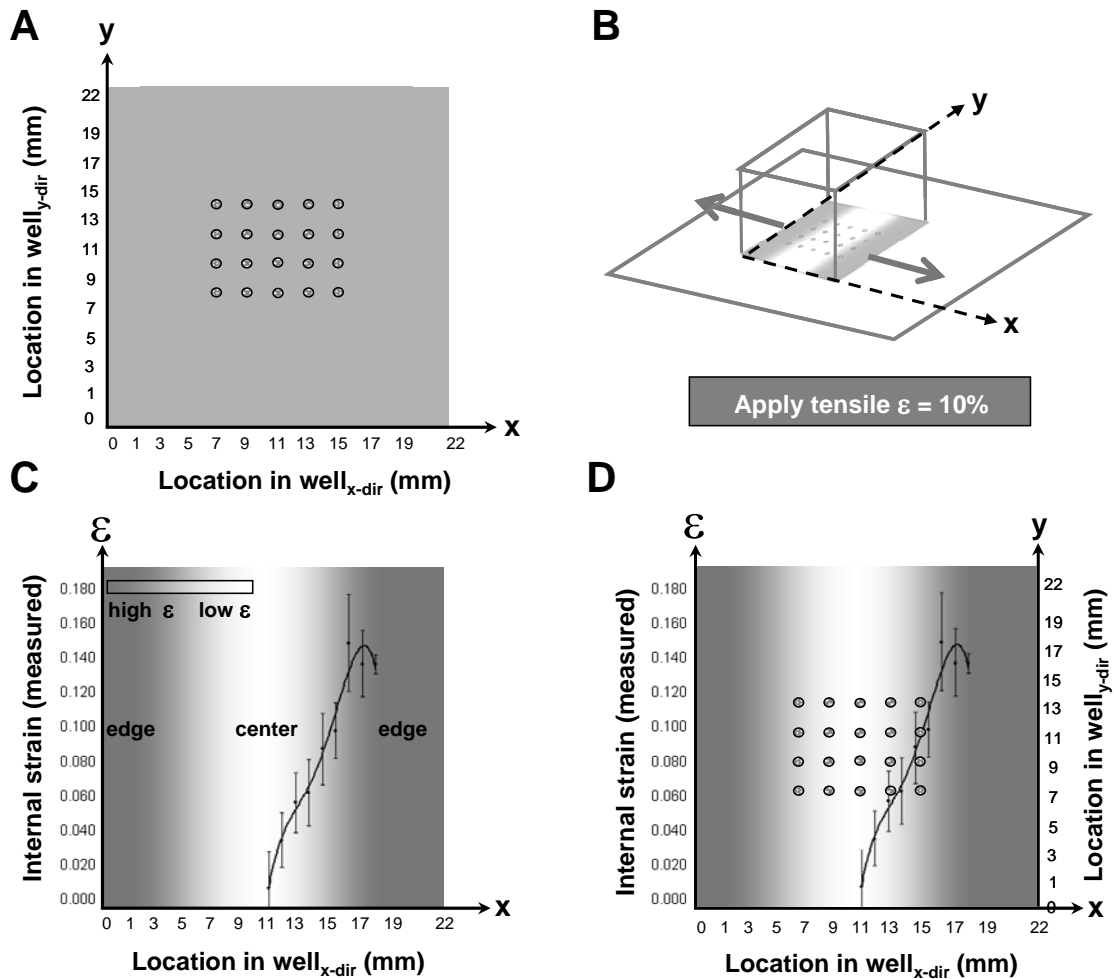


Figure 5.2 A-D: Array of vascular cell colonies in PDMS well with strain gradient
 Patterned array of vascular cell colonies on PDMS culture well that presents a gradient in surface strain (A) Dimension and coordinates of cell colony array on PDMS well (B) Direction of strain application ($\epsilon=10\%$) with respect to cell array coordinate (C) PDMS well strain profile (D) A combined view illustrating which cell colonies, at defined regions, are exposed to different levels of tensile strain.

Mathematical model to define PDGF concentration profile

The secretion of PDGF by HUVECs in response to cyclic strain is assumed as a continuous production from an EC colony point source. The equation below enables determination of diffusion length and concentration profile. The culture well system is assumed a semiinfinite medium, with negligible consumption of PDGF by SMCs due to continuous production and constant diffusion. The diffusion profile describes a solute at a distance r from an injection point (PDGF generated) and the mathematical model is as follows³⁰:

$$C(r, t) = \frac{Me^{-r^2/(4Dt)}}{8(\pi Dt)^{3/2}}.$$

The concentration (C) of PDGF, at a radial distance r from the point source as a function of time (t), where M is the mass of the PDGF source, and D is the diffusion coefficient ($1 \times 10^{-6} \text{ cm}^2/\text{s}$). Values for M were determined experimentally (0.0514 pmol/ HUVEC colony). This model predicts the maximum distance r that is required in order to ensure paracrine sensing proximity of PDGF from HUVECs, by HASMCs.

Quantification of HASMC Migration in Response to Chemotactic Gradients

HASMCs were seeded (1×10^4 cells/well) in basal media (SMBM-2) into the upper reservoir of a transwell chemotaxis insert (Corning Life Sciences, Wilkes-Barre, PA) and exposed to (1) a range of PDGF concentrations (1-100 ng/mL) (R & D Systems, Minneapolis, MN) and (2) to conditioned media from HUVECs from both cyclically strained samples or static cultures (with media exchanged every 24 hrs, taken from day 5). The bottom surfaces of the transwell inserts were coated with 2ug/mL of fibronectin (Sigma-Aldrich) for 24 hrs and rinsed in PBS prior to use. Cells were allowed to migrate

across a (3 μm pore) polycarbonate porous membrane for 24 hr in a humidified incubator with 5% CO_2 at 37°C. After 24 hrs, all cells that did not migrate remaining the top insert were removed by PBS rinsing and gentle cotton swabbing. Migrated cells on the bottom surface of the filter were subsequently fixed in 3.7% formaldehyde (Electron Microscopy Sciences, Hatfield, PA) for 15 minutes. The membrane was then rinsed in PBS and stained using DAPI (300nM) (Molecular Probes, Eugene, OR) for 15 min, cut and placed onto a microscope slide for fluorescent microscope imaging (Olympus IX81).

Neutralizing effects of SM membrane bound PDGF-receptor (PDGF-R) on SMC migration were assessed by pre-incubating HASMCs for 30 minutes in 100 $\mu\text{g}/\text{mL}$ anti-PDGFR (R & D Systems, Minneapolis, MN). Cells in five random fields (at 100x magnification) were counted to quantify average number of migrated cells per insert. Data represent means of the number of migrating cells per condition normalized to the negative control (no growth factor).

Immuncytochemistry of PDGF-R

Immunofluorescent visualization of PDGF-R expression on the membrane of HASMCs was performed using standard methods. HASMCs were cultured for 24 hrs on Lab-Tek chambers and activated PDMS substrates, both surfaces coated with 2 $\mu\text{g}/\text{mL}$ Fibronectin (Sigma). HASMCs were cultured for an additional 48hrs, those in Lab-Teks exposed to a range of rhPDGF concentrations (1-100 ng/mL) and those in PDMS wells both under static culture and strain application. Subsequent to removal from culture, cells were fixed in 3.7% formaldehyde (Electron Microscopy Sciences, Hatfield, PA) for 15 minutes, rinsed in PBS, and expression of PDGF-R was detected using a goat polyclonal antibody

against the human PDGF-R β (10 ug/mL; R&D Systems) followed by a secondary Alexfluor488 conjugated rabbit-anti-goat antibody (2ug/mL; Invitrogen). A fluorescent microscope (Olympus IX81) was used for image documentation. Quantification of PDGF-R expression was assessed by measuring the average relative fluorescence units (RFU) of images taken with a 10x objective (IPLAB 4.0).

5.3 Results

Strain magnitude alters vascular cell proliferation, average velocity and direction

The response of vascular cell migration to varying magnitudes of cyclic tensile strain was assessed by the fraction of cells that migrated out from original cell culture region, the average velocity outside of the original cell culture region, and the directionality of the cell colony, all at a frequency of 1Hz. Cyclic tensile strain enhanced the fraction of migrating HUVECs by 2-fold when an amplitude of 6% cyclic strain was applied, while at an amplitude of 13% cyclic strain, the fraction of cells migrating was enhanced nearly 4-fold (Figure 5.3A). The average velocity of HUVEC migration at 13% cyclic strain was 15-fold (Figure 5.3B) as compared to that at static conditions, amounting to an averaged velocity of $\langle v \rangle = 15 \mu\text{m/hr}$. Migration of HUVEC colonies exhibited a clear directionality, perpendicular to the line of strain application (Figure 5.3C). Two days of cyclic tensile strain similarly enhanced the fraction of migrating HASMCs nearly 3-fold at 13% strain as compared to non strained conditions, but only negligibly at 6% (Figure 5.4A). The average velocity of HASMC migration, at 13% strain

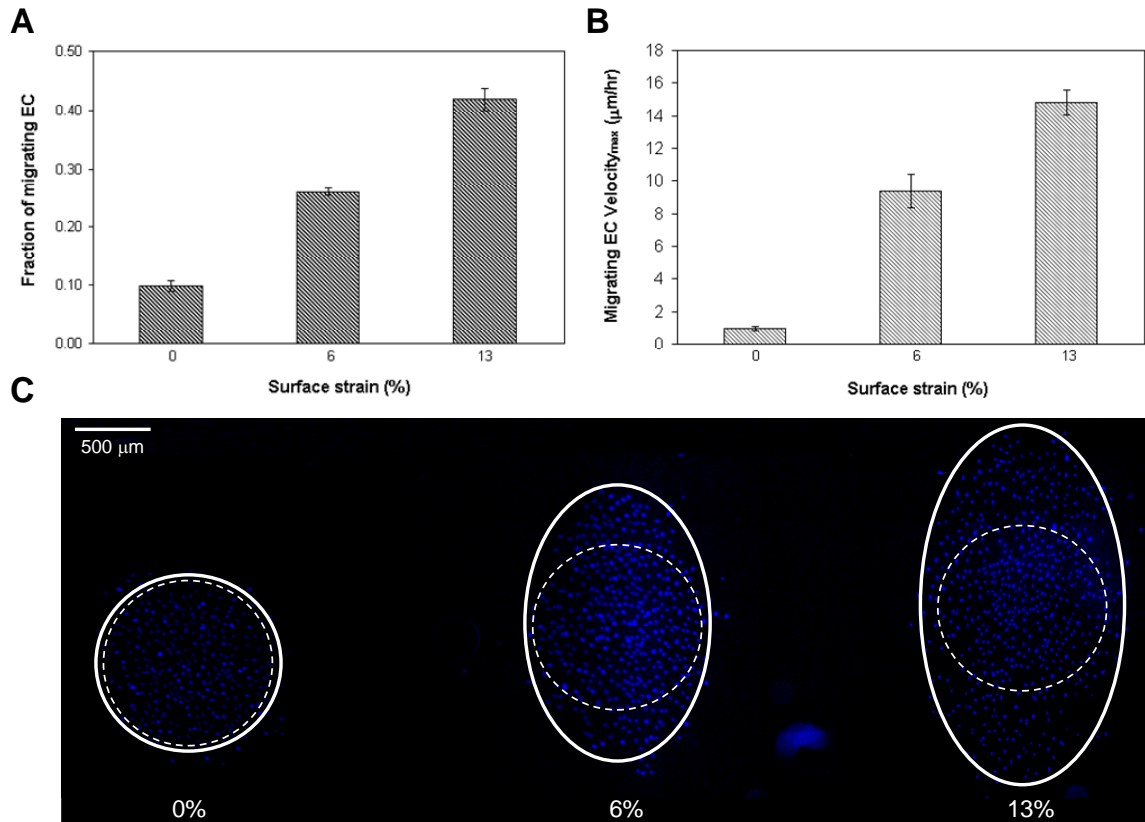


Figure 5.3 A-C: Response of EC migration to increasing strain magnitudes

HUVEC migration, velocity, and directionality are enhanced in response to increasing cyclic tensile strain magnitude. Migration of HUVEC was quantified after subject to 2 days of cyclic strain at varying magnitudes of strain: 0 (no strain), 6, and 13%. (A) Distance of migration out of the original seeding area and (B) velocity of migration, as taken from the maximum distance in the y-direction of cell colony perimeter over a 48 hr duration and (C) Fluorescent mosaic image combines over 30 images taken at (100x) with nucleus immunostained with (DAPI/blue) to show directionality of migrating ECs (n=3).

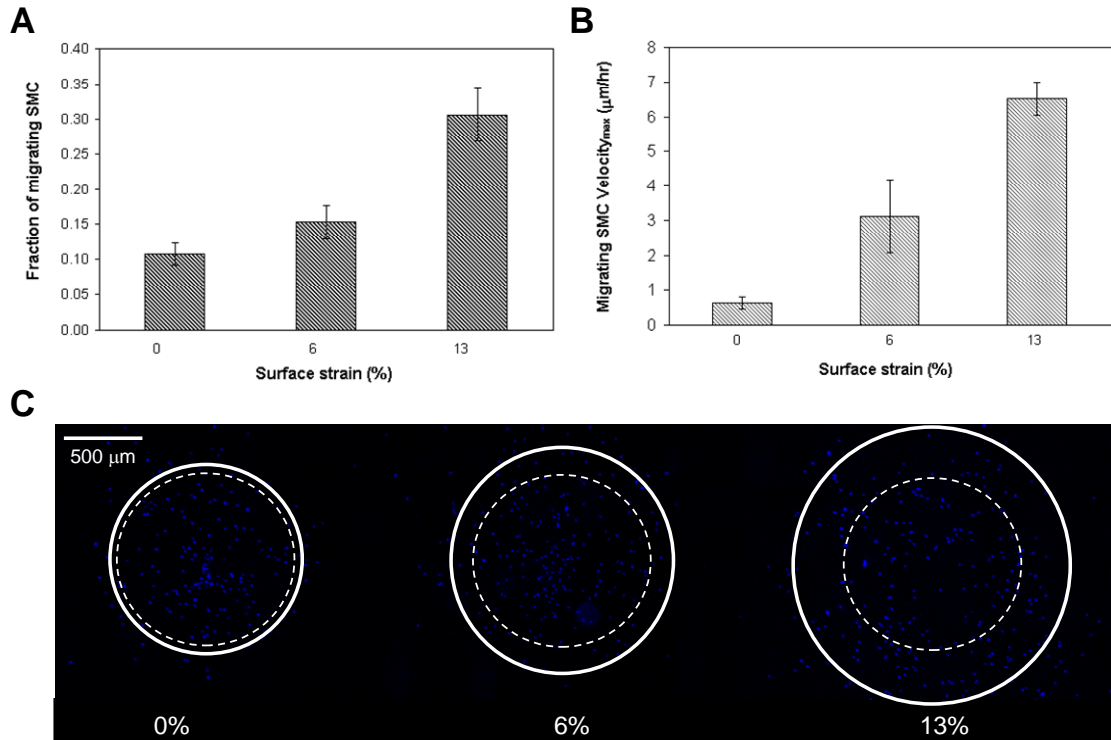


Figure 5.4 A-C: Response of SMC migration to increasing strain magnitudes

HASMC migration, velocity are enhanced in response to increasing cyclic tensile strain magnitude, with no clear directional migration. Migration of HASMC was quantified after 2 days of cyclic strain at varying magnitudes of strain: 0 (no strain), 6, and 13%.

(A) Distance of migration out of the original seeding area and (B) velocity of migration, as taken from the maximum distance in the y-direction of cell colony perimeter over a 48 hr duration and (C) Fluorescent mosaic image combines over 24 images taken at (100x) with nucleus immunostained with (DAPI/blue) to show lack of directionality of migrating SMCs (n=3).

was approximately 6-fold as compared to non strained conditions, notably slower than HUVEC migration rates (Figure 5.4B). Additionally, HASMCs over the 2 day strain duration did not demonstrate directional migration (Figure 5.4C).

SM migration enhanced by PDGF and EC conditioned media

To determine whether HASMCs were chemotactically responsive to PDGF (both recombinant human PDGF and endogenous PDGF secreted by HUVECs), HASMC migration was first assessed across porous transwell membranes. HASMCs migration increased when exposed to larger dosages of exogenous recombinant human PDGF (Figure 5.5A).

More physiologically relevant, conditioned media taken from strained ECs (demonstrated an upregulated secretion of PDGF, Chapter 3) demonstrated to enhance migration by nearly 2-fold, as compared to conditioned media taken from cells in non strained cultures. To determine whether the enhanced SM migration was a direct result of the strain-mediated increased PDGF levels, we neutralized PDGF-receptor (PDGF-R) on HASMCs and reassessed their response to conditioned media taken from strained ECs.

Interestingly, neutralizing HASMC responsiveness to PDGF (by neutralizing the PDGF-receptors) decreased migration by 45% (Figure 5.5B).

Next the migration of HASMCs migration on PDMS substrates was evaluated in response to (1) a depot of rhPDGF and (2) a depot of CM from strained. To first determine the validity of the distance of chemotactant from the HASMC colony, a

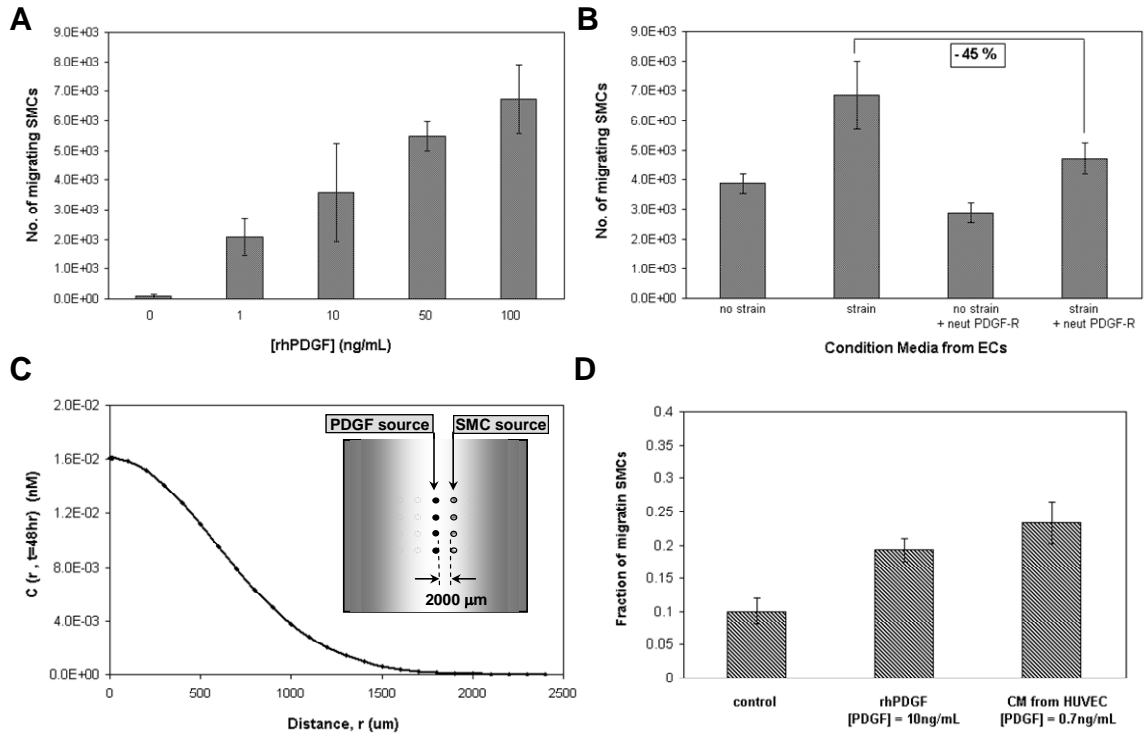


Figure 5.5 A-D: Model of PDGF concentration profile and SM migration to PDGF

PDGF enhances HASMC migration and recruits via chemotactic gradients (A)

Exogenous application of rhPDGF enhance SM migration across transwell inserts after 24 hrs in static culture with exposure increasing concentrations. (B) Application of endogenous PDGF secreted from strained HUVECs enhanced HASMC with and without PDGF-R neutralized, migration across transwell inserts. (C) Mathematical model representing the PDGF concentration profile from HUVEC point source. (D) SM migration was enhanced towards depo source: rhPDGF and CM from strained ECs over control (no growth factor).

mathematical model was used to approximate the diffusion length of PDGF (taken as a continuously generating point source). The concentration profile validates a diffusion length of 2 mm, from the originating PDGF source, therefore demonstrating that a chemotactic gradient exists (Figure 5.5C). The migration of HASMCs towards a depot of rhPDGF and a depot of CM from cyclic strained HUVECs demonstrated a respective 2-fold 2.25-fold enhancement in migration (Figure 5.5D) as compared a blank depot with no stimulants.

Bioactivity of PDGF-R on SMCs enhanced by PDGF and cyclic strain

To determine if HASMC bioactivity of PDGF-R was regulated by strain, HASM cultures were cyclically strained over a duration of 2 days and qualitatively assessed via immunostaining of the PDGF-R. Visual comparison clearly demonstrated that cyclic strain of HASMCs distinctly enhanced PDGF-R detection as compared to non strained conditions (Figure 5.6A). Next, SM PDGF-R bioactivity was examined in response to chemical stimulation of increasing rhPDGF levels. The relative fluorescent units (RFU) quantitatively showed that HASMC PDGF-R bioactivity increased with application of increasing rhPDGF (Figure 5.6B).

Directing SMC recruitment towards migrating ECs by cyclic strain

Strain activated, migrating HUVECs, and its secreted PDGF paracrine effects on HASMC migration, was assessed using 2D co-culture system (Figure 5.7A). Results demonstrated a 2-fold increase in SM migration (when coculture with non strained HUVECs), while when SMCs were co-cultured with strained HUVECs, the migration of

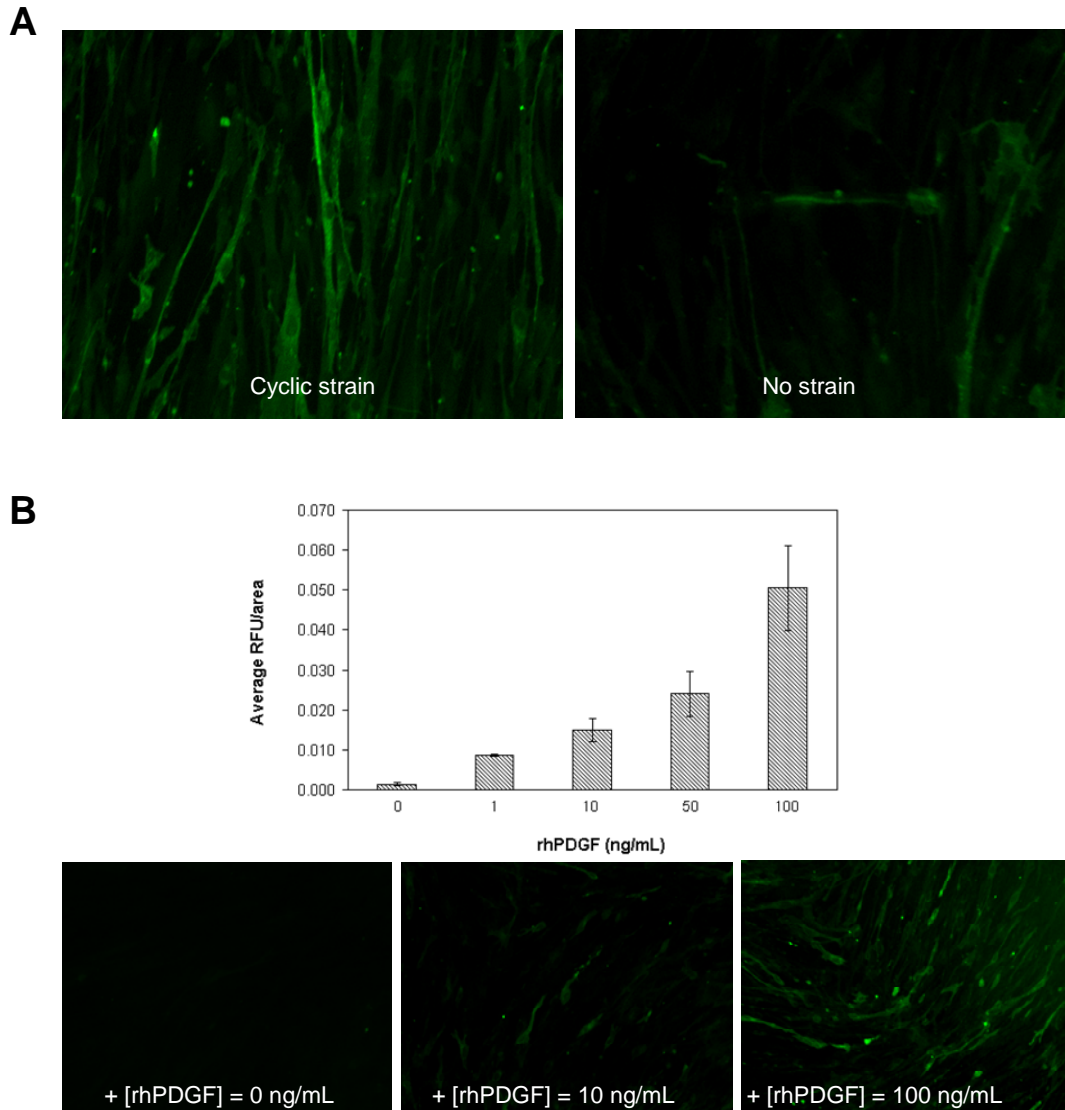


Figure 5.6 A-B: Bioactivity of SM PDGF-R enhanced by cyclic strain and rhPDGF

(A) Expression of PDGF-R was enhanced after 48 hrs of cyclic strain application to HASMCs and documented using fluorescent microscopy, with PDGF-R immunostained (Green). (B) Relative fluorescence Units (RFU) of immunostained PDGF-R was quantified in response to SMCs exposed to increasing rhPDGF concentrations over a 3 day duration (n=5).

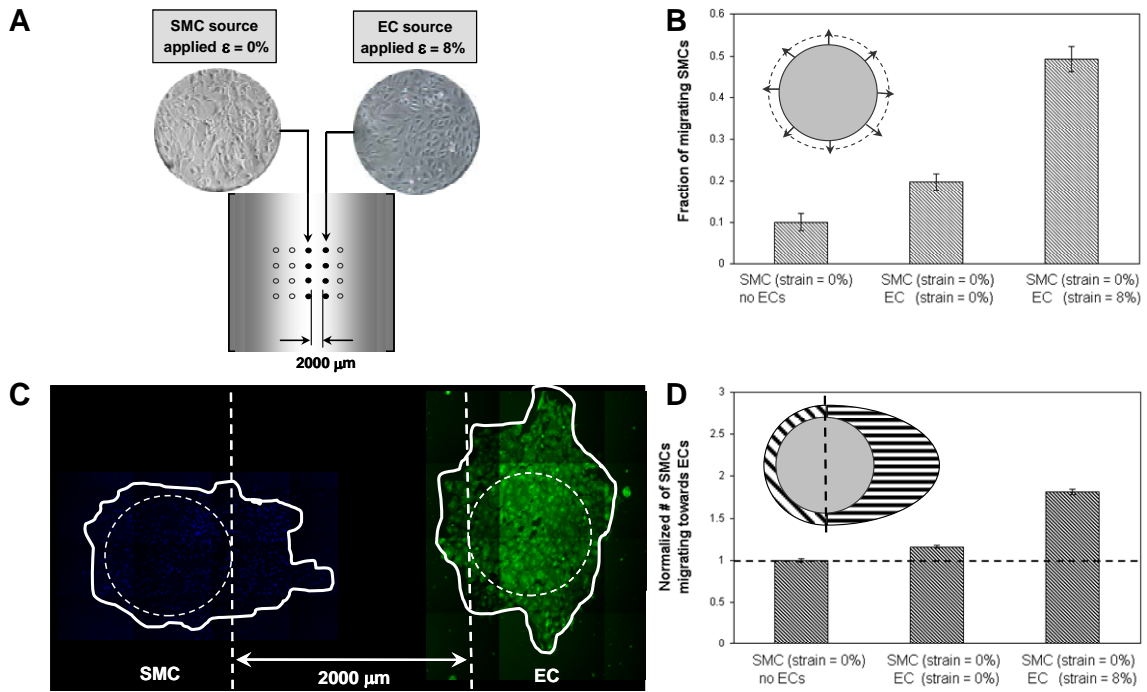


Figure 5.7 A-D: Cyclic strain mediates EC paracrine signaling on SMC recruitment
 HASMC migration via intercellular communication between HUVECs and HASMCs is enhanced in response to cyclic tensile strain. (A) Location of co-cultured cell colonies on PDMS well. (B) HASMC migration from original seeding location is enhanced when in co-culture with HUVECs, and particularly, under cyclic strain over 48 hrs. (C) Mosaic of 30+ images (at 100x) illustrating migration of HASMCs towards HUVECs. (D) Directionality of HASMC migration from original seeding location is polarized toward HUVECs, as analyzed by the hemisphere partition (D)

HASMCs were enhanced by 5-fold (Figure 5.7B), as compared to a negative control (SMCs with no co-culture, no strain). There was no notable directionality of HASMC migration when co-culture with non-strained HUVEC colonies. However, when co-cultured with strained HUVECs, the upregulated secretion of paracrine factors provided directional cues to direct the migration of HASMCs by 2-fold (Figure 5.7C-D) towards the migrating HUVEC colony.

5.4 Discussion

The results in this study demonstrate that cyclic strain can activate cues that result in directing HASMC migration towards HUVECs via a PDGF strain-regulated paracrine signaling mechanism. Cyclic strain increased HASMC responsiveness to PDGF and the directional migration of HASMCs towards cyclic strained HUVECs.

Previous studies report directing migration through immobilizing growth factors on culture surface^{31,32}, or chemotaxis chambers that generate gradients^{33,34}. A functional concentration gradient retains the concentration differential over time to enable visualization of the cell trajectories and migration velocities. Our method is unique because it employs a continuously generating chemotactic source where growth factors in other approaches that either immobilize factors, or delivery them at time gaps³⁵ would need to address the consumption and depletion of factors on culture surfaces or the lack of a gradient due to bolus applications. Altering the PDMS substrate in order to establish local differentials in strain for the purpose of directing SM growth migration is, to the best of our knowledge, not been previously documented. Others have attempted to

mimic local control cell migration to soluble stimuli by varying the extent to which the cells could spread over ECM^{36, 37}. However, our model is based on creating a substrate that is homogeneously treated to assess migration affects solely in response to strain. Lastly, although a 3-dimensional culture would provide a more physiologically relevant culture environment, technical inabilities to seed isolated (array of cell colonies, at time co-culture of HASMC and HUVECs) and precise (size of each colony precisely overlaid onto strain patterning locales) colonies of vascular cells limited our studies to monolayer culture.

Cyclic tensile strain was found in this study and by others³⁸ to enhance the expression of PDGF-R β on HASMCs. This enhanced responsiveness of signaling via the tyrosine kinase pathway (activated by ligand binding to PDGF-R) may implicate the mechanism by which cyclic strain upregulates HASMC migration. Cyclic strain regulation of molecules associated with the intracellular signaling pathway of PDGF-R has been widely documented, and was found to modulate ERK1/2^{39, 40}, PI3K⁴¹, p21^{42, 43}, tyrosine kinase^{40, 44}, and RhoA. However, the likelihood that cyclic strain may be enhancing other receptors is high, in particular stress response factors or other signaling molecules, all which may cooperatively lead to complex intracellular signaling pathways. The limitations of our studies in only detecting activation of one molecule may not be the most comprehensive in terms of understanding the overall strain mediated effects.

The sequential regulation by cyclic tensile strain on early (secretion of Ang2 followed by PDGF by HUVECs) and late (PDGF and strain activated recruitment of SM migration

towards HUVECs) stages of vascular remodeling, represents a highly relevant and critical role for mechanical signaling in angiogenesis. Reciprocal signaling of EC-induced SMC recruitment via PDGF has been examined in vivo^{9, 45} but not with events activated by external mechanical stimuli. None of the above described reciprocal signaling phenomenon in response to strain, has been documented in vitro.

The results of these studies demonstrate that modulating the presentation of substrate strain, can direct HASMC recruitment towards strain regulated HUVECs via paracrine intercellular signaling. Although beyond the scope of studies performed here, the possibility that other paracrine factors activated by straining ECs likely exist to contribute to the enhancing effect on SMCs. However, the results here identify one clear mechanism and provide added understanding of the role cyclic strain in the intercellular interaction governing SMC and HUVEC in context of neovessel formation during early stages of angiogenesis.

5.5 References

1. Hirschi, K.K. & D'Amore, P.A. Pericytes in the microvasculature. *Cardiovasc Res* **32**, 687-698 (1996).
2. Gerhardt, H. & Betsholtz, C. Endothelial-pericyte interactions in angiogenesis. *Cell Tissue Res* **314**, 15-23 (2003).
3. Jain, R.K. Molecular regulation of vessel maturation. *Nat Med* **9**, 685-693 (2003).
4. Raines, E.W. & Ferri, N. Thematic review series: The immune system and atherogenesis. Cytokines affecting endothelial and smooth muscle cells in vascular disease. *J Lipid Res* **46**, 1081-1092 (2005).
5. Sanders, M. Molecular and cellular concepts in atherosclerosis. *Pharmacol Ther* **61**, 109-153 (1994).
6. Abramsson, A. et al. Analysis of mural cell recruitment to tumor vessels. *Circulation* **105**, 112-117 (2002).
7. Morikawa, S. et al. Abnormalities in pericytes on blood vessels and endothelial sprouts in tumors. *Am J Pathol* **160**, 985-1000 (2002).
8. Ross, R. The pathogenesis of atherosclerosis: a perspective for the 1990s. *Nature* **362**, 801-809 (1993).
9. Hellstrom, M., Kalen, M., Lindahl, P., Abramsson, A. & Betsholtz, C. Role of PDGF-B and PDGFR-beta in recruitment of vascular smooth muscle cells and pericytes during embryonic blood vessel formation in the mouse. *Development* **126**, 3047-3055 (1999).
10. Westermarck, B., Siegbahn, A., Heldin, C.H. & Claesson-Welsh, L. B-type receptor for platelet-derived growth factor mediates a chemotactic response by

- means of ligand-induced activation of the receptor protein-tyrosine kinase. *Proc Natl Acad Sci U S A* **87**, 128-132 (1990).
11. Zerwes, H.G. & Risau, W. Polarized secretion of a platelet-derived growth factor-like chemotactic factor by endothelial cells in vitro. *J Cell Biol* **105**, 2037-2041 (1987).
 12. Hirschi, K.K., Rohovsky, S.A., Beck, L.H., Smith, S.R. & D'Amore, P.A. Endothelial cells modulate the proliferation of mural cell precursors via platelet-derived growth factor-BB and heterotypic cell contact. *Circ Res* **84**, 298-305 (1999).
 13. Montesano, R., Vassalli, J.D., Baird, A., Guillemin, R. & Orci, L. Basic fibroblast growth factor induces angiogenesis in vitro. *Proc Natl Acad Sci U S A* **83**, 7297-7301 (1986).
 14. Higashiyama, S., Abraham, J.A. & Klagsbrun, M. Heparin-binding EGF-like growth factor stimulation of smooth muscle cell migration: dependence on interactions with cell surface heparan sulfate. *J Cell Biol* **122**, 933-940 (1993).
 15. Dardik, A., Yamashita, A., Aziz, F., Asada, H. & Sumpio, B.E. Shear stress-stimulated endothelial cells induce smooth muscle cell chemotaxis via platelet-derived growth factor-BB and interleukin-1alpha. *J Vasc Surg* **41**, 321-331 (2005).
 16. Li, C., Wernig, F., Leitges, M., Hu, Y. & Xu, Q. Mechanical stress-activated PKCdelta regulates smooth muscle cell migration. *Faseb J* **17**, 2106-2108 (2003).
 17. Haga, J.H., Li, Y.S. & Chien, S. Molecular basis of the effects of mechanical stretch on vascular smooth muscle cells. *J Biomech* **40**, 947-960 (2007).

18. Nikolovski, J., Kim, B.S. & Mooney, D.J. Cyclic strain inhibits switching of smooth muscle cells to an osteoblast-like phenotype. *Faseb J* **17**, 455-457 (2003).
19. Worth, N.F., Rolfe, B.E., Song, J. & Campbell, G.R. Vascular smooth muscle cell phenotypic modulation in culture is associated with reorganisation of contractile and cytoskeletal proteins. *Cell Motil Cytoskeleton* **49**, 130-145 (2001).
20. Smith, P.G., Moreno, R. & Ikebe, M. Strain increases airway smooth muscle contractile and cytoskeletal proteins in vitro. *Am J Physiol* **272**, L20-27 (1997).
21. Gunst, S.J. & Tang, D.D. The contractile apparatus and mechanical properties of airway smooth muscle. *Eur Respir J* **15**, 600-616 (2000).
22. Kakisis, J.D., Pradhan, S., Cordova, A., Liapis, C.D. & Sumpio, B.E. The role of STAT-3 in the mediation of smooth muscle cell response to cyclic strain. *Int J Biochem Cell Biol* **37**, 1396-1406 (2005).
23. Numaguchi, K., Eguchi, S., Yamakawa, T., Motley, E.D. & Inagami, T. Mechanotransduction of rat aortic vascular smooth muscle cells requires RhoA and intact actin filaments. *Circ Res* **85**, 5-11 (1999).
24. Ingber, D.E. Mechanical signaling and the cellular response to extracellular matrix in angiogenesis and cardiovascular physiology. *Circ Res* **91**, 877-887 (2002).
25. Gerthoffer, W.T. Mechanisms of vascular smooth muscle cell migration. *Circ Res* **100**, 607-621 (2007).
26. Kallenbach, K. et al. A quantitative in vitro model of smooth muscle cell migration through the arterial wall using the human amniotic membrane. *Arterioscler Thromb Vasc Biol* **23**, 1008-1013 (2003).

27. Lanza, G.M. et al. Targeted antiproliferative drug delivery to vascular smooth muscle cells with a magnetic resonance imaging nanoparticle contrast agent: implications for rational therapy of restenosis. *Circulation* **106**, 2842-2847 (2002).
28. Kanda, K., Matsuda, T. & Oka, T. Mechanical stress induced cellular orientation and phenotypic modulation of 3-D cultured smooth muscle cells. *Asaio J* **39**, M686-690 (1993).
29. Kakisis, J.D., Liapis, C.D. & Sumpio, B.E. Effects of cyclic strain on vascular cells. *Endothelium* **11**, 17-28 (2004).
30. Haugh, J.M., Codazzi, F., Teruel, M. & Meyer, T. Spatial sensing in fibroblasts mediated by 3' phosphoinositides. *J Cell Biol* **151**, 1269-1280 (2000).
31. DeLong, S.A., Moon, J.J. & West, J.L. Covalently immobilized gradients of bFGF on hydrogel scaffolds for directed cell migration. *Biomaterials* **26**, 3227-3234 (2005).
32. Griffith, L.G. Emerging design principles in biomaterials and scaffolds for tissue engineering. *Ann N Y Acad Sci* **961**, 83-95 (2002).
33. Wells, C.M. & Ridley, A.J. Analysis of cell migration using the Dunn chemotaxis chamber and time-lapse microscopy. *Methods Mol Biol* **294**, 31-41 (2005).
34. Zicha, D., Dunn, G.A. & Brown, A.F. A new direct-viewing chemotaxis chamber. *J Cell Sci* **99** (Pt 4), 769-775 (1991).
35. Kumar, N., Zaman, M.H., Kim, H.D. & Lauffenburger, D.A. A high-throughput migration assay reveals HER2-mediated cell migration arising from increased directional persistence. *Biophys J* **91**, L32-34 (2006).

36. Chen, C.S., Mrksich, M., Huang, S., Whitesides, G.M. & Ingber, D.E. Geometric control of cell life and death. *Science* **276**, 1425-1428 (1997).
37. Ingber, D.E. Fibronectin controls capillary endothelial cell growth by modulating cell shape. *Proc Natl Acad Sci U S A* **87**, 3579-3583 (1990).
38. Ma, Y.H., Ling, S. & Ives, H.E. Mechanical strain increases PDGF-B and PDGF beta receptor expression in vascular smooth muscle cells. *Biochem Biophys Res Commun* **265**, 606-610 (1999).
39. Cheng, T.H. et al. Reactive oxygen species mediate cyclic strain-induced endothelin-1 gene expression via Ras/Raf/extracellular signal-regulated kinase pathway in endothelial cells. *J Mol Cell Cardiol* **33**, 1805-1814 (2001).
40. Ikeda, M., Takei, T., Mills, I., Kito, H. & Sumpio, B.E. Extracellular signal-regulated kinases 1 and 2 activation in endothelial cells exposed to cyclic strain. *Am J Physiol* **276**, H614-622 (1999).
41. Ikeda, M., Kito, H. & Sumpio, B.E. Phosphatidylinositol-3 kinase dependent MAP kinase activation via p21ras in endothelial cells exposed to cyclic strain. *Biochem Biophys Res Commun* **257**, 668-671 (1999).
42. Iwasaki, H., Yoshimoto, T., Sugiyama, T. & Hirata, Y. Activation of cell adhesion kinase beta by mechanical stretch in vascular smooth muscle cells. *Endocrinology* **144**, 2304-2310 (2003).
43. Li, C., Hu, Y., Mayr, M. & Xu, Q. Cyclic strain stress-induced mitogen-activated protein kinase (MAPK) phosphatase 1 expression in vascular smooth muscle cells is regulated by Ras/Rac-MAPK pathways. *J Biol Chem* **274**, 25273-25280 (1999).

44. Lehoux, S. & Tedgui, A. Cellular mechanics and gene expression in blood vessels. *J Biomech* **36**, 631-643 (2003).
45. Zeller, P.J., Skalak, T.C., Ponce, A.M. & Price, R.J. In vivo chemotactic properties and spatial expression of PDGF in developing mesenteric microvascular networks. *Am J Physiol Heart Circ Physiol* **280**, H2116-2125 (2001).

CHAPTER 6

SUMMARY, CONCLUSIONS, IMPLICATIONS AND FUTURE DIRECTIONS

6.1 Summary

The completion of this thesis brings together device development, molecular biology, engineering and material studies to address whether cyclic strain can direct vascular cells throughout specific, concerted stages of angiogenesis.

The first aim focused on developing a high precision strain device designed to concurrently run a large number of studies in parallel, and on creating custom elastomeric culture wells to present defined strain profiles for both 2D and 3D. Vascular cell studies, in aims 2 and 3, utilized this strain system to critically examine the role of cyclic tensile strain in regulating vascular cells during early and late stage angiogenesis.

Application of cyclic strain enhanced the migration and sprout formation of endothelial cells (Figure 4.3). In addition, cyclic strain was found to increase secretion of angiogenic cytokines, primarily Angiopoietin-2 (Figure 4.4B) and PDGF (Figure 4.4A) by ECs. Exogenous Ang-2 was also found to mediate EC migration (Figure 4.5E) and sprout formation (Figure 4.5A). However, RNAi knockdown of Ang-2 production by ECs

decreased EC responsiveness to strain regulated processes of migration (Figure 4.6C) and sprout formation (Figure 4.6D).

Increasing levels of cyclic strain magnitudes regulated the average velocity of EC and SMC migration (Figure 5.3 and 5.4), and EC directionality (Figure 5.3C). Cyclic strain enhanced SM expression of PDGF-receptor (Figure 5.6A). Chemotactic effects by exogenous rhPDGF on SM were validated (Figure 5.5A) and secreted PDGF by ECs yielded similar enhancing effects SM migration (Figure 5.5D).

6.2 Conclusions

We can therefore draw several conclusions from the results summarized above. The computer controlled strain device enabled the application of high precision strain and the ability to systematically characterize vascular cell phenotype and protein production necessary for our studies. The enhanced EC angiogenic phenotypes, represented by migration and sprout formation, demonstrated a clear role for mechanical cues in angiogenesis. Moreover, autocrine signaling via activation of Ang-2 may be the mechanistic pathway by which endothelial cells transduce mechanical signals to process a physiologic, angiogenic response. Cyclic strain modulated the intercellular communication between EC and SMC by upregulating chemotactic paracrine factors secreted by ECs to recruit SMCs. A co-culture model system examining vascular cell interactions during angiogenesis enabled us to conclude that local strain gradients regulate chemotactic gradients to direct ECs and SMCs, respectively. Our studies showed that the application of precise local cyclic tensile strain signals enables one to

regulate the behavior of cells at the molecular level by regulating autocrine and paracrine signals between vascular cells, to ultimately direct angiogenic phenotypes at physiologic length scales.

6.3 Implications and Future Directions

The results from this thesis demonstrate that vascular cells, when exposed to mechanical stimuli, are capable to secrete factors necessary to induce physiologically relevant angiogenic responses.

The SMART system developed in this thesis provides a platform to quantitatively assess the role of cyclic mechanical strain on tissue development. Physiologically, numerous tissues are exposed to either a sustained, occasional, or a continuous level of strain. The ability of cells in various tissues types to accommodate strains from the time of development throughout adult life suggest that strain signals may hold a regulatory homeostatic cue. Our studies have shown that cyclic mechanical strain plays an important role in altering blood vessel homeostasis. Many diseased states represent cases where tissues either lack or lose the ability to transduce normal levels of mechanical signals e.g. mechanically flawed tissues, such as atherosclerotic lesions¹ or change in mechanical stiffness in cancerous tissues^{2,3}. The strain system and the ability to present specific levels of strain will allow one to understand the role of strain signals and the complex combinatorial effect with its interaction with endogenous cues.

The ability to evaluate strain effects on neovascularization in 3D substrates, developed and utilized in this thesis, provides knowledge essential to understanding the mechanisms that regulate this process in a more physiologically relevant environment. This system enables one to advance further and engineer 3D strain gradient fields to induce the formation of networks, crucial and representative of various organs throughout our physiology. A possible approach to achieve 3D strain gradients can be the use of spatially patterned crosslinked polymers (PDMS, collagen, alginate, etc.). Such variations in material properties could be achieved by applying photolithographic methods. The studies performed here advance and provide a crucial tool set to better delineate how mechanical properties and the material interactions of cells regulate tissue formation.

Analysis of intercellular communication between vascular cells via paracrine signaling using a novel co-culture system revealed that ECs and SMCs, in the context of angiogenesis, are highly dependent on strain-mediated mitogenic signals. To address the role of strain in the development of other tissue types, proper management of the diffusion lengths balanced with understanding the levels of strain-mediated enhancement of mitogenic factors can be useful in better understanding co-culture interaction and communication. The knowledge gained from these in vitro models gives insight to the role of strain signals derived from the pulsation of blood flow, and can be used as a model system to study intercellular communication in other co-culture systems.

Knowledge from these studies can impact clinical approaches to curing vascular diseases by contributing to our current understanding of critical cues that regulate vascular development⁴. By understanding the key factors of how these processes develop can also aid in understanding how these similar processes fail during diseased states⁵. Current tissue engineering approaches rely primarily on engineering delivery systems for mitogenic molecules. Understanding how physiologic networks of interactions, mechanical stimuli and bioactive molecules, function together in the physical context of living cells and tissues is a challenge for future research. In the native environment, cells are exposed to numerous and simultaneous signals. Therefore, elucidating how cells selectively detect and filter signals to produce one concerted response could have large impact on a number of therapeutic approaches to diseases extending beyond those associated with blood vessel failure. An environment that is oversaturated with mitogens would not likely be the most appropriate approach. Thus, an alternative approach to using engineered delivery systems is to induce formation of vascular networks directly during tissue formation. An improved understanding of how mechanical signals induce activation of angiogenic processes has important implications. Mechanical signals can influence large length scales that are physiologically relevant, which greatly exceed those accessible to diffusional mass transport of purely chemical stimuli. Diffusional mass transport is limited to a few hundred micrometers, and is therefore fails to fully explain how mitogens alone can influence physiologic distances during adult vascular remodeling. The use of mechanical fields as signaling pathways may enable organisms to overcome the intrinsic length scale limitations and apply directed signals simultaneously to wide ranges of length scales to induce complex local angiogenic processes. Mechanical

signals thereby play a role as a key signaling mechanism to complements chemotactant stimulation. Since mechanical signals are present over a broad range of length scales, angiogenesis can be induced at multiple locations, independently. This multitude of local nucleation sites leads to the characteristic fractal structures of blood vessel networks, where local mitogenic factors come into play to regulate anastomosis of existing vessels, as illustrated in Figure 6.1. The SMART, strain gradient surfaces, 3D delivery of strain and a strain gradient co-culture system development and utilized throughout this thesis can be used to study similar concepts of chemomechanical coupling prevalent in biological processes.

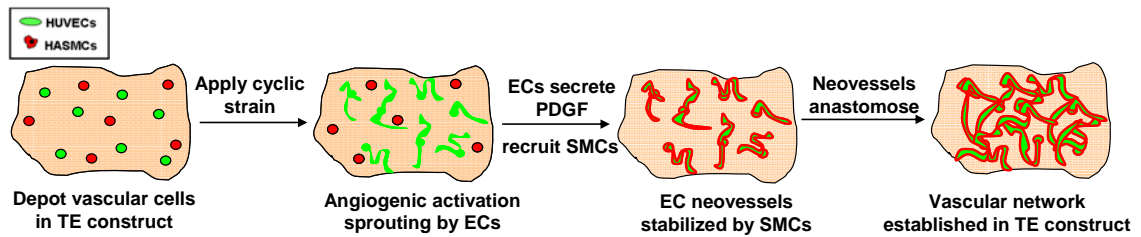


Figure 6.1: Suggestion for a new tissue Engineering Approach

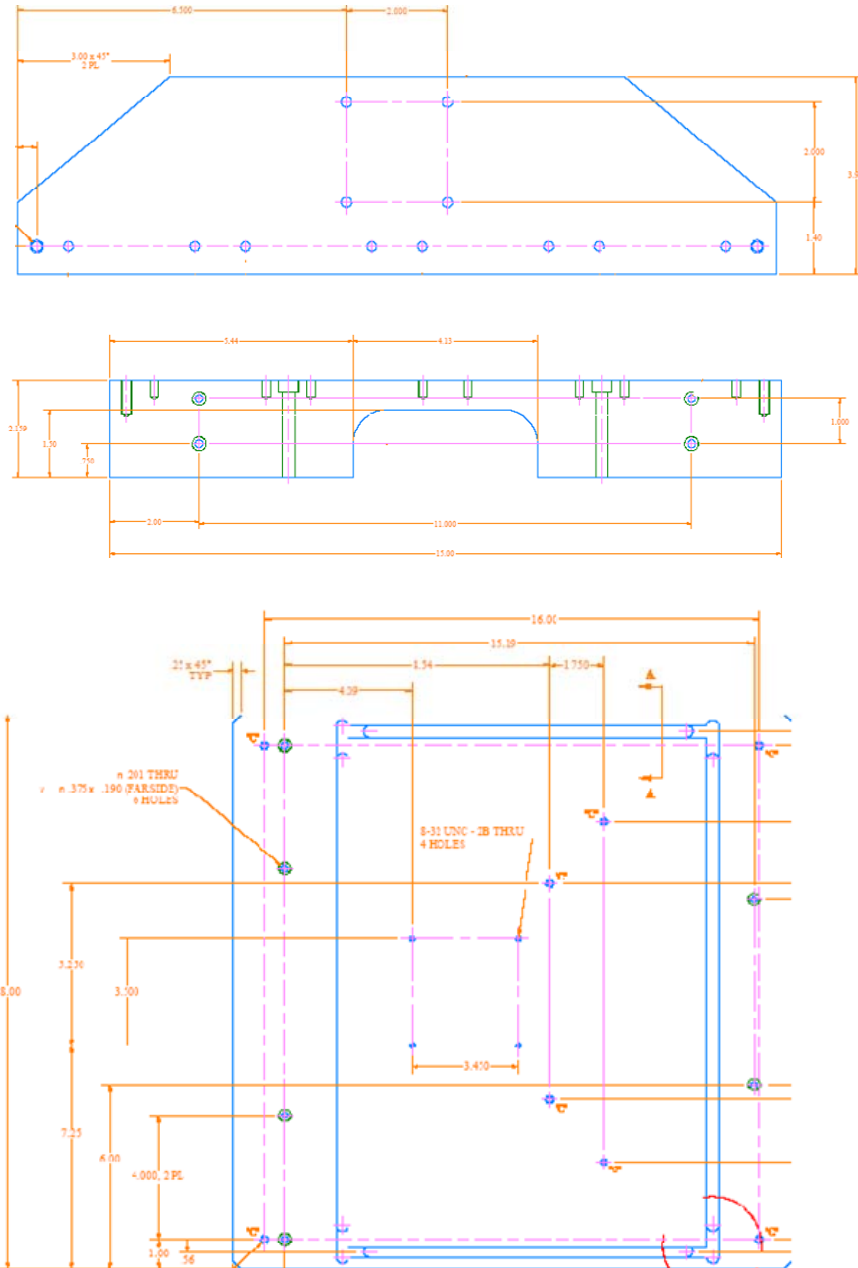
The concept is based on creating vascular networks using cyclic tensile strain to overcome the diffusional mass transport limitation (approximately 200 μm). This method addresses the question how mitogens alone can influence physiologic distances of vascular formation in tissue engineered constructs. Mechanical fields are used as signaling pathways to overcome the intrinsic length scale limitations, by applying directed signals across the entire tissue construct to induce multiple sites of local angiogenic activation. The multitude of local nucleation sites then leads to the characteristic fractal structures of blood vessel networks. Subsequent anastomosis of existing vessels can occur once these local sites begin to interact.

6.4 References

1. Ross, R. The pathogenesis of atherosclerosis: a perspective for the 1990s. *Nature* **362**, 801-809 (1993).
2. Greenleaf, J.F., Fatemi, M. & Insana, M. Selected methods for imaging elastic properties of biological tissues. *Annu Rev Biomed Eng* **5**, 57-78 (2003).
3. Discher, D.E., Janmey, P. & Wang, Y.L. Tissue cells feel and respond to the stiffness of their substrate. *Science* **310**, 1139-1143 (2005).
4. Conway, E.M., Collen, D. & Carmeliet, P. Molecular mechanisms of blood vessel growth. *Cardiovasc Res* **49**, 507-521 (2001).
5. Carmeliet, P. Angiogenesis in health and disease. *Nat Med* **9**, 653-660 (2003).

APPENDIX A

Schematics for S.M.A.R.T.



APPENDIX B

Protocol to create Mosaic Images

This script will systematically capture and combine over 100 images (using a 10x objective) to create a high resolution mosaic image of your sample on a macro-scale (ex: sample 10x10mm). It is programmed in IPLAB 4.0 and fully automated for use on Olympus IX81 (Mooney Lab, ESL-4th floor inverted fluorescence) and requires a functional computer controlled stage.

Useful for: imaging whole histological samples or migration of localized cell colony.

Scripts required

Main script (choose one depending on need)

For DIC images: YC array mosaic non6D.IPS

For DAPI + GFP images: YC array mosaic non6D FL.IPS

Supplemental script (required)

Array yu ching grab dapi_fitc.IPS

Method

1. Open script (choose one depending on need):
2. Bring focus to upper left corner to sampling image locale.
3. Focus and (if applicable) select exposure time
4. Press continue
5. Calculate # images in x-dir and y-dir you require: (see conversion table below)

Conversion Table for image pixel (at 10x) : length (um)

(at 10x) 1307.11 pixels = 780um

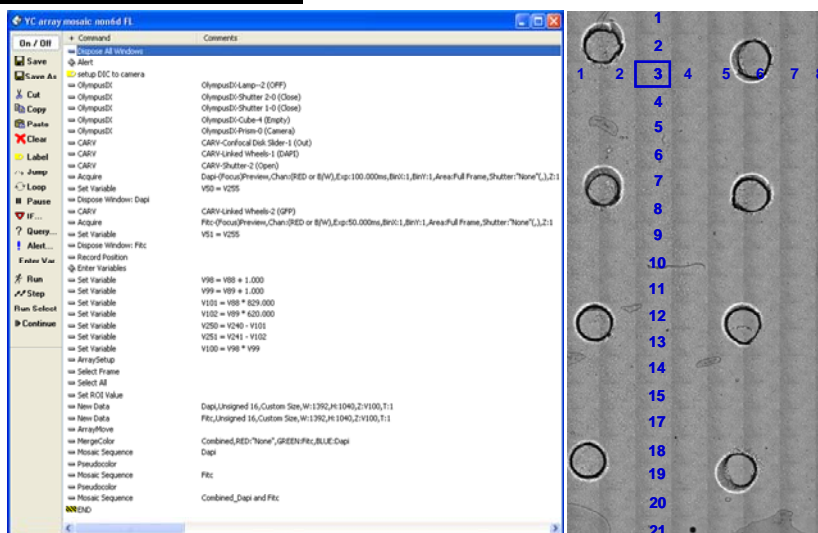
Unit conversion = 0.596 um/pixel

Full frame (at 10x) = (1392 x 1040) pixels/frame = (830 x 620) um²/frame

Example: if you want a mosaic image that has a sample length in the x-dir = 3 mm, you should enter (image # in x-dir = 4 , overshooting slightly).

6. Press run (time to complete, ranges from 2-5 minutes)

Script and samples mosaic image



APPENDIX C

Protocol to Sprouting Assay

Cell Culture

1. Culture cells so that they are confluent at day of culturing cells onto beads

Prepare microcarriers for cell coat - 1 day prior to gel prep

1. Weigh out 50 mg of dextran beads and hydrate in PBS solution for 2hrs (min) at room T (store in 50mL tube)
2. Carefully aspirate PBS (after beads settled to bottom of tube), exchange with new PBS.
3. Autoclave beads in 5mL PBS (use tubes that can be autoclaved)
4. Store beads at room T for a max of 2 days before use.

Culture cells onto sterilized dextran beads (to form: cell coated beads)

1. Confirm cells confluent in T75 (approx 2-4E6 cells)
2. Thaw trypsin and warm media and PBS in warm water bath
3. Carefully remove PBS from dextran beads and replace with 5mL culture media. Place in incubator.
4. Pipette 15 mL culture medium into a steril spinner flask. with 5ml of beads containing medium and incubate for a few minutes. (with stirring)
5. Trypsinize and centrifuge to pellet cells from a confluent T75.
6. Reconstitute cells (approximately 2-4E6 cells in 5mL culture media)
7. Pipette 5mL dextran beads in culture media along with 5mL cell soln into spinner flask.
Add 2-4E6 cells /5 ml EGM-2 medium in flask, and start stirring (every 30 min stop and go for 2 hrs)
8. Place spinner flask (closed loosely) onto magnetic stirrer.
9. Alternate with dynamic and static culture every 15 mins for 2 hrs.
10. After 2 hrs, dynamic culture overnight.
11. After 24 hrs: Transfer cell-bead soln from spinner flask into a 50mL tube.
12. Exchange with 15mL of fresh culture medium and split uniformly (5mL/flask) into 3 T25 flasks.

Encapsulating cell coated beads into fibrin gels

1. 30 min prior to gel casting: Pipette 1 ml of (uniform) cell coated bead solution from T25 flask and exchange with 1mL of fresh culture medium. Store in incubator
2. Make 2 solutions: (Soln 1) gel-cell soln (Soln 2) enzyme soln

Soln (1)	ratio
Fibrinogen	0.682
Aprotinin	0.091
cell coated beads	0.227

Soln (2)	ratio
Thrombin	0.083
PBS	0.917

3. First pipette Soln (1) into all wells (uniform distribution), then pipette Soln (2) and mix by thorough pipetting.
4. Prepare mixture at designated proportions: Soln (1) = 55.5% (of total V) and Soln (2) = 44.4% (of total V)
5. Place gels into incubator for 20 min to allow for gel polymerization.
6. Have specific growth factor in media dilutions prepared. (depends on your individual conditions)
7. Carefully pipette media into each well and place into incubator

APPENDIX D

Protocol to Cloning pSilencer-neo

Reconstitute single stranded oligos in distilled water

$C_{\text{final}} = [100 \mu\text{M}]$ ssOligos in ddH₂O

- 1 spin down (collect all mass @ bottom of vial)
- 2 pipette + reconstitute in ddH₂O
- 3 turn upside down
- 4 vortex to ensure uniform mixing
- 5 spin down
- 6 use 1 uL of each sense/antisense and store remaining at T = -20°C

Anneal to form dsOligos

-ddH ₂ O	23 ul
-sense oligo	1 ul
-antisense oligo	1 ul
-2X annealing buffer	25 ul

- incubate 4 minutes at 95°C
- incubate 10 minutes at 70°C
- slowly cool down the annealed oligos to 4°C (Store at -20°C)

2X Annealing buffer:
 200 mM potassium acetate
 60 mM HEPES-KOH pH 7.4
 4 mM Mg-acetate

Ligation of pSil-neo vector with dsOligo to make circular DNA

- Dilute 1 μL of annealed oligos in 19 μL of water to make: diluted (1:20) dsOligo
- Ligate 1 μL of diluted annealed oligos to (25.7 fmol = 0.764 uL pSil-neo) linearized pSil-neo in a 10 μL reaction.
- Incubate at room temperature overnight

• Transform 2 μL of ligation (circular DNA with dsOligo inserted)

- Propagate overnight
- Isolate DNA via miniprep
- Digest miniprep s:

Samples: Hind III - EcoRI = 396 bp (insert + U6)	793-397 = 396
Control: BamHI - EcoRI = 333 (U6, no insert)	793-731 = 62

- Positive clones will release a fragment ~ 62 bp larger than control, empty vector
- Use a 2% agarose gel to detect the shift.
- Positive clones should be sequence verified.

	dsOligos (top-bot annealed)
1	p Sil / Ang 2 - 874
2	p Sil / Ang 2 - 1156
3	p Sil / Ang 2 - 1447
4	p Sil / Ang 1 - 696
5	p Sil / Ang 1 - 914
6	p Sil / Ang 1 - 260
Control	p Sil / empty vector (linear)

pSilencer-neo (4.52 kb)

	V-1 (uL)	V-2 (uL)
vector (pSil-neo)	0.8	0.8
diluted (1:20) dsOligo	1	2
10x buffer	1	1
ligase	1	1
ddH ₂ O	6.2	5.2
	total = 10 uL	total = 10 uL

Control (pSil-neo, empty vector)

	V-1
vector (pSil-neo)	0.8
diluted (1:20) dsOligo	0
10x buffer	1
ligase	1
ddH ₂ O	6.8

APPENDIX E

Protocol to Pattern Array of Vascular Cell Colonies

Make PDMS wells and fuse glass strip covalently bond using Plasma O2

Create Mask using Imm punch and prototype pattern array

Surface treatment (sterilize, UV treat, 2um/mL FN coat)

Place mask onto base of PDMS well

Preparation: Cell seeding into mask

	total cells starting	
cells in media	2.50E+06	cells/mL
put 16uL (cell soln) in	4.00E+04	total cells in 50uL
add Soln 2 (40.5 uL)		(now V=0.0905mL)
#cell / (V _{tot} =S1+S2=)	4.42E+05	cells/mL
# cells in V = 2uL	6.94E+02	cells in 2uL

Preparation: Cell seeding into entire PDMS-medium well

Soln (1)	% of soln 1+2	total V (soln 1)	250 uL	50 uL
		% of tot soln	V (uL)	V (uL)
Fibrinogen	0.682	0.379	168.8	34.1
cells in media	0.318	0.177	78.7	15.9
		total V (soln 2)	200 uL	40.5 uL
Soln (2)	% of soln 1+2	% of tot soln	V (uL)	V (uL)
Thrombin	0.083	0.037	16.8	3.4
PBS	0.917	0.408	185.7	37.1

Prepare fibrin gels with cells embedded, quickly seed 1.5uL cell-fibrin gel soln into each well (diam = 1mm)

Change tips and make new cell-gel mixture when needed until entire array is seeded

Prepare media containing optimized plasmin (to slowly degrade fibrin to provide monolayer culture over 24 hrs)

Preparation: Media + 10ug/mL Plasmin

mass Plasmin bought = 1500ug + 1.5mL = 1000ug/mL (stock)
 stock [Plasmin] = 1000ug/mL final [Plasmin] in media = 10 ug/mL
 using medium PDMS wells (2mL media/ well)

	V1 (mL)	C1 (ug/mL)	V2 (mL)	C2 (ug/mL)
HUVECs				
HASMCs	0.160	1000	16	10

After 24 hrs, remove mask to reveal patterned array of cell colonies.